THE EFFECTS OF 12-LIPOXYGENASE METABOLITES ON VASCULAR PERMEABILITY IN THE RAT SKIN

by

Mei Mei Wang

A thesis submitted in conformity with the requirements
for the degree of Master of Science
Graduate Department of Pharmacology
University of Toronto

ABSTRACT

The Effects of 12-Lipoxygenase Metabolites on Vascular Permeability in the Rat Skin

Degree of Master of Science 1996
Mei Mei Wang
Graduate Department of Pharmacology
University of Toronto

Increased vascular permeability is one of the features of acute inflammation. Metabolites of the arachidonic acid (AA) cascade have long been associated with this condition. In this study, the vascular permeability effects evoked by 12-HETE and hepoxilins (Hx), AA products of 12-lipoxygenase, were examined in the rat skin in the presence and absence of bradykinin (BK) and platelet-activating factor (PAF). 12-HETE was able to induce an increase in vascular permeability on its own while the hepoxilins were inactive. In the presence of BK, 12-HETE had no additional effects, while the specific forms of $HxA_3(8R)$, $HxB_3(10R)$ and $Hx\Delta A_3(LP)$ were able to potentiate the BK effects. Conversely, only $HxB_3(10R)$ and $Hx\Delta B_3(LP)$ were able to cause potentiation of PAF-induced vascular permeability. Establishment and implementation of a fluorescence detection system using ADAM to the label carboxylic acid group demonstrated that BK- and PAF-stimulated skin preparations (*in vitro* and *in vivo*) produced predominantly 12-HETE. The results suggest that 12-HETE may act directly on the vascular endothelium to create gaps to increase vascular permeability, while hepoxilins may modulate the effects of other mediators.

ACKNOWLEDGEMENTS

TABLE OF CONTENTS

LIST OF FIGURES

LIST OF ABBREVIATIONS

AA — arachidonic acid
ACN — acetonitrile
ADAM — 9-anthryldiazomethane
BK — bradykinin
BSA — bovine serum albumin
$CaCl_2$ — calcium chloride
DDH_2O — double distilled water
D-PBS — Dulbecco's phosphate buffered saline
EB — Evans blue
EDTA — ethylenediaminetetraacetic acid
EtOAc — ethyl acetate
EtOH — ethanol
HCl — hydrochloric acid
HPLC — high-pressure liquid chromatography
HxA_3 — hepoxilin A_3;
  8(S/R)-hydroxy-11(S),12(S)-*trans*-epoxyeicosa-5Z, 9E, 14Z-enoic acid
HxB_3 — hepoxilin B_3;
  10(S/R)-hydroxy-11(S),12(S)-*trans*-epoxyeicosa-5Z, 8Z, 14Z-enoic acid
$Hx\Delta A_3$ — hepoxilin ΔA_3, cyclopropane analogue
$Hx\Delta B_3$ — hepoxilin ΔB_3, cyclopropane analogue
LTB_4 — leukotriene B_4
  5(S),12(R)-dihydroxy-6,14-*cis*-8,10-*trans*-eicosatetraenoic acid
MeOH . — methanol
$MgSO_4$ — magnesium sulfate
N_2 — nitrogen gas
PAF — platelet-activating factor
KCl — potassium chloride
KH_2PO_4 — potassium phosphate
PG — prostaglandin
RA — ricinoleic acid
NaCl — sodium chloride
$NaHCO_3$ — sodium bicarbonate
Na_2HPO_4 — sodium phosphate
NaOH — sodium hydroxide
PLA_2 — phospholipase A_2
TLC — thin layer chromatography
Tris-HCl — tris(hydroxymethyl)aminomethane hydrochloride
$TrXA_3$ — trioxilin A_3
$TrXB_3$ — trioxilin B_3
5-HETE — 5-hydroxy-6,8,11,14-eicosatetraenoic acid
8-HETE — 8-hydroxy-5,9,11,14-eicosatetraenoic acid
9-HETE — 9-hydroxy-5,7,11,14-eicosatetraenoic acid
11-HETE — 11-hydroxy-5,8,12,14-eicosatetraenoic acid
12-HETE — 12-hydroxy-5,8,10,14-eicosatetraenoic acid
15-HETE — 15-hydroxy-5,8,11,13-eicosatetraenoic acid
12-HPETE — 12-hydroperoxy-5,8,10,14-eicosatetrenoic acid

SECTION ONE: INTRODUCTION

1.1   THE SKIN

The skin is the largest organ in the body constituting 16% of body weight. It is composed of an epithelial layer (epidermis), a connective tissue layer (dermis) and a subcutaneous, adipose layer (hypodermis) (for review see Eckert, 1989; Mukhtar *et al.*, 1992). The skin has numerous functions all of which depend on the structure and individual components of the various regions. Some of these functions include protection from injury and desiccation, temperature regulation and water balance, sensation, as well as communication and expression. By far one of the most important functions of the skin is to provide protection between the individual and the environment.

1.1.1 The Epidermis

Structure

The epidermis is a tightly bound, stratified squamous epithelium that covers the entire outer surface of the body. The five strata of the epidermis are (from outermost to innermost, refer to Figure 1-1) corneum, lucidum, granulosum, spinosum, and basale (Figure 1-1). Each layer represents the various stages of differentiation (Green, 1977; Stenn, 1983), a process in which keratinocytes undergo keratinization to form the dead superficial layers of the skin.

These superficial cells are continuously lost from the surface and are replaced by cells that arise as a result of mitotic activity of the basal cells in the epidermis. As the generation of new cells move upwards, they accumulate keratin in their cytoplasm. Eventually keratin replaces all metabolically active cytoplasm, and the cell is finally shed. This process of cell turnover occurs every 15-30 days.

In the epidermis there exists four cell types: keratinocyte, melanocyte, Merkel cell (Jimbow *et al.*, 1976) and Langerhan cell (Rowden, 1981). The keratinocyte is the predominant cell type and accounts for more than 90% of the total cell population (Green, 1977; Stenn, 1983; Holbrook and Wolff, 1987; Eckert, 1989). Whereas, the other three cell types reside mainly in strata spinosum and basale, keratinocytes are distributed among the layers of the epidermis. Melanocytes produce melanin (Quevedo and Fleischmann, 1980), the pigment responsible for shades of brown. Langerhan cells bear surface antigens common to B and some T lymphocytes and monocytes, signifying immunological importance (Rowden, 1981). Merkel cells are associated with intraepithelial nerve endings and may serve a role in sensory perception.

Function

Although the thickness of the epidermis ranges between 0.07-0.12mm throughout most of the body, it serves as the first line of defense against the environment. Stratification has provided a resilient and abrasion-resistant surface to protect the replenishing stem cell population from injury, while keratin, the fibrous protein product of cell differentiation, provides a tough, insoluble covering essential for protection. Furthermore, melanin (the product of melanocytes) protects against ultraviolet irradiation.

The epidermis is also a major site of drug metabolism. Cytochrome 1A1 activity is high, accounting for 1% of the dealkylation activity of the liver (Finnen *et al.*, 1985; Mukhtar and Khan, 1989). Other enzyme systems include epoxide hydrolase (MacNicoll *et al.*, 1980; Bickers *et al.*, 1982), glucuronosyl transferase, sulfotransferase (Harper and Calcutt, 1960) and glutathione transferase (Mukhtar and Bresnick, 1976; Summer and Goggelmann, 1980; Baars *et al.*, 1981).

1.1.2 The Dermis

Structure

The free surface of the skin is not smooth but marked by delicate grooves. The complicated patterns of ridges in the epidermis correspond to complementary patterns on the surface of the dermis. This delineates the sharp boundary between these two regions.

The dermis, averaging a thickness between 0.5-3.0mm, is composed of two strata: the papillary layer which is in contact with the epidermis, and the reticular layer which houses the numerous sensory nerves and blood vessels (Figure 1-1). Although the densities of the connective tissue differ, both layers consist of collagenous fibres and numerous elastic fibres. The main cell types are fibroblasts and macrophages.

Function

As the largest fraction of the skin endowed with a generous proportion of connective tissue, the dermis provides the skin with its structural strength and high resilience to physical injury. The dermis also serves to anchor the downward extensions of sweat glands and hair follicles which are originally derived from the epidermis.

1.1.3 The Hypodermis

Structure

The epidermis and dermis lie on a soft insulating cushion of fibro-fatty tissue called the hypodermis (Figure 1-1: subcutaneous tissue). Where the fibrous elements are well defined between the former two regions, this demarcation is less evident between the dermis and hypodermis.
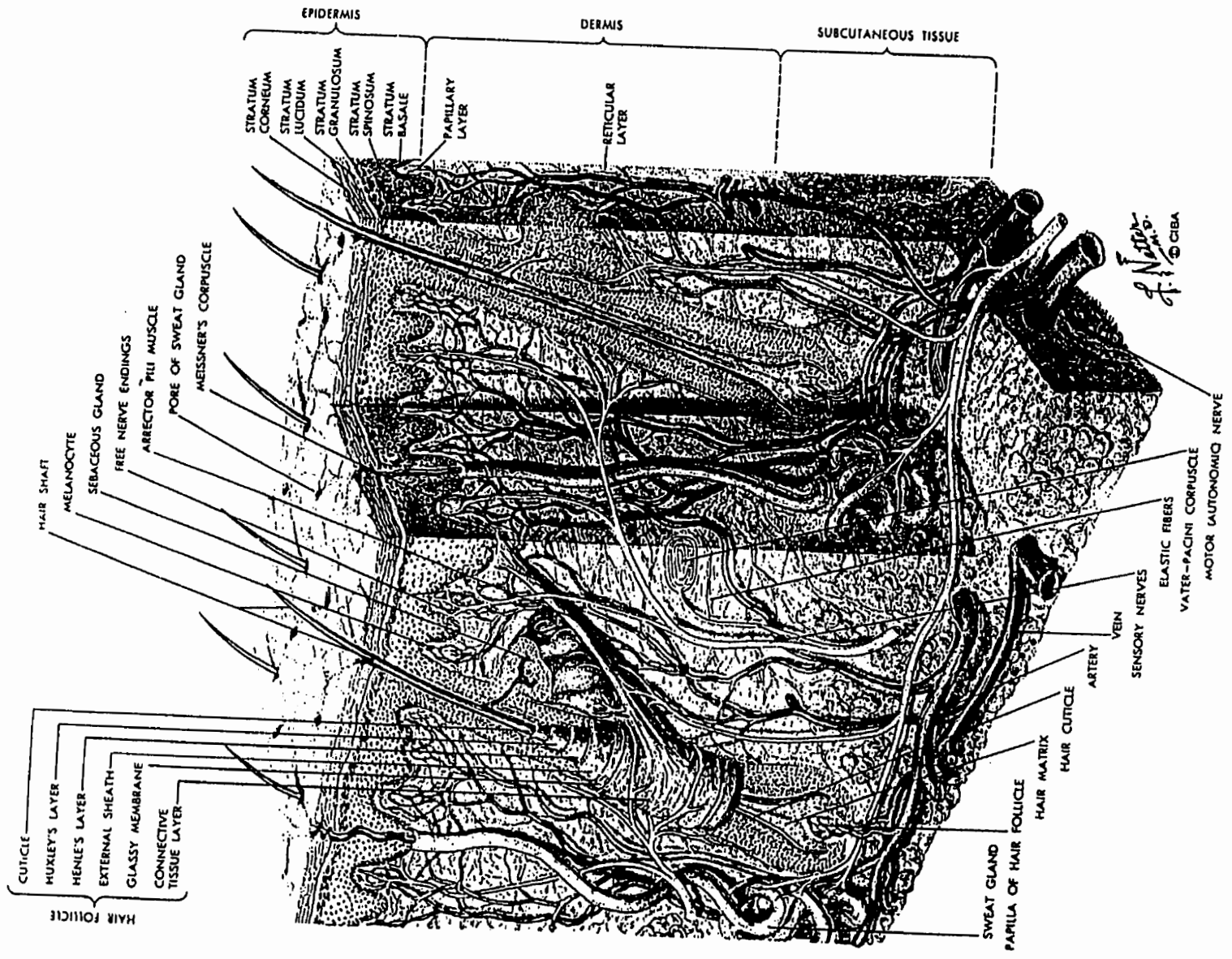
Figure 1-1. The structure of the skin. Reprinted from Habif (1990)

Clinical Dermatology: A Color Guide to Diagnosis and Therapy

This layer of loose connective tissue made of collagenous and elastic fibres is a continuation of the reticular layer of the dermis. Fat cells occur in this subcutaneous layer; their numbers varying with location. The hypodermis is also richly supplied with blood vessels and nerve trunks.

Function

The cushion structure of the hypodermis provides added protection against temperature and traumatic fluctuations for the other skin layers and internal structures.

1.2 INFLAMMATION

"Inflammation is a process typical of vascularized tissues, whereby fluid and white blood cells accumulate at the site of injury. The overall significance of inflammation is that of a defense mechanism." (Ryan and Majno, 1977). The inflammatory reaction can be mediated by any noxious stimulus falling generally into one of the following broad categories: (i) physical (e.g. mechanical trauma, irradiation, cold or heat), (ii) chemical (e.g. acids, alkalis and other irritants), and (iii) infection due to a living organism (e.g. viruses, bacteria, fungi).

The four cardinal signs of inflammation as first described by Celsus (30 BC-AD 38) evoke changes in *rubor* (redness), *tumor* (swelling), *calor* (temperature) and *dolor* (pain). The fifth was addressed by Hunter (1728-1773) who later added *functio laesa* (loss of function). The inflammatory response involves a series of events, and variation in its duration and intensity depend largely on the type of injury and degree of damage. Interest in the pathological etiology and pharmacological control of the inflammatory response originated from the realization that many dermatological diseases (psoriasis, atopic eczema) and conditions (rheumatoid arthritis, allergic reactions) arise from processes that accompany inflammation. A clearer understanding of the role of the mediators and their actions may lead to rational therapies.

Cutaneous inflammation consists of two phases: acute and chronic inflammation. Acute inflammation is the local reaction of living tissue to injury and polymorphonuclear leukocytes (PMNL) predominate in its early stages. Chronic inflammation is exhibited in extreme circumstances when the noxious stimulus persists and activated fibroblasts undergo mitosis to provide collagen to encapsulate the lesion (Dunn and Willoughby, 1989). The most severe inflammatory disease states are generally chronic in nature.

In 1889, Cohnheim described vascular changes as the cornerstone of an acute inflammatory reaction. These three basic events are hyperemia, increased vascular permeability and extravasation of circulating cells.

1.2.1 Hyperemia

After the initial insult, a distinct vascular response ensues. First, there is a transient vasoconstriction followed immediately by vasodilatation of the entire vascular network. This increase in blood flow rate develops rapidly and lasts 30-45 minutes. Eventually, there is a slowing of flow, presumably due to the movement of fluid out of the vessel and into the interstitial spaces. The major determinant of blood flow is arteriolar tone which passively produces capillary and venous distention.

1.2.2 Vascular permeability

Changes in vascular permeability result from alterations in the blood vessel wall such that normally impermeable molecules leak into the extravascular tissue leading to the formation of an edema. The mechanism of leakage may be a result of direct injury to the vessel itself or activated via mediators arising from the damaged tissue. The effect of the former, is a generalized leakage of the entire microcirculatory network, while the mediators of the latter affect mostly the post-capillary venules. These mediators can be categorized into three groups: direct-acting, vasodilators and leukocyte-dependent.

Direct-acting mediators include bradykinin (BK, Figure1-2) and platelet-activating factor (PAF, Figure 1-3). These compounds along with histamine and serotonin are believed to create gaps between endothelial cells of post-capillary venules (Majno and Palade, 1961; Majno *et al.*, 1961).

H - Arg - Pro - Pro - Gly - Phe - Ser - Pro - Phe - Arg - OH
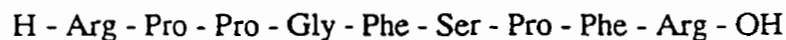
Figure 1-2. Chemical structure of bradykinin, a nonapeptide.

$CH_2O(CH_2)_{15-17}-CH_3$

$CHOCOCH_3$

$CH_2O - P - OCH_2CH_2N^+ - CH_3$
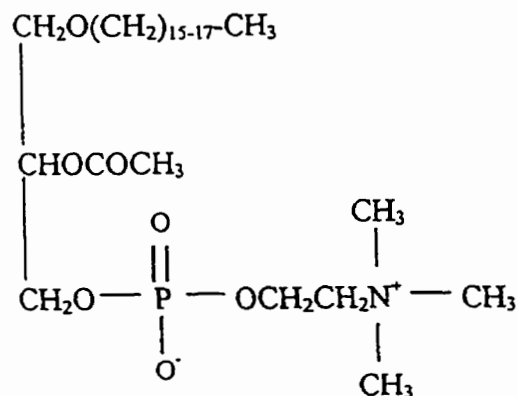
Figure 1-3. Chemical structure of platelet-activating factor.
A part of the phospholipid family designated as acetyl-glyceryl-ether-phosphorylcholine.

Vasodilators such as prostaglandins (PGs, particularly the E-types) and nitric oxide relax the pre-capillary arterioles to cause vasodilatation. Alone they have little effect (although this also varies with species) but can substantially potentiate the effects of other compounds (Williams and Morley, 1973; Williams and Peck, 1977; Khalil and Helme, 1992; Teixeira et al., 1993).

Leukocyte-dependent mediators of which C5a (the peptide fragment from the complement system), leukotriene B4 (LTB4) and N-formyl-methionyl-leucyl-phenylalanine (FMLP) belong, share traits from the two aforementioned groups. They possess little ability to increase vascular permeability on their own, but are potentiated by PGs. Unlike direct-acting mediators, depletion of circulating PMNL results in complete abolition of their effects even on co-administration with PGs (Wedmore and Williams, 1981).

The way in which the three mediator groups interact is complex and still unclear. It is believed that histamine and other direct-acting mediators predominate in the early stages of inflammation while formation of leukocyte-dependent mediators occur later.

1.2.3 Extravasation of circulating cells

During hyperemia, leukocytes already present in the blood adhere to the venule walls, pass across the basement membranes through interendothelial and mediator-induced gaps and emigrate toward the site of injury. In this way, neutrophils, eosinophils and monocytes (not lymphocytes) are able to contain and destroy the inflammatory stimulus. As well, circulating albumin and other proteins, as well as some erythrocytes escape into the extravascular tissue.

1.3 CAUSES OF INFLAMMATION

Inflammation can come about in many ways, at any time. The ability of an organism to recognize the infliction triggers a series of events culminating in an inflammatory reaction. Although many factors interact to cause inflammation, it is beyond the scope of this thesis to describe them all. Instead, a general overview of a particular system, the arachidonic acid cascade, and its role in the skin will be examined.

1.3.1 Arachidonic acid

In nature there exists hundreds of fatty acids with chain length ranging from three to more than thirty carbons and containing up to seven or eight double bonds. The substrates for all known lipoxygenase, epoxygenase and cyclooxygenase enyzmes include the majority of 18, 20 and 22 carbon polyunsaturated fatty acids (PUFA). PUFA are highly susceptible to autooxidation by light, redox-active transition metals and molecular oxygen (O_2). Carbon atoms flanked by double

bonds are prone to carbon-hydrogen cleavage which result in formation of carbon radicals. Such radicals are then attacked by O_2 producing fatty acid peroxides.

Arachidonic acid (AA, Figure 1-4) is a 20 carbon length PUFA containing four double bonds. In membrane phospholipids, AA is esterified in the sn-2-position. Upon phospholipase stimulation (induced directly by phospholipase A_2 or indirectly by phospholipase C via stimulation of phosphatidylinositol turnover), AA is de-esterified and becomes available to metabolizing enzymes (Lands and Samuelsson, 1968; Irvine, 1982).
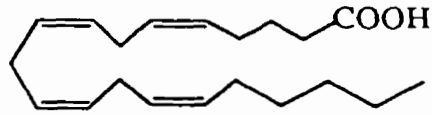
Figure 1-4. Chemical structure of arachidonic acid.

1.3.2 Arachidonic acid metabolism

AA can be metabolized into a variety of products (refer to Figure 1-5) depending on the enzyme system present in the tissue. The resulting metabolites are known to mediate the regulation and modulation of important physiologic functions and pathologic conditions. The two main systems are the cyclooxygenase and lipoxygenase pathways.

Cyclooxygenase pathway

AA is metabolized by a series of peroxidations and cyclizations leading to ephemeral intermediates (PGG_2) and then, via isomerizations and reductions, to prostaglandins (PGE_2, Figure 1-6A), thromboxane (Figure 1-6B) and prostacyclin (Figure 1-6C). In the skin, PGE_2 and PGD_2 (a structural isomer of PGE_2 in which the C9 keto and C11 hydroxy groups are interposed) are the predominant products (Camp et al., 1978; Hammarstrom et al., 1979; Hensby et al., 1980; Mayer et al., 1984).

A. Prostaglandin E_2   **B. Thromboxane**   **C. Prostacyclin**
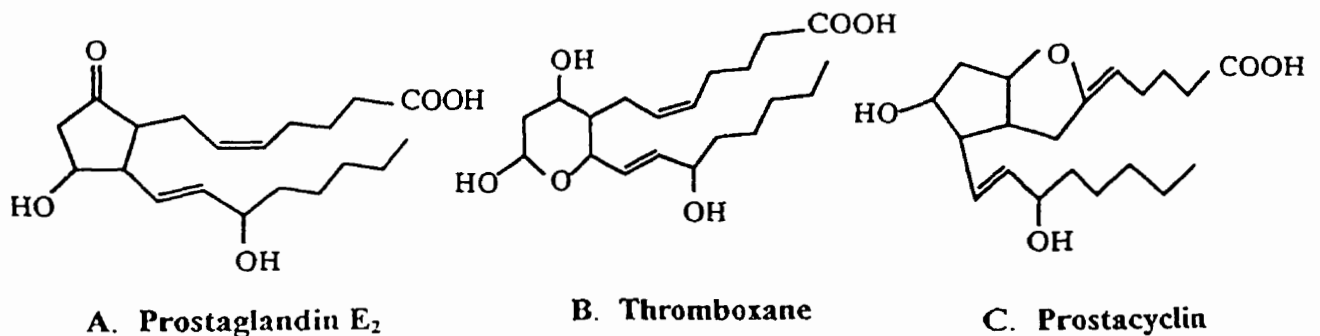
Figure 1-6. Cyclooxygenase compounds.

Phospholipids

Phospholipase A₂ —

Arachidonic acid

12-lipoxygenase	*8-lipoxygenase* *9-lipoxygenase* *11-lipoxygenase* *15-lipoxygenase*	*5-lipoxygenase*	*cyclooxygenase*	*cytochrome p450*

| 12-HPETE | 8-HPETE
9-HPETE
11-HPETE
15-HPETE | 5-HPETE | Prostaglandins
Prostacyclin
Thromboxane | AA-epoxide |

12-HETE	Hepoxilin A₃ Hepoxilin B₃	8-HETE 9-HETE 11-HETE 15-HETE	5-HETE	Lipoxin A₄ Lipoxin B₄	LTA₄

LTB₄   LTC₄
LTD₄
LTE₄

Figure (1-5): The arachidonic acid cascade outlining the major enzymatic pathways, intermediates and products

Lipoxygenase pathway

Lipoxygenases can act on AA to form hydroperoxides, which are then transformed either enzymatically or non-enzymatically to other compounds (Figures 1-5 and 1-7A-F). Monohydroxy derivatives of arachidonic acid, possessing hydroxyl groups in the 5, 8, 9, 11,12, or 15 positions have been shown to be synthesized by neutrophils (Borgeat and Samuelsson, 1979; Goetzl and Sun, 1979). Interactions between the 5- and 15-lipoxygenase pathways have further yielded di- and tri-hydroxyeicosatetraenoic acids (Maas *et al.*, 1982; Turk *et al.*, 1982; Serhan *et al.*, 1984a; Serhan *et al.*, 1984b).

Transformation of AA by 5-lipoxygenase results in the formation of 5-HETE and leukotrienes (LT). LTA_4, the 5,6-epoxy intermediate can be hydrolyzed to 5(S),12(R)-dihydroxy-6,8,10,14-eicosatetraenoic acid (LTB_4) or conjugated with glutathione to form LTC_4, LTD_4 and LTE_4.

In the skin, 5- and 15-HETE as well as traces of LTB_4 have been detected (Hammarstrom *et al.*, 1975; Kragballe *et al.*, 1986; Cameron *et al.*, 1990).

A. 5-HETE   B. 8-HETE   C. 9-HETE

D. 11-HETE   E. 15-HETE   F. LTB₄
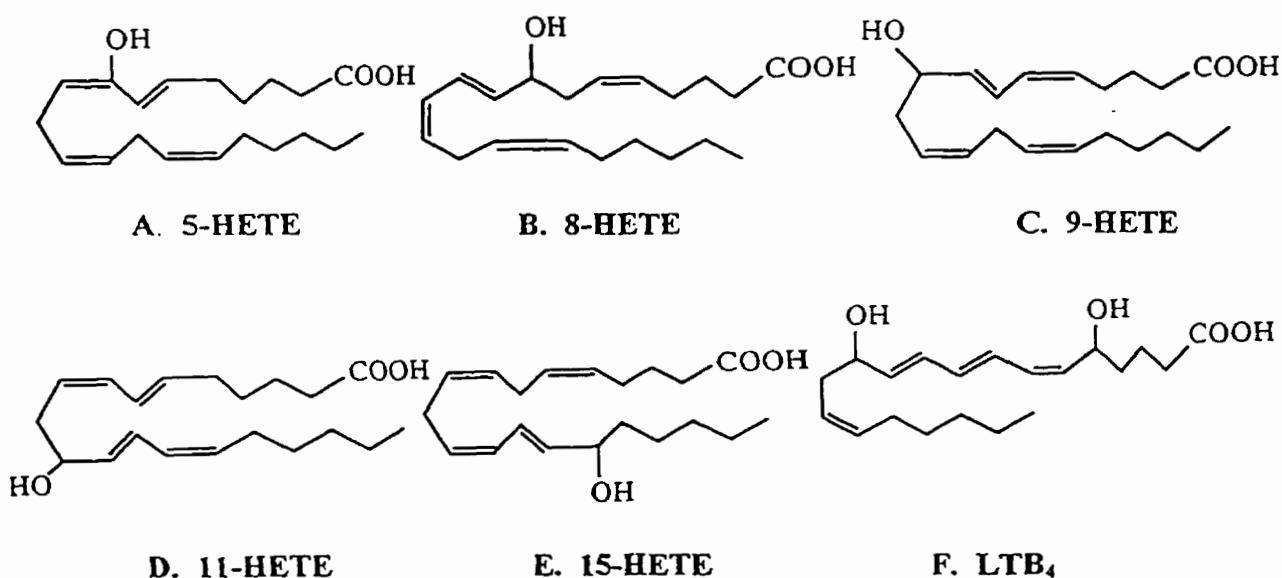
Figure 1-7. Lipoxygenase compounds.

1.3.3 12-lipoxygenase compounds

12-lipoxygenase catalyzes the incorporation of one oxygen molecule into AA to yield 12-hydroperoxyeicosatetraenoic (12-HPETE) acid. This compound serves as the precursor to 12-HETE and hepoxilins.

12-HETE

Reduction of 12-HPETE to its monohydroxy analogue 12-HETE (Figure 1-8) has been attributed to a peroxidase activity associated with 12-lipoxygenase. In the skin, human keratinocytes possess a high capacity to transform AA to 12-HETE (Hammarstrom *et al.*, 1979; Ruzicka *et al.*, 1983; Gschwendt *et al.*, 1986; Nugteren and Kiviti, 1987).
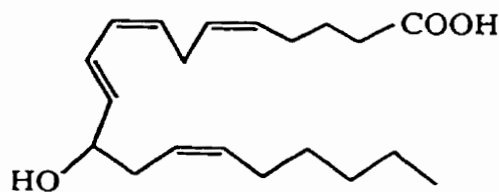
Figure 1-8.   12-HETE

Hepoxilins

Recently, a new class of 12-lipoxygenase compounds called hepoxilins (Pace-Asciak and Martin, 1984), has been reported. Hepoxilins are monohydroxyepoxide products formed by brain (Pace-Asciak, 1988; Reynaud *et al.*, 1994a; Reynaud *et al.*, 1994b), blood vessels (Laneuville *et al.*, 1991a), human neutrophils (Reynaud *et al.*, 1995) and pancreatic islets (Pace-Asciak *et al.*, 1985). Hepoxilin formation is carried out by a specific heat-labile protein (hepoxilin A_3 synthase) which catalyzes the transformation of 12(S)-HPETE (Pace-Asciak *et al.*, 1983; Reynaud *et al.*, 1994b) to mostly hepoxilin A_3 (Figure 1-9A) and minor amounts of hepoxilin B_3 (Figure 1-9B) (Pace-Asciak *et al.*, 1993).
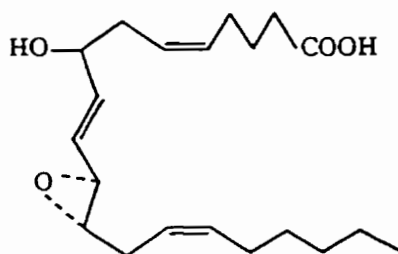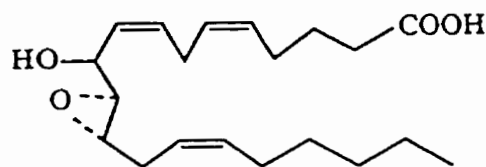
A. Hepoxilin A_3   **B. Hepoxilin B_3**

Figure 1-9. Naturally occurring hepoxilins.
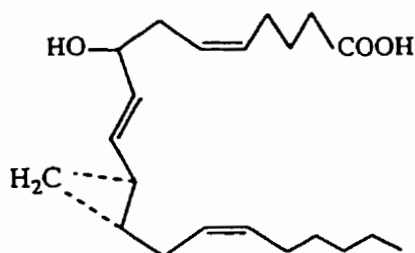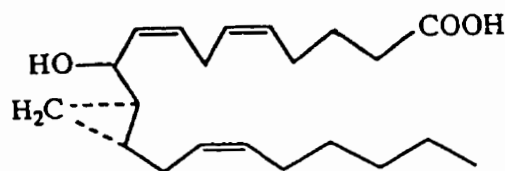
A. Hepoxilin ΔA_3   **B. Hepoxilin ΔB_3**

Figure 1-10. Chemically synthesized hepoxilin analogs

1.4 RATIONALE AND OBJECTIVES

Over the years, the lipoxygenase pathway has garnered considerable attention. LTB_4 has been shown to be a potent chemotactic agent both *in vivo* and *in vitro* (Bray *et al.*, 1980; Ford-Hutchinson *et al.*, 1980; Smith *et al.*, 1980; Bhattacherjee *et al.*, 1981; Carr *et al.*, 1981), while LTC_4, LTD_4 and LTE_4 comprise the components of slow-reacting substances of anaphylaxis (Kellaway and Trethewie, 1940). Other compounds such as 15-HETE participate in regulatory interactions between various lipoxygenase pathways (Vanderhoek *et al.*, 1982a; Vanderhoek *et al.*, 1982b) while conjugated triene diols, also derived from 15-lipoxygenase, have been reported to exert chemotactic activity on human neutrophils (Shak *et al.*, 1983).

In lieu of the fact that lipoxygenase compounds have been shown to mediate an array of inflammatory reactions, one of our first objectives was to determine if recently discovered hepoxilins (HxA_3 and HxB_3) and their synthetic structural analogs (Figure 1-10, $Hx\Delta A_3$ and $Hx\Delta B_3$) could also contribute to the condition. We have adopted a classical method of examining acute inflammation by testing the effects of these compounds on vascular permeability in the rat skin, alone and in combination with BK and PAF and comparing it to the effects of 12-HETE.

Our second objective involved implementing and expanding the use of a fluorescence labeling system to detect and quantitate production of lipoxygenase compounds, as a way to elucidate the mechanism of action of these compounds and of that of BK and PAF.

The results of these studies may provide insight into the pathophysiology of common inflammatory skin diseases such as psoriasis which have been shown to contain elevated levels of AA and lipoxygenase products (Hammarstrom *et al.*, 1975; Hammarstrom *et al.*, 1979). This better understanding may lead to the development of improved therapies.

SECTION TWO: MATERIALS AND METHODS

2.1 *IN VIVO* VASCULAR PERMEABILITY PROTOCOL

A schematic representation of this section (2.1) is illustrated in Figure 2-1.

2.1.1 Materials

The solutes used for the Krebs' buffer (NaCl, D-(+)glucose, $NaHCO_3$, KCl, KH_2PO_4, $MgSO_4$, $CaCl_2$), Evans blue dye, bradykinin (acetate salt) and platelet-activating factor were purchased from Sigma Chemical Co. (St. Louis, MO). Standard racemic 12-HETE and 12-HPETE were obtained from Cayman Chemical Co. (Ann Arbor, MI). The double distilled (DDH_2O) solvent was distilled water filtered on a Barnstead/Thermolyne HN Ultrapure cartridge (Dubuque, IO). Ethanol was obtained from The Hospital for Sick Children Stores (Toronto, ON), dried over Mg/I_2, distilled and used to dissolve hepoxilins, 12-HETE, 12-HPETE and PAF. The formamide (analytical grade) used for extraction of Evans blue from the tissue and as solvent for the standard curve was obtained from BDH (Toronto, ON). Nitrogen gas for drying samples came from Praxair Inc. (Brampton, ON).

2.1.2 Animal preparation and surgery

Male Wistar rats (170-220g, Charles River Ltd., St. Constant, Quebec) were anaesthetized with Inactin (100mg/kg, i.p., BYK-Gulden, Constanz, Germany) and their dorsal skin shaved with a clipper (Oster Model 23) and cleansed with EtOH. The trachea and left jugular vein were cannulated (PE-200, PE-50, University of Toronto Stores) for respiration and fluid administration respectively. Body temperature was maintained at 37°C by placing animals on a thermostatically controlled heating box.

2.1.3 Plasma protein extravasation

Changes in vascular permeability were based on the leakage of plasma protein-bound dye into the extravascular compartment of the skin (Udaka *et al.*, 1970; Laneuville *et al.*, 1991b) Thirty-five mg/kg of Evans blue was administered intravenously 5 minutes prior to skin injections. The methyl ester forms of the hepoxilins were supplied by Dr. Peter Demin in our laboratory, as previously described (Demin *et al.*, 1994). Hepoxilins were dissolved in EtOH and aliquots were added to Krebs' vehicle (in mM: 118 NaCl, 11 glucose, 25 $NaHCO_3$, 4.62 KCl, 1.2 KH_2PO_4, 1.2 $MgSO_4$, 2.5 $CaCl_2$) to make an injection volume of 100µL. Similarly, BK, PAF, 12-HETE and 12-HPETE were diluted with Krebs' and appropriate amounts of EtOH were added such that all 100µL injections contained no more than 3%EtOH. It had been observed that EtOH increased vascular permeability in a dose-dependent manner (data not shown) but at the 3%EtOH level, these effects were negligible.

male Wistar rats

shave, cannulate, administer Evans blue (i.v.),
inject (i.d.) test compounds into selected skin sites

decapitate, excise skin patches containing
injection site, weigh, incubate in formamide
for 18hrs, 65°C

centrifuge 500g for 5 minutes

read spectrophotometrically at 620 nm

plot standards and calculate

OD @ 620nm

Evans Blue (μg)
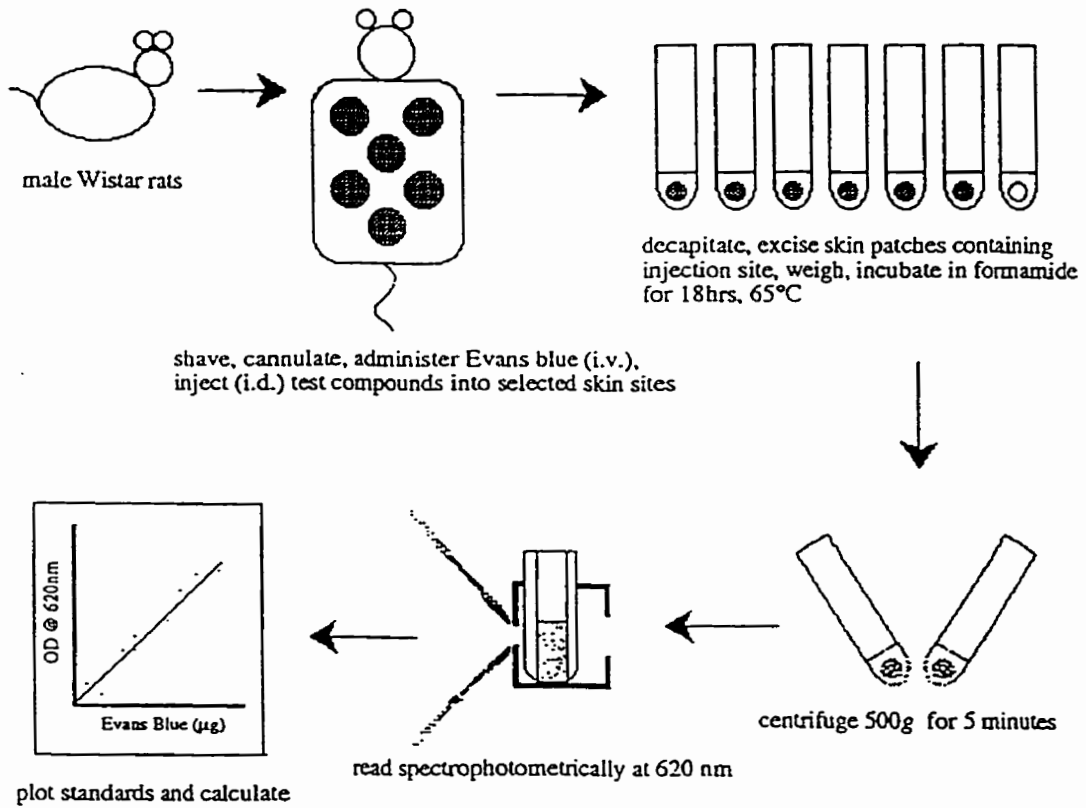
Figure 2-1. **Vascular permeability measurements (*in vivo*).**

In random order, the hepoxilins (40ng), 12-HETE (40ng), 12-HPETE (40ng), BK (1-500ng) or PAF (1-20ng) and Krebs' were injected intradermally (see below for detailed description of injection technique) using 30 1/2 GA needles (Becton Dickinson & Co.) into six positions in the dorsal skin according to the pattern in Figure 2-1, with rotation of injection sites between animals to avoid bias due to difference among sites. Dye leakage was localized within the area of the injection site such that cross-contamination with other sites were minimized.

Intradermal injection technique (Figure 2-2): A 1cm flap of dorsal skin was raised with thumb and index finger. The needle pierced the upper portion of the raised skin at an angle of 180° (i.e. parallel) to the dorsal skin and was pushed further until it was past the bevel (see inset). The contents of the syringe were slowly injected (100μL in 10 seconds). A slight resistance could be felt during the injection, indicative of an intradermal versus a subcutaneous injection. The resulting 'bulge' spanned 1cm and gradually subsided during the 30 minutes incubation time *in vivo*.
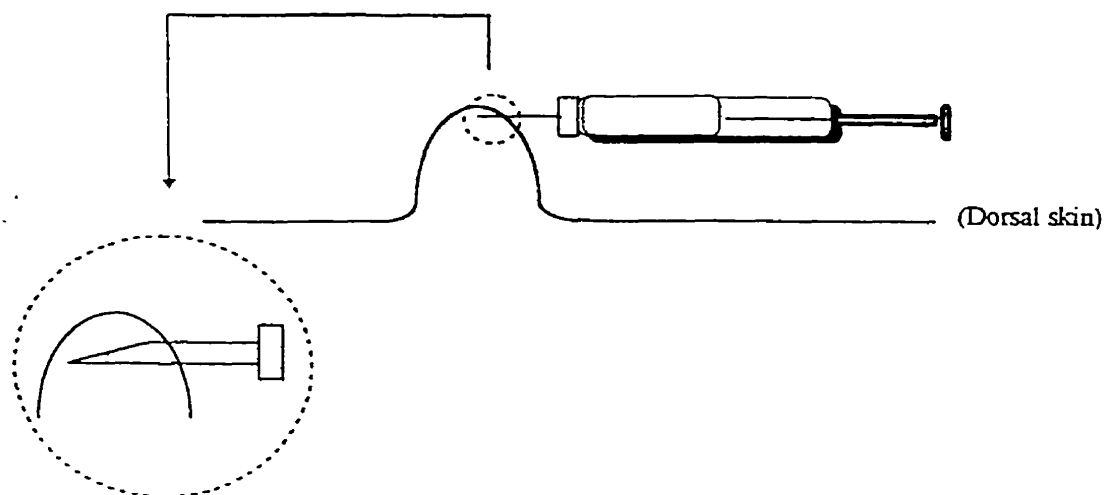
Figure 2-2. Intradermal injection technique. The needle was pushed into the skin until the bevel was no longer seen (*inset.*).

After 30 minutes, the animals were decapitated. Circular patches of skin (diameter 1.5 cm) containing the injection site were excised with a metal puncher, weighed, and incubated in 3mL of formamide at 70°C. An additional, untreated patch of skin was collected and used as a measure of background. After 18 hours, the vials were centrifuged (Sorvall GLC-1) for 5 minutes at 500g, the supernatant removed, placed in a glass cuvette and the colour read spectrophotometrically (Beckman D-65) at 620nm.

2.1.4 Statistics

The amount of plasma protein leakage is expressed as mean$\pm$SEM of 8-12 samples. Student's t-test (for paired samples) was performed to compare the colour intensity of BK (or PAF) + test compounds (Hx, 12-HETE or 12-HPETE) to BK (or PAF) alone, and of BK, PAF or test compounds to Krebs' vehicle. Results were considered significant at the 0.05 level.

2.2 FLUORESCENT LABELING OF LIPOXYGENASE COMPOUNDS WITH ADAM

2.2.1 Materials

Authentic 12-HETE and LTB$_4$ were purchased from Cayman Chemical Co. (Ann Arbor, MI). Ricinoleic acid and silicic acid were obtained from Sigma Chemical Co. (St. Louis, MO) A HETE mixture containing 5-, 8-, 9-, 11-, 12-, and 15-HETEs was synthesized previously by photooxidation of arachidonic acid and purified through HPLC. Integrity of the HETE mixture was obtained by TLC using EtOAc/acetic acid (99/1 v/v) as a developing system. Radiolabelled [^{14}C]12-HETE (without antioxidants, specific activity 54mCi/mmol) was purchased from Amersham (Oakville, ON). All standards were dissolved in EtOH with the exception of [^{14}C]12-HETE which came in toluene solution. ADAM (9-anthryldiazomethane) was obtained from Research Organics Inc. (Cleveland, OH). All chemicals were stored in a -20°C freezer until ready for use.

Solvents used for silicic acid column chromatography and HPLC (MeOH, EtOAc and hexane) were of analytical and/or HPLC grade and were obtained from Caledon (Georgetown, ON).

2.2.2 Derivatization

Derivatization of LTB$_4$, HETEs and ricinoleic acid with 9-anthryldiazomethane (ADAM) produced fluorescent esters (refer to section 4.1.1 for details). The process was performed as followed. The mixture of standards was taken to dryness with a gentle stream of nitrogen. ADAM (50μg/mL) was dissolved in EtOAc. 2mL of the ADAM-EtOAc solution was added to the dried sample. The reaction mixture was wrapped in aluminum foil and stirred continuously for one hour using a one-piece molded Alnico V permanent magnet (VWR) in darkness. After the reaction was complete, the magnet was removed and washed with 1mL of EtOAc. Finally the sample was taken to dryness and redissolved in 1mL of hexane.

2.2.3 Silicic acid column chromatography

Silicic acid chromatography was performed in 5mm diameter glass columns packed with a small piece of glass wool (Pyrex fibre glass Sliver 8μm, Corning Glassworks) and 0.4g of silicic acid (mesh size -325) dissolved in MeOH. The column was washed twice with MeOH and five times with hexane prior to use. Four fractions of the sample were collected in the following order: i) 5mL hexane: to elute non-polar compounds ii) 10mL EtOAc/hexane, 3/97 (v/v): to elute yellow ADAM reagent iii) 5mL EtOAc/hexane, 50/50 (v/v): to elute mono- and dihydroxy acids and iv) 5mL EtOAc: to elute all remaining polar compounds. Nitrogen gas was used to assist the eluents through at a pace of 45-50 drops/minute. All work in this section was done using siliconized (0.5% Aquasil, Pierce) glassware.

2.2.4 Reverse-phase high-pressure liquid chromatography (RP-HPLC)

RP-HPLC was performed on a column (3.9mm x 300mm Nova-Pak C18 packed with 4mm spherical silica-based particles) purchased from Waters. ADAM derivatized compounds were monitored using a Kratos FS-950 fluorescent detector (excitation$\geq$254nm and emission$\geq$400nm) and a Waters Lambda-Max Model 480 LC ultraviolet (λ=235nm) spectrophotometer. The signal was monitored on a Macintosh computer using NewDynamax HPLC Method Manager v.1.1 software. The mobile phase consisted of a mixture containing ACN/DDH$_2$O, 75/25 (v/v). Analyses were performed at a solvent rate of 1.4mL/min [2700psi] and 25°C. Derivatized samples and authentic ADAM standards were taken to dryness and injected in 200μL of HPLC solvent.

The areas of the peaks on the chromatograms were calculated and compared to that observed for ricinoleic acid internal standard.

2.3 APPLYING THE ADAM PROTOCOL TO AN *IN VITRO* PREPARATION

2.3.1 Materials

The solutes used to prepare the different buffers (NaCl, Na$_2$HPO$_4$, KCl, KH$_2$PO$_4$), BK, PAF, trypsin (type III, from bovine pancreas, dialyzed and lyophilized essentially salt-free), tris(hydromethyl)aminomethane hydrochloride (Tris-HCl), bovine serum albumin (BSA), leupeptin, ethylenediaminetetraacetic acid (EDTA) and NaOH were all purchased from Sigma Chemical Co. (St. Louis, MO). HCl (reagent grade) was obtained from Caledon (Georgetown, ON). All other chemicals have been cited elsewhere.

male Wistar rat (350g),
decapitate, shave

excise circular patches of skin
with metal puncher

cut into 1.0x0.3 cm strips

float in 0.25% trypsin in D-PBS at
4°C overnight (dermis side down)

place epidermal sheets in D-PBS for 20 minutes

peel epidermis from
dermis with fine forceps

filter cells through 118μm
nylon mesh discard filtrate

divide cells into
two tubes each
containing 4mL
Tris-HCl/EDTA
and 20μM
leupeptin

homogenize 10s and ice for 30s

aliquot 300μg
into eppendorf
tubes and freeze
at -20°C

centrifuge at 10000g , 4°C

combine supernatants and measure protein content

Figure 2-3. Epidermal lipoxygenase preparation.

2.3.2 Epidermal enzyme preparation

A schematic representation of this section (2.3.2) is illustrated in Figure 2-3.

Animal Preparation

Male Wistar rats (350g) were killed by decapitation using a guillotine. The dorsal skin was shaved with clippers (Oster Model 23) and then depiled using liquid soap (Huntington Wash) and a clean single edge blade (University of Toronto Stores). The soap was rinsed with DDH_2O and the area was cleansed with EtOH and allowed to dry.

Buffer preparation

The trypsin incubation buffer followed Gibco's formulation (Base catalogue no. 21300) for Dulbecco's phosphate buffered saline (D-PBS in mM: 136.89 NaCl, 9.58 Na_2HPO_4, 2.68 KCl, 1.47 KH_2PO_4, pH 7.1). The Tris-HCl/EDTA homogenization buffer contained 100mM Tris-HCl and 1mM EDTA, pH 8. Buffers were prepared fresh each day (with DDH_2O at room temperature) and placed on ice prior to their use.

Epidermal enzyme preparation

The dorsal skin was removed and circular patches of skin (1.5cm diameter) were cut using a metal puncher. Approximately 20-25 patches could be obtained per rat with each patch having a wet weight of about 0.36g. The patches were further cut into 1cm x 0.3cm strips and floated, dermis-side down, in Petri dishes (Becton Dickson Labware, 100mm x 20mm) containing trypsin solution (0.25% w/v in D-PBS) at 4°C overnight.

The next morning, in a dry dish the epidermis (thin yellow film) was peeled from the dermis (thick white tissue) using fine forceps and transferred into cold D-PBS for 20 minutes to dilute traces of trypsin. Identification of the desired layer was confirmed histologically using hematoxylin/eosin staining of 10% formalin-fixed skin pieces (Hospital for Sick Children, histology department, Figure 2-4). The dermis surface was scraped 10 times with medium force using a single edge blade to remove basal rich epidermal cells. This mixture was filtered using a nylon screen mesh (Nitex 118µm, Thompson Co. Ltd.) and the filtrate discarded. The cells were divided into two 50mL plastic tubes and 4mL of Tris-HCl/EDTA homogenization buffer with 20µM of leupeptin were added to each tube and placed on ice.

The polytron homogenizer (Brinkman) was rinsed with Tris-HCl/EDTA buffer and wiped dry prior to use. Each tube was homogenized twice at setting speed #3 for 10 seconds and placed on ice for 30 seconds. The resulting homogenate was cream-coloured and possessed a smooth texture. Next, the tubes were centrifuged (Beckman Model J2-21, JA-20 rotor) at 10 000g for 20 minutes at 4°C. Finally, the supernatants were combined into a 15mL Falcon tube using plastic transfer pipettes (Fisher Scientific) and placed on ice.
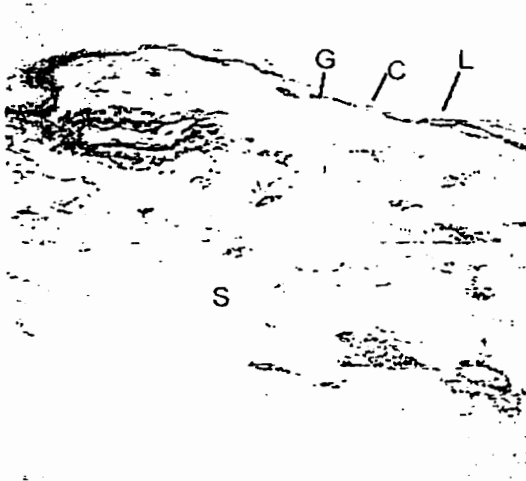
Figure 2-4A. Epidermal layer. Photograph of the hematoxylin/eosin staining of peeled epidermis after whole rat skin sections were incubated overnight in 0.25% trypsin solution. Note the four outer most strata:

C - corneum

L - lucidum

G - granulosum

S - spinosum

Magnification x12.5.
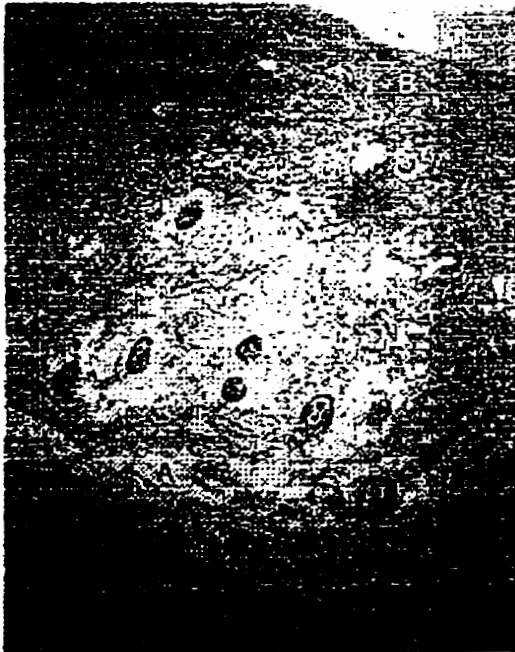
Figure 2-4B. Dermal and subcutaneous layers. Photograph of the hematoxylin/eosin staining of peeled dermis and subcutis after whole rat skin sections were incubated overnight in 0.25% trypsin solution. Note that the stratum basale (B) of the epidermis remains attached to the papillary layer (P) of the dermis. There is also an abundance of adipose cells (A) in the subcutis.

Magnification x5.

Bio-Rad protein assay (Bio-Rad) was performed on a 200μL aliquot of preparation using BSA as standard. Once protein amount was determined, 300μg aliquots of the protein solution were put into 1.5mL eppendorf tubes and were stored at -20°C. This amount was comparable to the amount of protein in one skin patch *in vivo*.

2.3.3 Incubation and extraction

A schematic representation of this section (2.3.3) is illustrated in Figure 2-5.

A 1mL volume of Tris-HCl/EDTA containing 300μg of enzyme was incubated for 60 minutes at 37°C with vigorous shaking (setting #15 using Blue M Electric Co. waterbath) with various amounts of AA (1μg), BK (1, 10, 50, 100ng) and PAF (0.5, 1, 5, 10ng) dissolved in 10μL EtOH. Lipoxygenase compounds were recovered by acidifying the buffer to pH3 with 1N HCl and extracting 3 times with 2mL EtOAc. Each EtOAc fraction was washed with DDH_2O and combined. The internal standard, the free-acid form of ricinoleic acid, was added immediately following incubation (100ng in 10μL EtOH) and extracted with the lipoxygenase compounds as described.

The sample was purified through silicic acid column chromatography (refer to 2.2.2) and was analyzed on RP-HPLC (refer to 2.2.3) as previously described.

2.3.4 Statistics

Lipoxygenase production is expressed as mean±SD of 3 samples. The areas of the peaks on the chromatograms were calculated and compared to that observed for ricinoleic acid. Dose-response curves were subjected to a one-way ANOVA and then each dose was compared to the EtOH control using a Student's *t*-test. Results were considered significant at the 0.05 level.

2.4 APPLYING THE ADAM PROTOCOL TO AN *IN VIVO* PREPARATION

Similar preparatory and injection techniques as the *in vivo* vascular permeability section were used here, with the exception of Evans blue administration. Refer to section 2.1 for further details.

2.4.1 Materials

Components of the Krebs' vehicle, BK and PAF were purchased from Sigma Chemical Co. (St. Louis, MO). All other chemicals have been cited elsewhere.
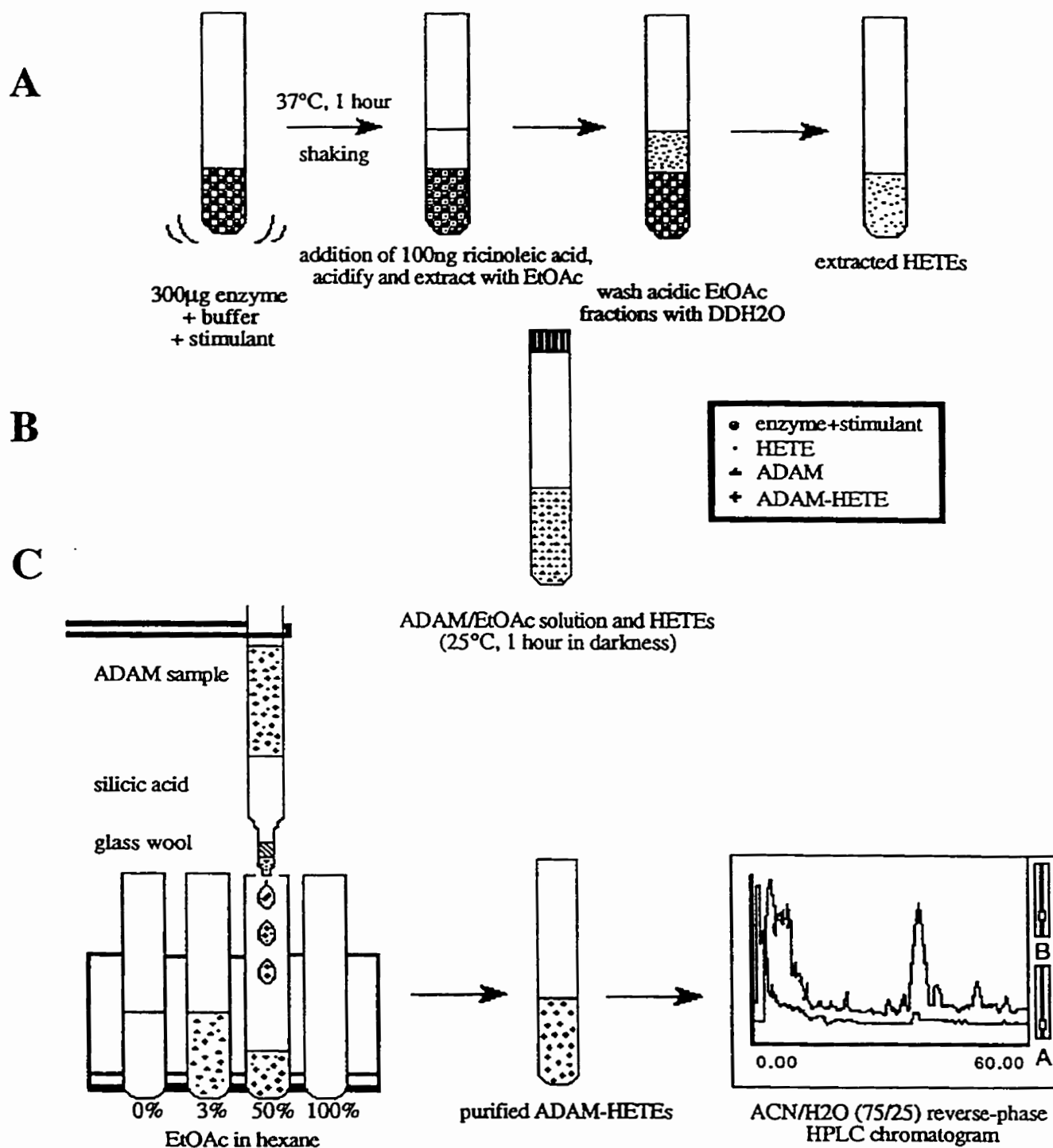
Figure 2-5. Applying ADAM protocol to an *in vitro* preparation.
A) Stimulation and extraction of lipoxygenase compounds. B) Derivatization
with ADAM. C) Silicic acid column purification and analysis on HPLC.

2.4.2 Animal preparation

Male Wistar rats (230-280g) were anaesthetized with Inactin (100mg/kg, i.p.). The dorsal skins were shaved with an electric clipper and cleansed with EtOH. Body temperature was maintained at 37°C by placing animals on a thermostatically controlled heating box.

2.4.3 Intradermal injection

BK and PAF were diluted with Krebs' vehicle (in mM: 118 NaCl, 11 glucose, 25 NaHCO$_3$, 4.62 KCl, 1.2 KH$_2$PO$_4$, 1.2 MgSO$_4$, 2.5CaCl$_2$). EtOH was added such that each 100µL injection contained 3%EtOH. In random order, BK, PAF and Krebs' were injected intradermally using 30 1/2 GA needles into 3 areas of the dorsal skin.

After 30 minutes, the animal were decapitated and the dorsal skin removed. Circular patches of skin were excised at the injection site using a metal puncher and each patch was scraped of its dermal layer using a clean single edge blade.

2.4.4 Extraction procedures

Each tissue scraping was placed in 4mL EtOAc on ice. The sample was homogenized with a polytron (Brinkman) for 20 seconds. Residual tissue adhering to the homogenizer was washed with an additional 1mL of EtOAc. The sample was centrifuged at 500g for 15 minutes and the supernatant was transferred into another tube. 1mL of DDH$_2$O was added and acidified to pH3 with 1N HCl. The acidified EtOAc layers were extracted into a second tube and washed neutral with DDH$_2$O and finally transferred to a third tube. This process was repeated twice with 2mL of fresh EtOAc each time. 100ng of ricinoleic acid was added prior to the acidification step.

The extracted EtOAc layers were combined and taken to dryness with nitrogen and derivatized into ADAM esters as previously described. The sample was purified through silicic acid column as before and the 50%EtOAc/hexane fraction was analyzed on RP-HPLC.

2.4.5 Statistics

Lipoxygenase production is expressed as mean±SD of 3 samples. The areas of the peaks on the chromatograms were calculated and compared to that observed for ricinoleic acid. A one-way ANOVA was used to determine statistical significance among the Krebs' control, BK and PAF samples, and a further comparison between the Krebs' control and BK (or PAF) was performed using a Student's t-test. Results were considered significant at the 0.05 level.

SECTION THREE: RESULTS

3.1 THE EFFECTS OF 12-LIPOXYGENASE PRODUCTS ON VASCULAR PERMEABILITY

3.1.1 Direct-acting mediators: bradykinin and platelet-activating factor

Figures 3-1A and 3-1C show the dose-dependent responses of BK and PAF respectively. 50ng of BK and 5ng of PAF represented the mid-range doses from which possible potentiating or inhibiting effects could be detected. There was no significant difference between the amount of dye leakage exhibited by BK and PAF at these threshold levels. For all compounds tested, 50ng BK and 5ng PAF were significantly higher than Krebs' control. Figure 3-1B illustrates the time-course of BK-induced permeability. Plasma protein leakage was maximum at 30 minutes. All subsequent *in vivo* experiments were performed at this time point. A dose of 40ng was selected as the threshold dose for the hepoxilins, 12-HETE and 12-HPETE. Doses lower than this did not demonstrate reproducible results with BK (data not shown).

3.1.2 12-HPETE and 12-HETE

The effects of 12-HPETE, the intermediate of 12-lipoxygenase action on AA, and 12-HETE are shown in Figures 3-2A and 3-2B respectively. On their own, both 12-HPETE and 12-HETE produced an increase in vascular permeability over Krebs' (12-HPETE: +286% and 12-HETE: +214%, $p \leq 0.05$) but neither had any additionally significant effects over the BK-induced vascular permeability.

3.1.3 Naturally occurring hepoxilins: HxA₃ and HxB₃

On their own, the naturally occurring hepoxilins displayed no significant effects over Krebs'. Of the two epimer forms, only a combined injection of HxA₃(8R) with BK was significantly higher than with BK alone (Figure 3-3A: +160%, $p \leq 0.05$). When combined with PAF, neither forms of HxA₃ had any additional effects on leakage (Figure 3-4).

A combined injection of HxB₃ with BK demonstrated an increase in dye leakage over that induced by BK alone (Figure 3-3B: +176%, $p \leq 0.005$). This increase was stereospecific in that only HxB₃(10R) was active (Figure 3-3B). Similarly, a combined injection of HxB₃(10R) with PAF demonstrated an increase over PAF effects alone (Figure 3-4B: +150%, $p \leq 0.005$).

The difference between the potentiation of the BK effects by HxA₃(8R) and HxB₃(10R) as shown in Figures 3-3A and 3-3B was not statistically significant.

A
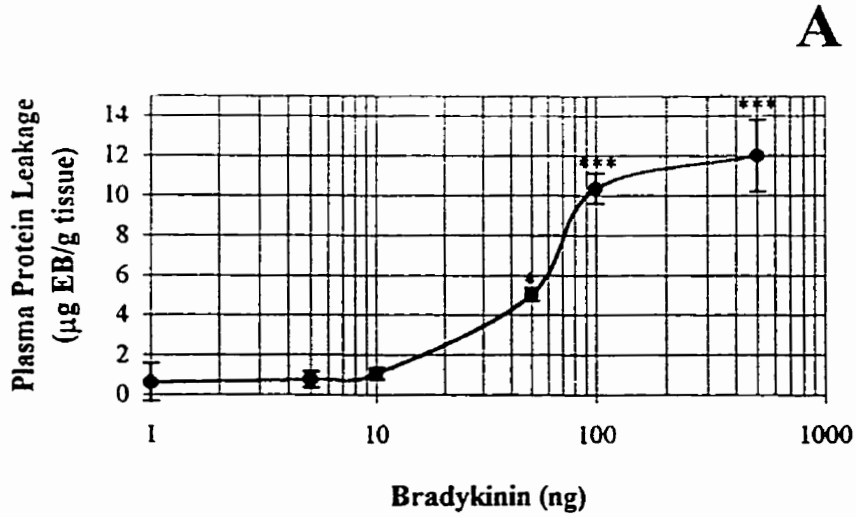
Figure 3-1A. Dose-dependent effects of BK. Plasma protein leakage induced by 100μL intradermal injections. Mid-range dose is 50ng. (*p<0.05, ***p<0.0005 vs Krebs'). n=8 for each point.

B

Figure 3-1B. Time-dependent effects of BK. Plasma protein leakage induced by 50ng BK. Subsequent experiments performed at 30 minute level. n=8 for each point.

C
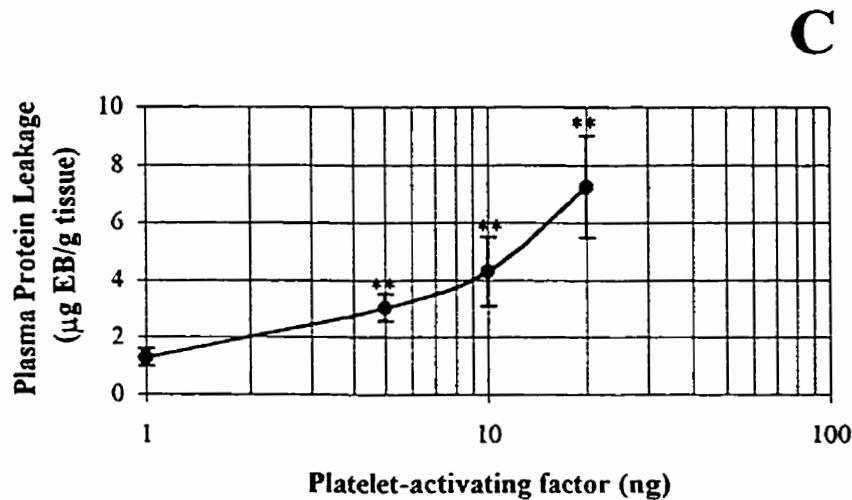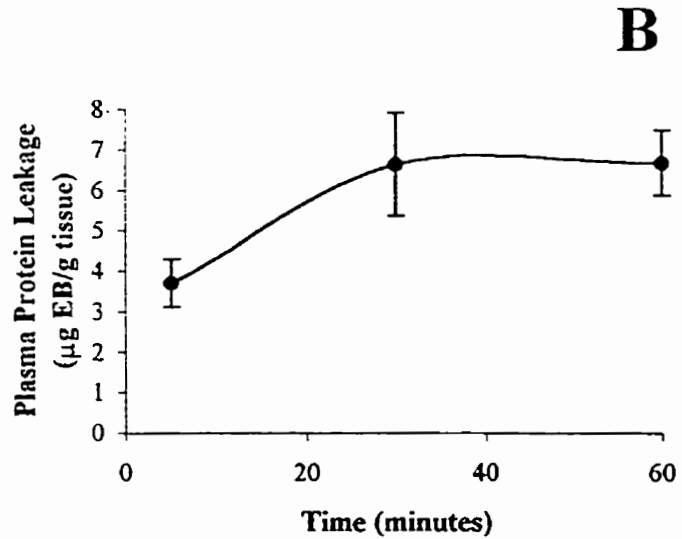
Figure 3-1C. Dose-dependent effects of PAF. Plasma protein leakage induced by 100μL intradermal injections. Mid-range dose is 5ng. Leakage not significantly different from BK threshold dose. (**p<0.005 vs Krebs'). n=8 for each point.
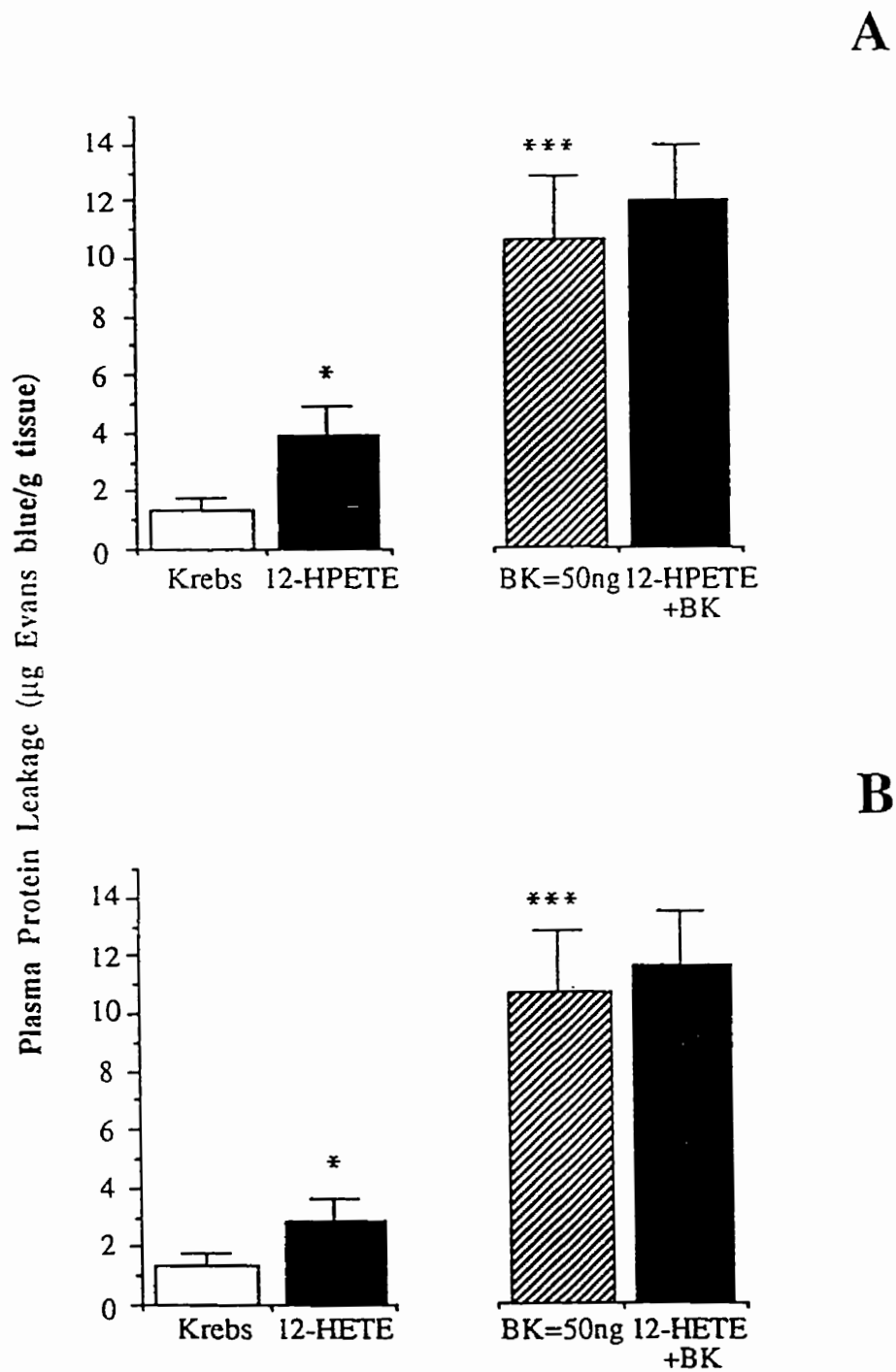
Figure 3-2. The vascular permeability effects of 100μL intradermal injections of (A) 12-HPETE and (B) 12-HETE; alone (40ng) and in combination with bradykinin. Each point represents mean±SEM of 8 samples. (*p≤0.05, ***p≤0.0005 vs Krebs).
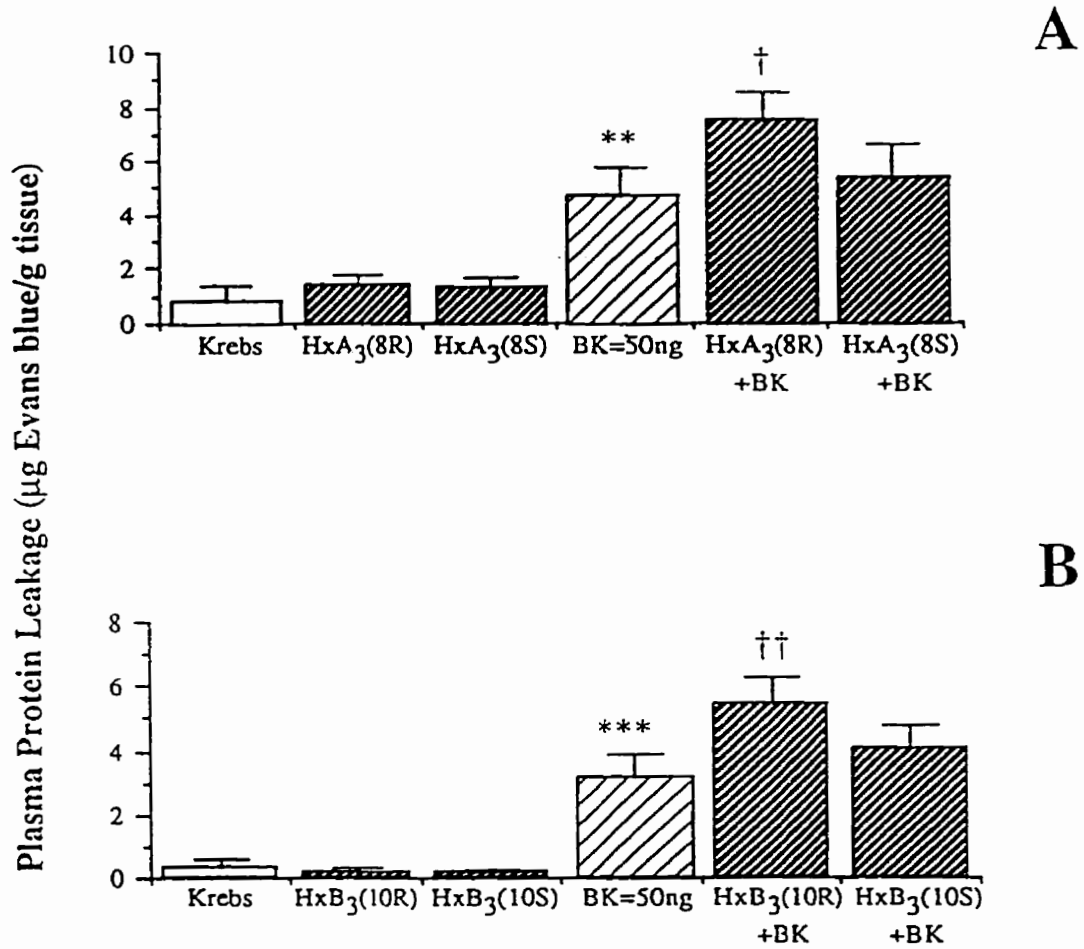
Figure 3-3. The vascular permeability effects of 100μL intradermal injections of (A) hepoxilin A_3 and (B) hepoxilin B_3; alone (40ng) and in combination with bradykinin. Each point represents mean±SEM of 12 samples. (**$p \leq 0.005$, ***$p \leq 0.0005$ vs Krebs and +$p \leq 0.05$, ++$p \leq 0.005$ vs BK).
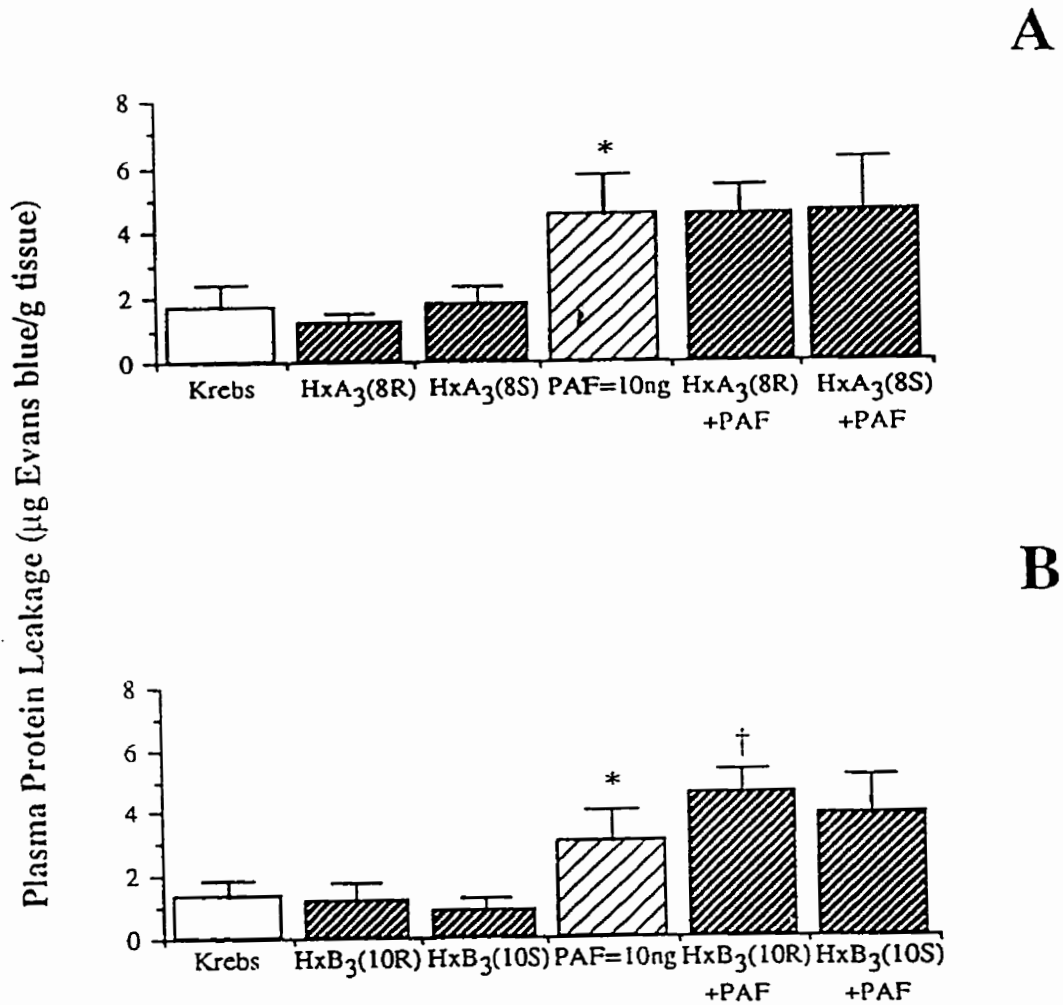
Figure 3-4. The vascular permeability effects of 100μL intradermal injections of (A) hepoxilin A₃ and (B) hepoxilin B₃; alone (40ng) and in combination with platelet-activating factor. Each point represents mean±SEM of 12 samples. (*p≤0.05 vs Krebs and +p≤0.05 vs PAF).
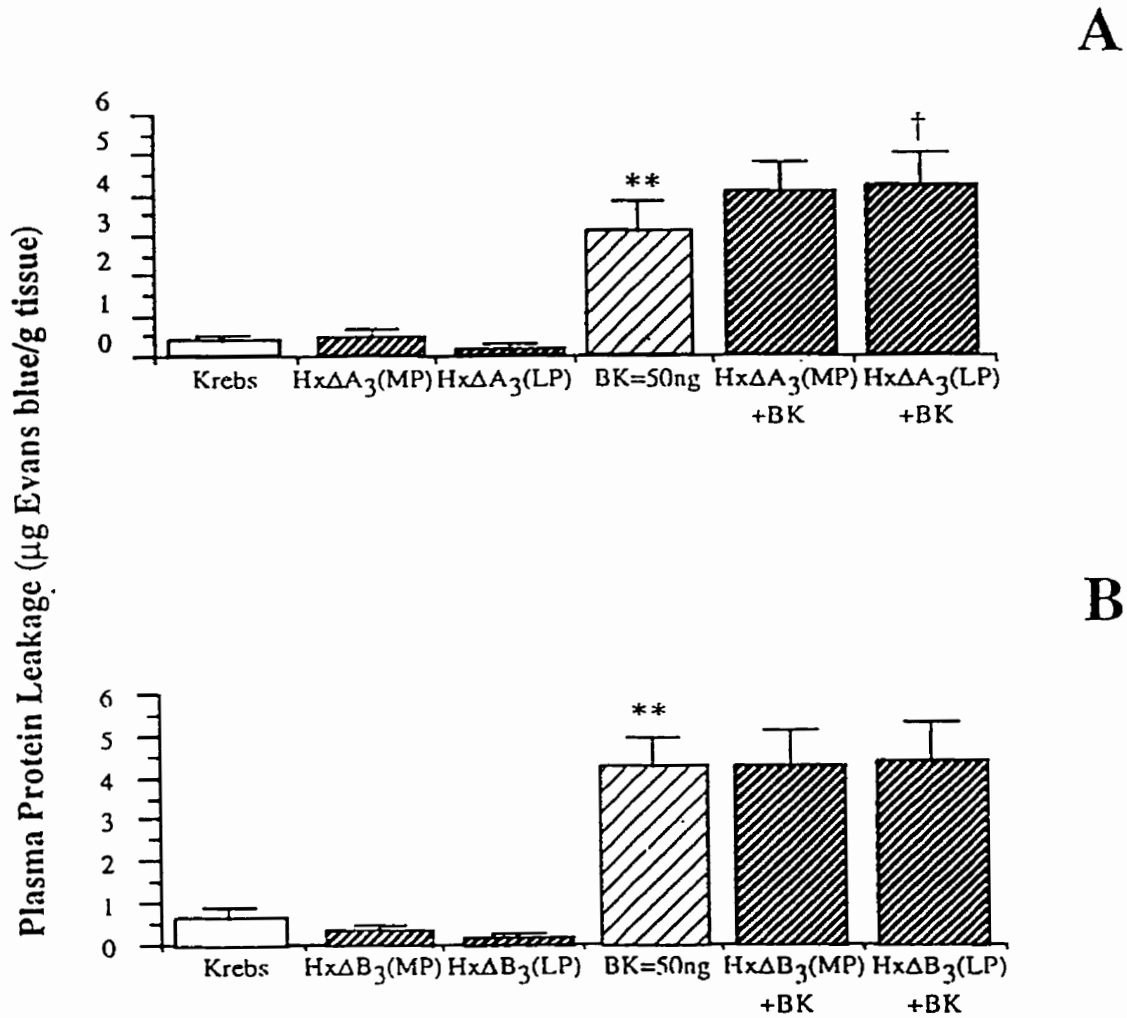
Figure 3-5. The vascular permeability effects of 100μL intradermal injections of (A) hepoxilin ΔA₃ and (B) hepoxilin ΔB₃; alone (40ng) and in combination with bradykinin. Each point represents mean±SEM of 12 samples. (**p≤0.005 vs Krebs and +p≤0.05 vs BK).

A

B

Y-axis label: Plasma Protein Leakage (μg Evans blue/g tissue)
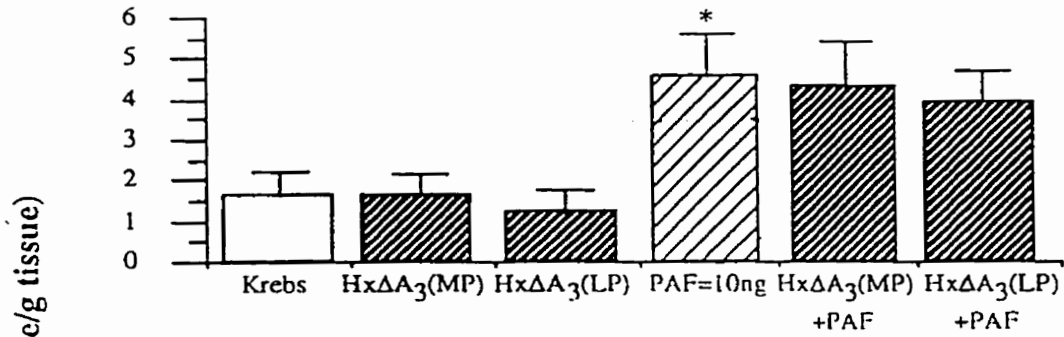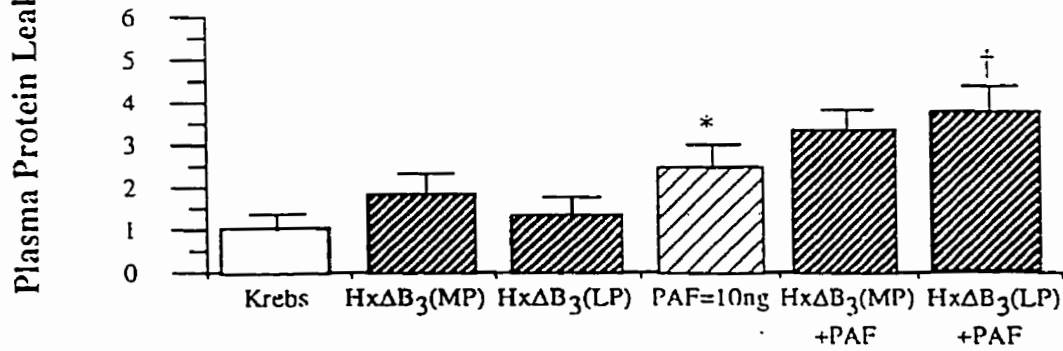
Figure 3-6. The vascular permeability effects of $100\mu L$ intradermal injections of (A) hepoxilin ΔA_3 and (B) hepoxilin ΔB_3; alone (40ng) and in combination with platelet-activating factor. Each point represents mean$\pm$SEM of 12 samples. (*$p \leq 0.05$ vs Krebs and +$p \leq 0.05$ vs PAF).

3.1.4 Synthetic hepoxilins: HxΔA$_3$ and HxΔB$_3$

On their own, the chemically synthesized hepoxilins displayed no significant effects over Krebs'. A combined injection of HxΔA$_3$(LP) with BK demonstrated an increase in leakage over that induced by BK alone (Figure 3-5A: +137%, p$\leq$0.05). Neither the MP epimer of HxΔA$_3$ nor the two epimers of HxΔB$_3$ were active when coinjected with BK. Conversely, the combined injection of HxΔB$_3$(LP) with PAF elicited an increase over PAF alone (Figure 3-6B: +149%, p$\leq$0.05). There was no difference between the degree of HxΔA$_3$(LP) effect on BK with HxΔB$_3$(LP) effect on PAF.

In summary, while HxA$_3$(8R) and HxB$_3$(10R) were capable of enhancing the BK-induced vascular permeability (the corresponding S epimers being inactive), only HxB$_3$(10R) was active in the PAF-induced studies. With the structural analogs, only the HxΔA$_3$(LP) epimer enhanced the BK effect, while the HxΔB$_3$(LP) enhanced the PAF effect.

3.2 DEVELOPMENT OF THE ADAM PROTOCOL

Radiolabelled [^{14}C]12-HETE (free-acid) was used to trace its recovery during derivatization with ADAM, purification with silicic acid column chromatography and analysis on HPLC. The internal standard (ricinoleic acid), a mixture of HETEs (15-, 12-, 11-, 9-, 8-, and 5-) and LTB$_4$ were later added to investigate their recovery through the procedure.

The red, solid crystals that characterize ADAM turned yellow upon addition of EtOAc. This yellow colour persisted throughout the derivatization process and subsequent analysis.

3.2.1 Derivatization

Concentration dependence

Figure 3-8 illustrates the concentration-dependent effects of ADAM on derivatization of 12-HETE and ricinoleic acid as measured by HPLC. A concentration of 50μg/mL, a solution of ADAM-EtOAc that possessed a visibly yellow colour, was arbitrarily chosen. Subsequent dilutions were made from this concentration.

This concentration was sufficient to derivatize >90% of the initial starting material (Figure 3-7) and was maintained for all subsequent experiments by screening the concentration spectrophotometrically (λ=400nm) prior to derivatization.

Time dependence

Figure 3-10 shows TLC analysis of the time-dependent effects of ADAM on derivatization using the concentration that would provide the best conversion of the free-acid compounds into their ADAM-derivatives (i.e. 50μg/mL). Shorter reaction times (0-30 minutes) produced
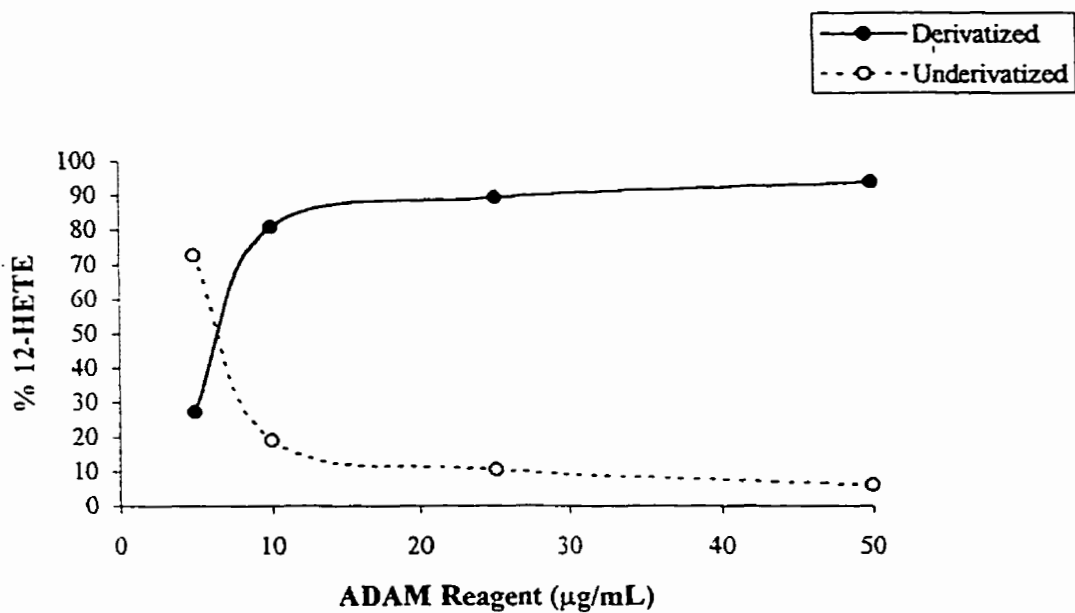
Figure 3-7. Concentration-dependent effects of ADAM reagent in derivatization. [^{14}C]12-HETE samples were derivatized with various concentrations of ADAM-EtOAc solution and purified through silicic acid column chromatography. Results demonstrate the different 50%EtOAc fractions counted for radioactivity (indicative of ADAM-12-HETE)
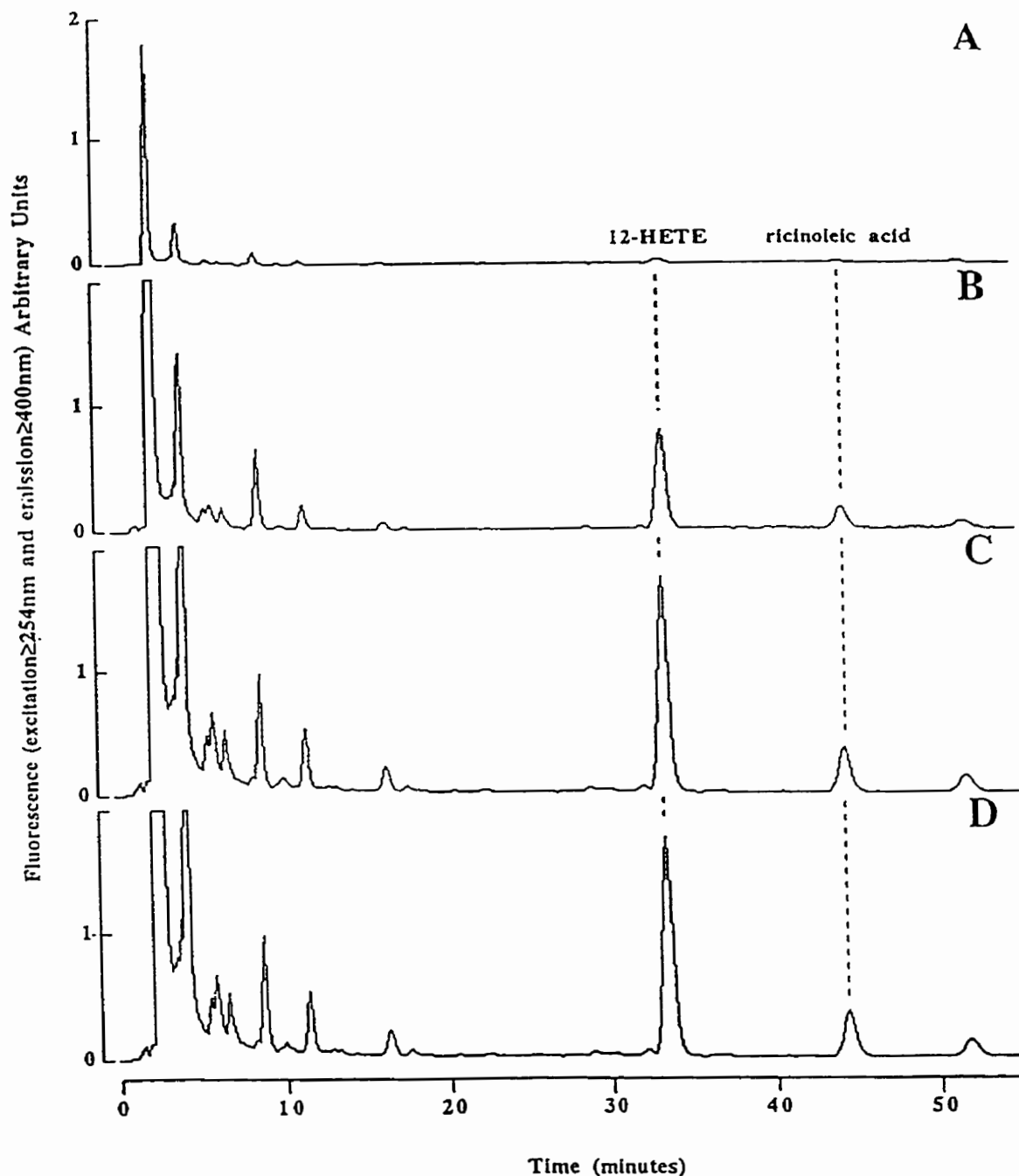
Figure 3-8. **Concentration-dependent effect of ADAM reagent in derivatization.** $[^{14}C]$12-HETE + 5μg ricinoleic acid samples were derivatized with various concentrations of ADAM-EtOAc solution and purified through silicic acid column chromatography. Chromatograms illustrate the different 50%EtOAc fractions: (A) 5μg/mL (B) 10μg/mL (C) 25μg/mL (D) 50μg/mL, analyzed on reverse-phase HPLC (75%ACN/25%H$_2$O solvent system, flow rate 1.4mL/min). The level of sensitivity of fluorescence detection for all chromatograms is the same.
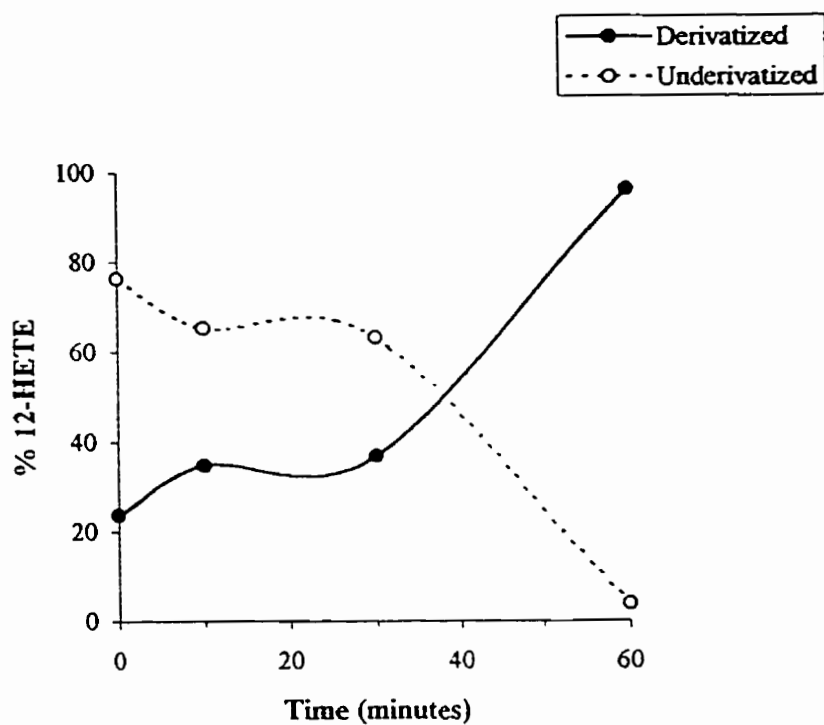
Figure 3-9. Time-dependent effects of ADAM reagent in derivatization.
[^{14}C]12-HETE samples were derivatized with 50μg/mL ADAM-EtOAc
solution. Reactions were stopped at the times indicated and samples were
spotted on TLC (100%EtOAC system, 45 minutes). Results summarize the
amount of radioactivity present at the origin and ADAM-12-HETE zones.
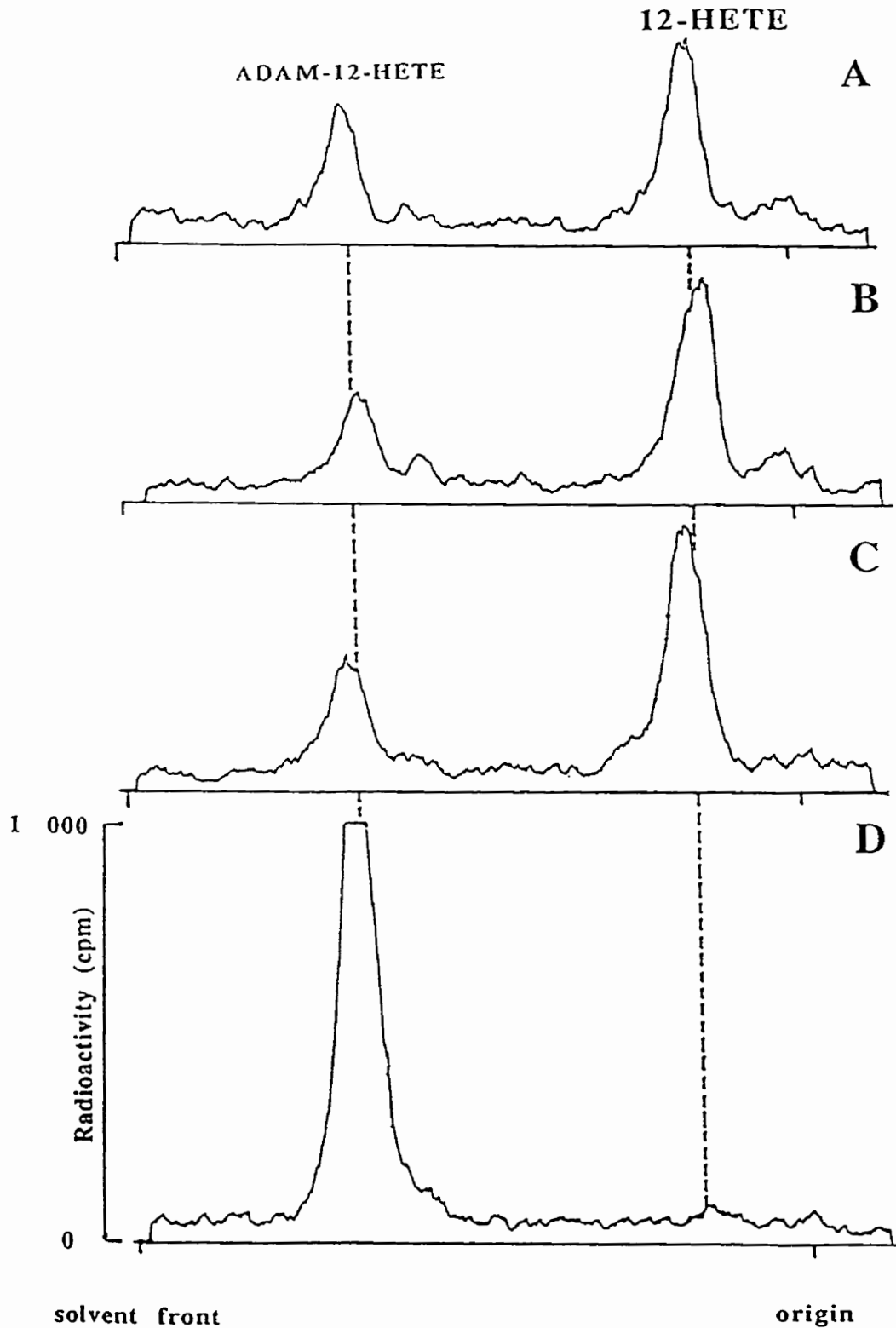
Figure 3-10. Time-dependent effects of ADAM-reagent in derivatization. TLC scans of figure 3-9 of the four time points: (A) 0 minutes (B) 10 minutes (C) 30 minutes (D) 60 minutes, prior to scraping and counting.

variability in derivatization capacity while at 60 minutes, >90% of the initial starting material was consistently derivatized (Figure 3-9). This later time point was subsequently used as the minimum reaction time for all derivatization experiments.

Note that the ADAM-12-HETE was considerably less polar than the original 12-HETE free-acid (Figures 3-10A-D).

3.2.2 Silicic acid column chromatography

Initial experiments involved derivatization with ADAM followed by direct analysis on reverse-phase (RP) HPLC. Figure 3-11 shows the effect of such a procedure on a sample of (A) ADAM reagent only and (B) 40ng 12-HETE. Note the presence of numerous large, extraneous peaks throughout the profiled range, particularly in the ADAM-trioxilin (6-8 minutes), ADAM-LTB$_4$ (10-11 minutes) and ADAM-hepoxilin (20-24 minutes) ranges. In order to extend this protocol for use in future studies, it became necessary to include a purification step to separate the yellow by-products of the ADAM reagent prior to injection on HPLC. Column chromatography using silicic acid as the packing material was chosen as an efficient way to quickly perform this task. Figure 3-12 (A and B) illustrates two similar samples after passage through silicic acid. (Note that Figures 3-11 and 3-12 have been adjusted to carry the same fluorescence sensitivity).

Establishing silicic acid column conditions

Radiolabelled 12-HETE was used to determine the conditions best suited to elute it as its ADAM-ester form from silicic acid.

Hexane served as the base solvent as it did not elute the desired ADAM-derivatives from the column. Polarity of the eluents was increased by adding increasing volumes of EtOAc to hexane. Figure 3-13A shows the effects of increasing polarity (+5%EtOAc in hexane, 1mL total v/v). Each fraction was collected, its colour noted and counted. A distinct yellow region at the lower polarity levels was observed. This colour progressively faded as the polarity increased.

The prominent peak between 5% and 20% EtOAc in Figure 3-13A, which contained >90% of the total radioactivity, was collected and re-analyzed (eluent volumes were increased to 5mL, each 1mL was collected, its colour noted and counted for radioactivity) to produce Figure 3-13B. Again there was a region (early 5%EtOAc concentration) where most of the yellow colour was eluted which contained very little radioactivity (<10%). Most of the counts (>80%) eluted just after this yellow region and a second radioactive peak accounting for 10% of the total counts can be observed at the 50%EtOAc level.

Three fractions from 3-13B: (Line A) first 2mL of 5%EtOAc, (Line B) last 3mL of 5%EtOAc + first 1mL of 15%EtOAc, and (Line C) last 4mL of 15%EtOAc were spotted on TLC (100%EtOAc solvent system for 45 minutes) and the results shown in Figure 3-14.

Since the ADAM contaminants and the radioactive counts began eluting at the 5%EtOAc level, the column was refined by lowering the concentration of the first EtOAc eluent to 3% and
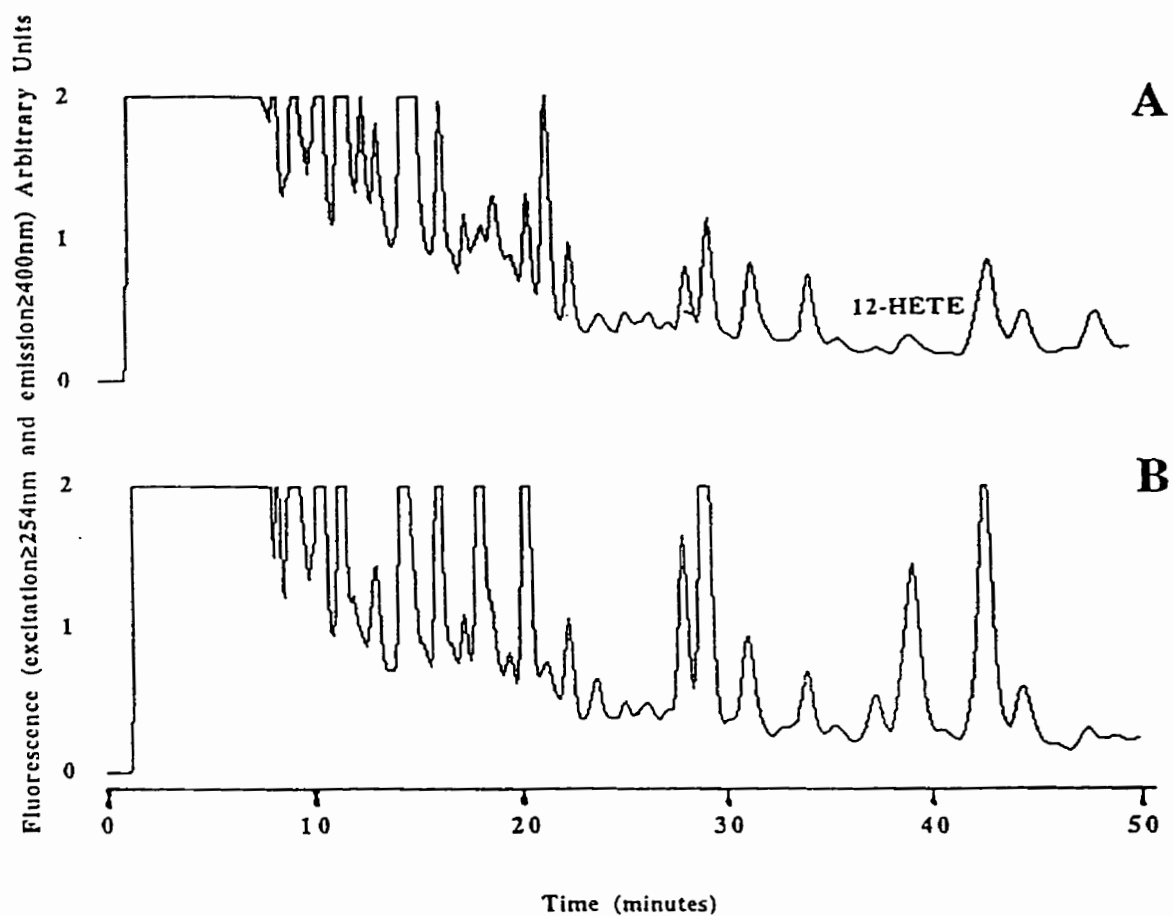
Figure 3-11. Derivatization with ADAM without silicic acid column chromatography purification.
(A) ADAM reagent only. (B) ADAM-12-HETE (40ng). Sensitivity of fluorescence detection of figures 3-11 and 3-12 is the same.
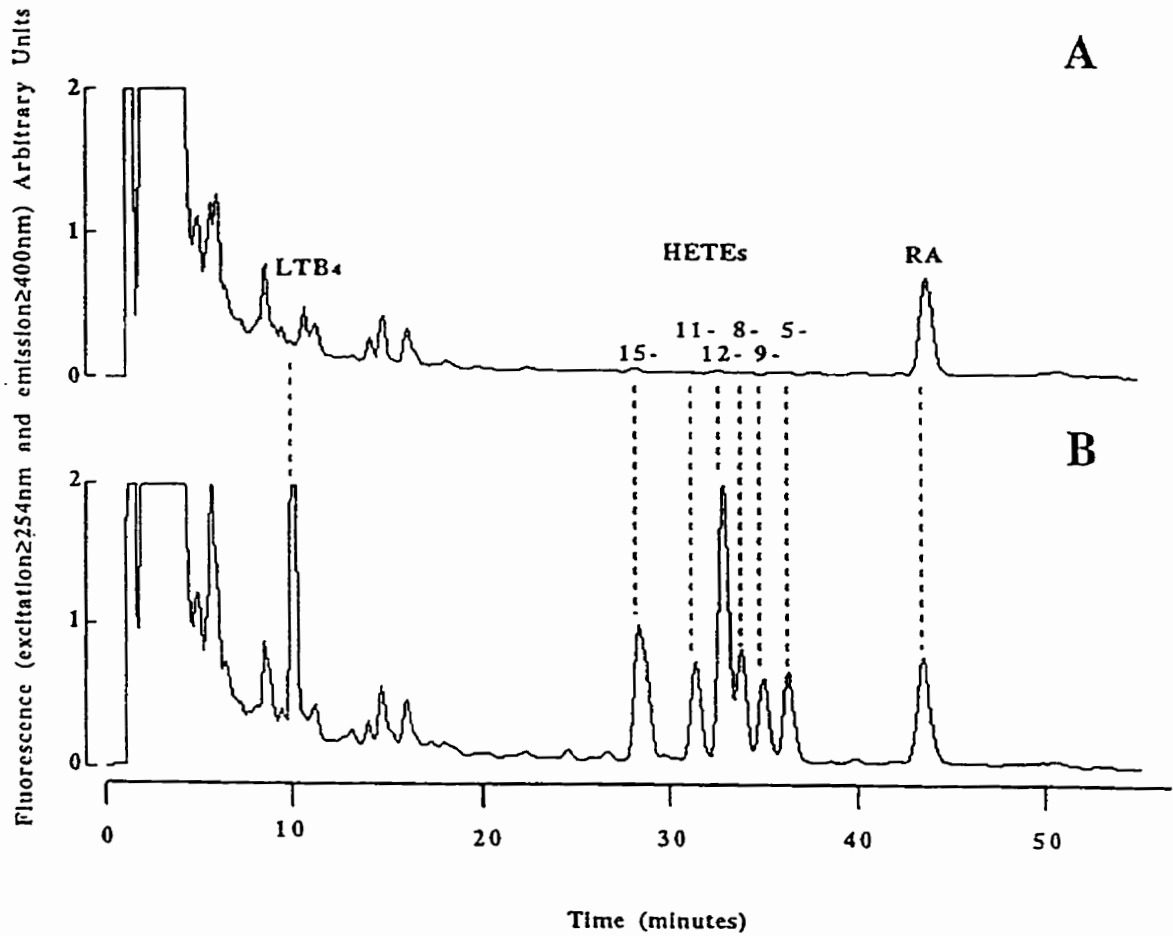
Figure 3-12. Derivatization with ADAM followed by silicic acid column chromatography purification.
(A) ADAM reagent + 100ng RA. (B) ADAM sample containing 100ng LTB₄ + 100ng 12-HETE + 50ng each of
5-,8-,9-,11-,15-HETE + 50ng RA. Sensitivity of fluorescence detection of figures 3-11 and 3-12 is the same.
RA=ricinoleic acid (internal standard).

A
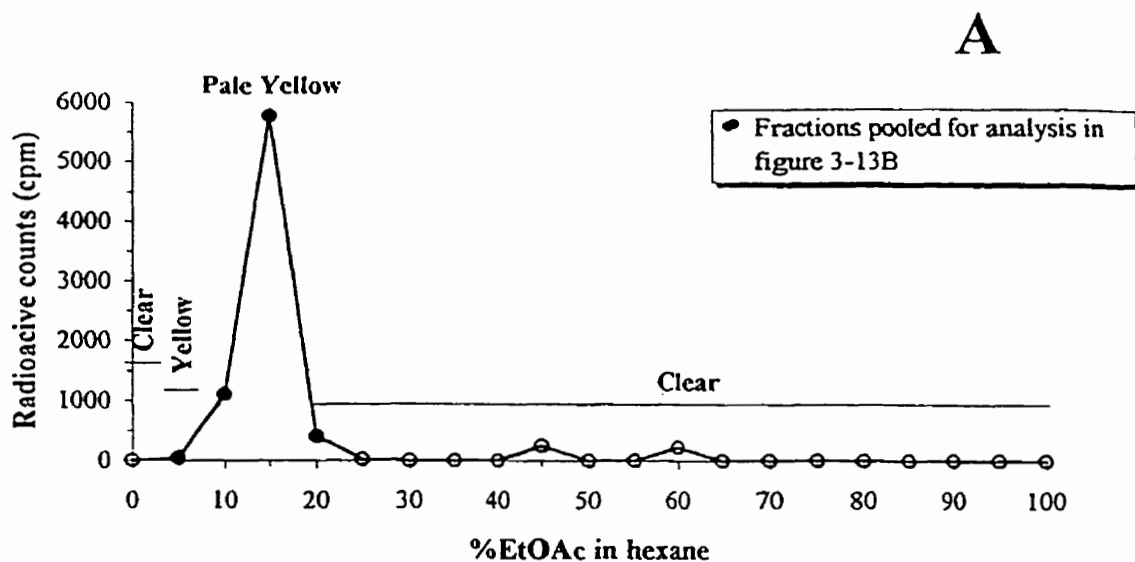
Figure 3-13A. Initial separation trial using silicic acid column chromatography. [^{14}C]12-HETE sample was derivatized and crudely purified through silicic acid using 1mL volume of eluents containing increasing EtOAc in hexane. Indicated fractions (containing majority of counts and colour) were pooled.

B
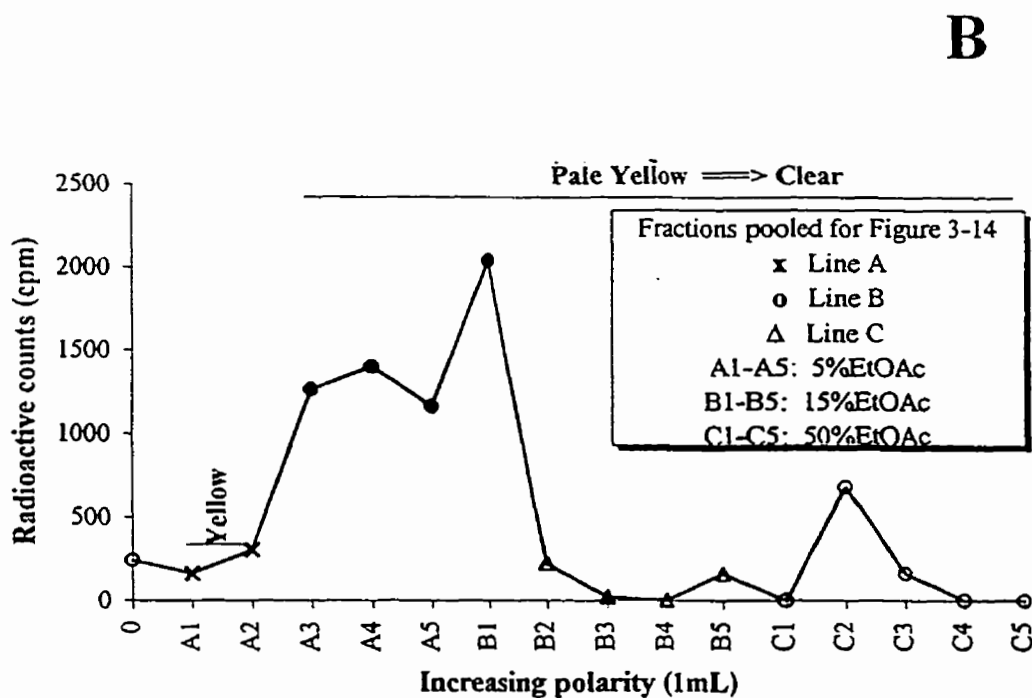
Figure 3-13B. Pooled fractions from 3-13A separated a second time using silicic acid column chromatography. Concentrations of eluents narrowed to 5%, 15% and 50%EtOAc and volumes increased to 5mL at each concentration. Indicated fractions pooled.
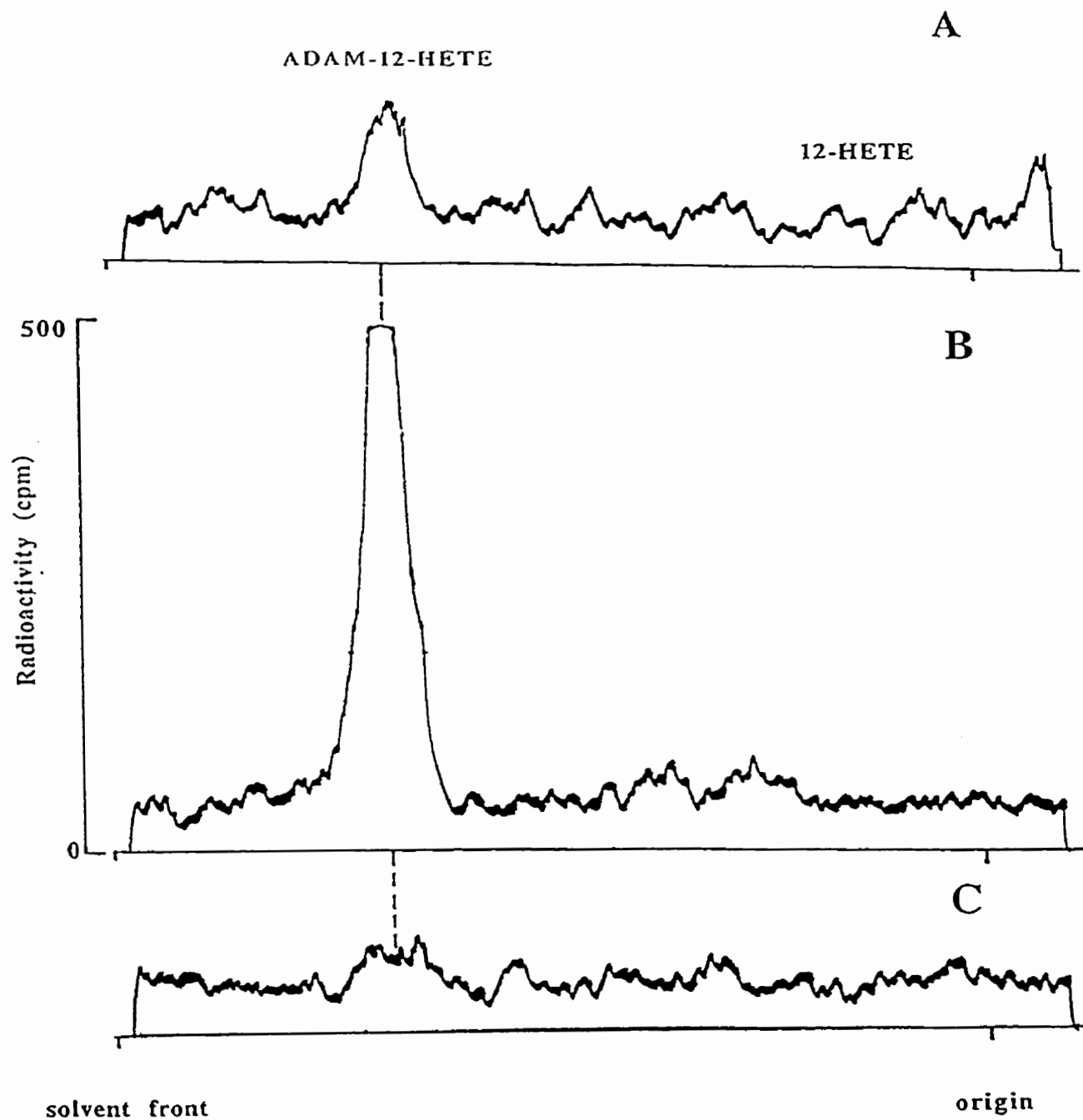
Figure 3-14. Pooled fractions from figure 3-13B were spotted on TLC (100%EtOAc, 45 minutes) and scanned for radioactivity. Line A contained the majority of the yellow colour. Line B contained the majority of the radioactive ADAM-12-HETE and was pale yellow. Line C was clear.

increasing the eluent volume to 10mL. The concentration of the second eluent was also increased to 10% and the volume was increased to 10mL.

The internal standard, HETEs and LTB$_4$

Also at this time an internal standard was selected. Ricinoleic acid (RA) was chosen because it satisfied the following criteria:

1. derivatized with ADAM
2. eluted under the same conditions as ADAM-12-HETE using silicic acid column chromatography
3. possessed a reasonable retention time on HPLC with respect to other lipoxygenase products
4. did not exist in nature.

For each sample, a known quantity of the internal standard was added. Its recovery as ADAM-ricinoleic acid on HPLC was an indication of recovery of all the other compounds.

Figure 3-15C shows the chromatogram of a derivatized sample of an unlabeled HETE mixture containing 5-, 8-, 9-, 11-, 12-, and 15-HETE, RA and some radioactive 12-HETE. Greater than 90% of the starting material was retrieved as calculated by the recovery of the internal standard.

The last compound incorporated into the lipoxygenase profile was LTB$_4$. Figure 3-15D illustrates that ADAM-LTB$_4$ was more polar than the ADAM-HETEs and ADAM-RA and was therefore eluted in the 50%EtOAc fraction. For the purpose of recovering all products (HETEs, RA and LTB$_4$), the eluents of the silicic acid column were finalized to the following:

1. 5mL hexane
2. 10mL 3%EtOAc in hexane
3. 5mL 50%EtOAc in hexane
4. 5mL 100%EtOAc.

3.2.3 Reverse-phase high-pressure liquid chromatography

Figure 3-16 shows the profile of pure standards (free-acid forms) which have been derivatized into ADAM-esters, purified through silicic acid column chromatography and analyzed on HPLC (panel D). It is coupled with a pair of chromatograms of authentic ADAM standards (panel A and B) and a reagent sample containing only the internal standard as a background control (panel C). The retention times of the ADAM standards are: trioxilin(A$_3$)<trioxilin(B$_3$)<LTB$_4$< HxA$_3$(8S) <HxA$_3$(8R)<HxB$_3$(10R)< HxB$_3$(10S)<15-<11-<12-<8-<9-<5-HETEs<RA. Note that ADAM-trioxilins and ADAM-LTB$_4$ co-elute closely with the large peaks of decomposed ADAM products, rendering their detection (on this HPLC system) difficult if their quantities are low (e.g. less than 50ng, refer to Figure 3-17). However, the remainder of the profile has been considerably improved with the addition of the silicic acid purification step.
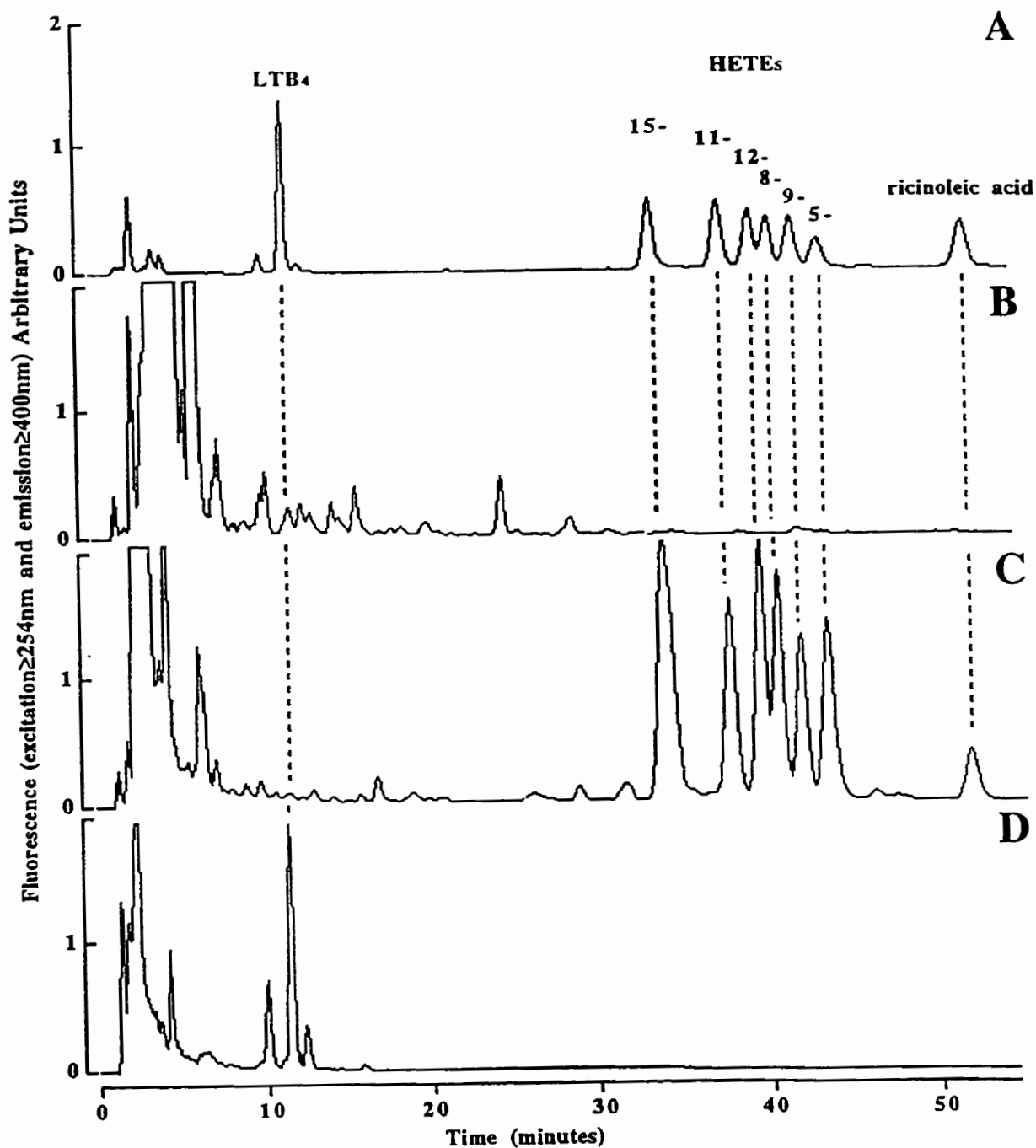
Figure 3-15. Chromatograms of the different silicic acid column fractions. (A) authentic ADAM standards (50ng LTB$_4$ + 10ng each of 5-,8-,9-,11-,12-,15-HETE + 10ng RA). (B) 3%EtOAc/hexane fraction. (C) 10%EtOAc/hexane fraction. (D) 50%EtOAc/hexane fraction. ADAM sample (as fractionated through B-D) contained 100ng LTB$_4$ + 50ng each of 5-,8-,9-,11-,12-,15-HETE + 50ng RA. RA=ricinoleic acid (internal standard).
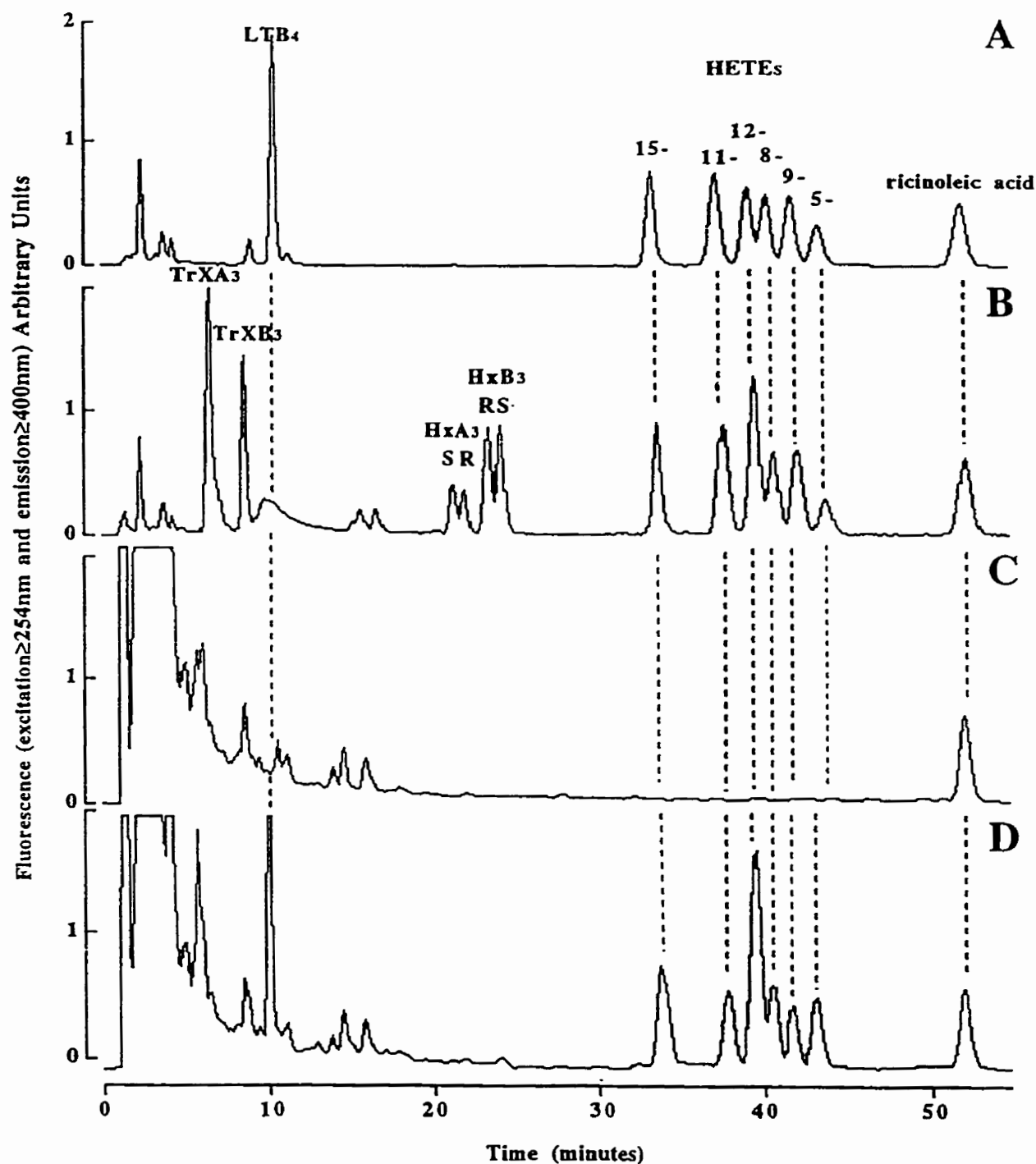
Figure 3-16. Final silicic acid column conditions and relative HPLC retention times. (A) authentic ADAM standards1 (100ng LTB₄ + 50ng each of 5-,8-,9-,11-,12-,15-HETE + 50ng RA). (B) authentic standards2 (50ng each TrXA₃, TrXB₃, HxA₃(R/S), HxB₃(R/S). (C) ADAM reagent + 50ng RA, 50%EtOAc/hexane fraction. (D) ADAM sample (100ng LTB₄ + 50ng each of 5-,8-,9-,11-,12-,15-HETE + 50ng RA), 50%EtOAc/hexane fraction. RA=ricinoleic acid (internal standard).
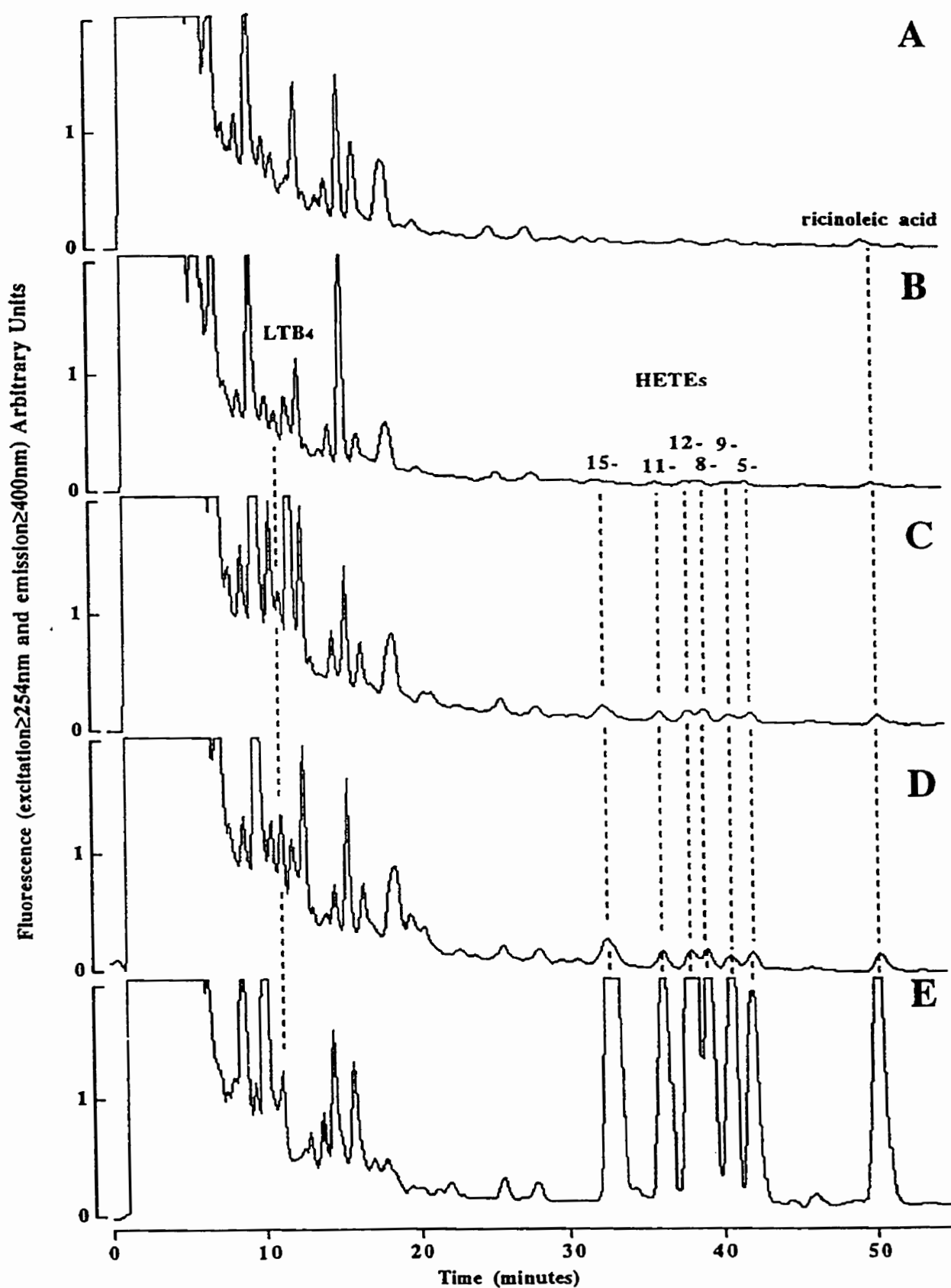
Figure 3-17. Dose-dependent limits of fluorescence detection of pure standards. (A) ADAM reagent + 1ng RA. (B) 1ng each of LTB₄, 5-,8-,9-,11-,12-,15-HETE and RA. (C) 5ng each LTB₄, 5-,8-,9-,11-,12-,15-HETE and RA. (D) 10ng each of LTB₄, 5-,8-,9-,11-,12-,15-HETE and RA. (E) 50ng each LTB₄, 5-,8-,9-,11-,12-,15-HETE and RA. All samples were derivatized, purified through silicic acid column and analyzed on HPLC as described in *Materials and Methods* section. Sensitivity of fluorescence detection for all chromatograms is the same.

Figure 3-17 demonstrates the dose-dependent limits of detection of the fluorescent esters using the same free-acid standard mixture. Note that the ADAM-HETEs and ADAM-RA become recognizable at the 5-10ng level.

3.3 APPLYING THE ADAM PROTOCOL TO AN *IN VITRO* PREPARATION

The rat skin preparation was a compilation of the works of various investigators (Ruzicka *et al.*, 1983; Cameron *et al.*, 1990; Falguetret *et al.*, 1990; von Zepelin *et al.*, 1991). An epidermal preparation was selected because this layer had been shown to possess AA metabolizing activities.

3.3.1 Enzyme preparation

Skin dissociation

The skin dissociation procedure was monitored by hematoxylin/eosin stains of formalin-fixed skin sections. An overnight incubation of depiled skin sections in 0.25% trypsin solution at 4°C led to the facile mechanical separation of epidermis from dermis (Figure 2-4). The dissociated epidermal elements isolated were composed of several cell types. The predominant cells were keratinocytes.

Profile of AA metabolites by different fractions of epidermis

As varying AA metabolizing abilities have been observed with different centrifuged fractions of the dissociated epidermis, each fraction (10 000g and 100 000g supernatants) was assayed. Figure 3-18 shows chromatograms obtained by analysis of each supernatant after incubation with [^{14}C]AA for 60 minutes at 37°C. Note that only the 10 000g supernatant (panel B) demonstrated any activity. Subsequent experiments therefore concentrated on this 10 000g supernatant. An additional experiment showed that the 12-lipoxygenase activity exhibited by this epidermal fraction was lost when thawed at 37°C (results not shown). As a result, the epidermal preparation was kept on ice and thawed at room temperature immediately prior to incubation.

3.3.2 Enzyme stimulation

Negative and positive controls

Figure 3-19 shows 15-HETE and 12-HETE production by the 10 000g supernatant. Figure 3-20 illustrates a typical chromatographic representation of these stimulations. The negative control contained the EtOH vehicle in the incubation mixture (Figure 3-20A) and the positive control was stimulated by 1μg AA (Figure 3-20B). There was endogenous release of 15- and 12-HETE and both were increased when AA was added (15-HETE: +195%, $p \leq 0.05$, 12-HETE: +514%, $p \leq 0.0005$ vs control). Neither LTB$_4$ nor hepoxilins were detected. If present, these compounds were below the limits of detection.
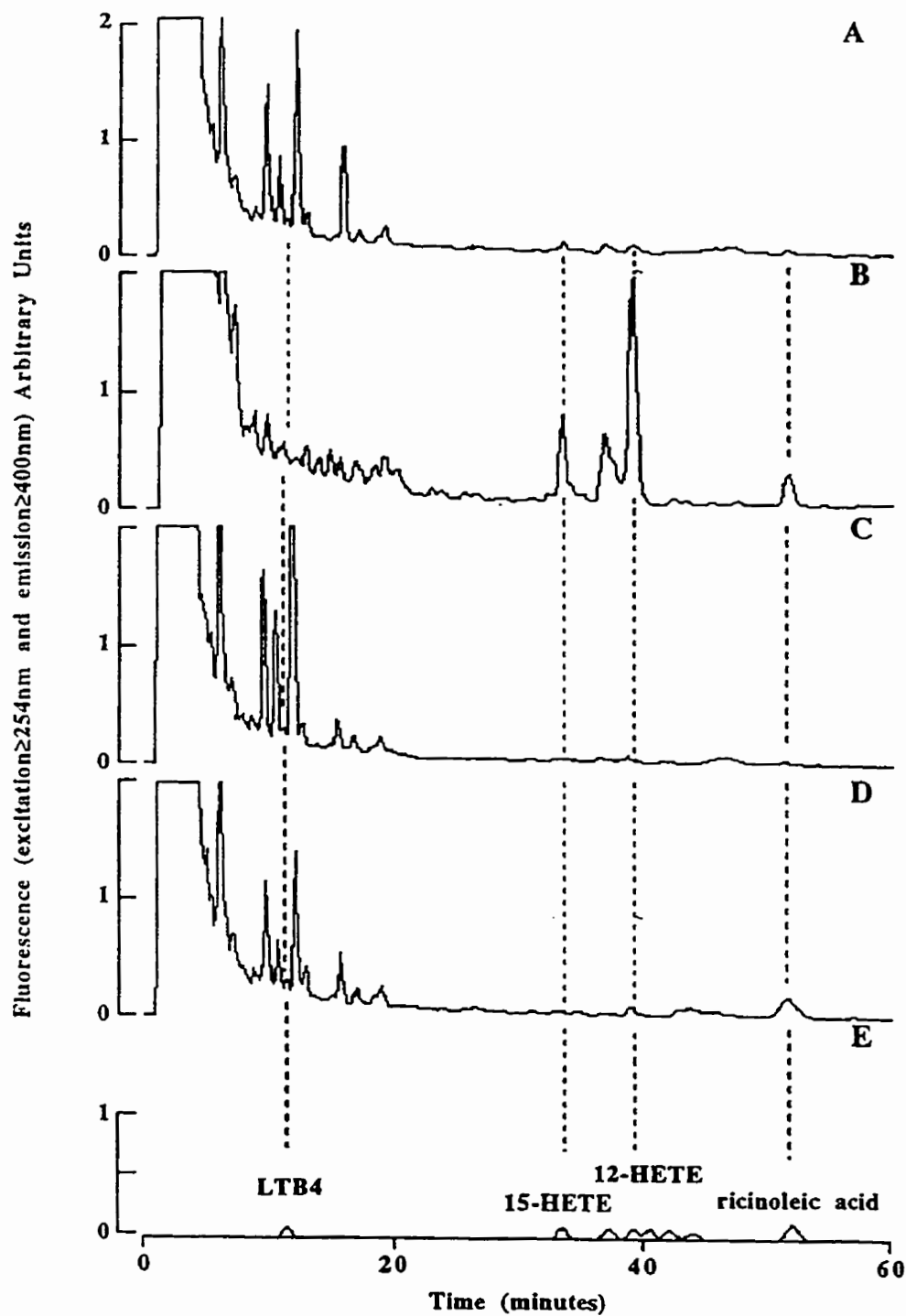
Figure 3-18. Testing of *in vitro* **enzyme batch.** (A) 10 000g control supernatant. (B) 10 000g supernatant + 1μg AA. (C) 100 000g control supernatant. (D) 100 000g supernatant + 1μg AA. (E) authentic ADAM standards (10ng each). Control samples received EtOH vehicle (used to dissolved AA).
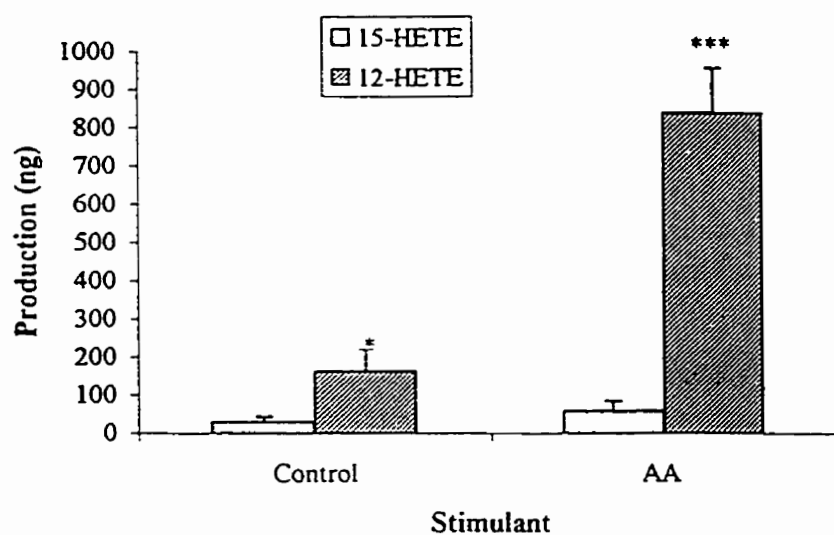
Figure 3-19. Application of ADAM derivatization and silicic acid column purification using *in vitro* model: 300µg of 10,000g supernatant enzyme batch + stimulants incubated at 37°C for 60 minutes. Control contained no stimulant (negative control) and 1µg AA (positive control). Calculations are based on a known amount of ricinoleic acid (internal standard) added. 12- and 15-HETEs were the only products detected using 75%ACN/25%H$_2$O HPLC solvent system (flow rate 1.4mL/min). Results are mean±SD of n=3 samples. (*$p \leq 0.05$, *** $p \leq 0.0005$ vs control).
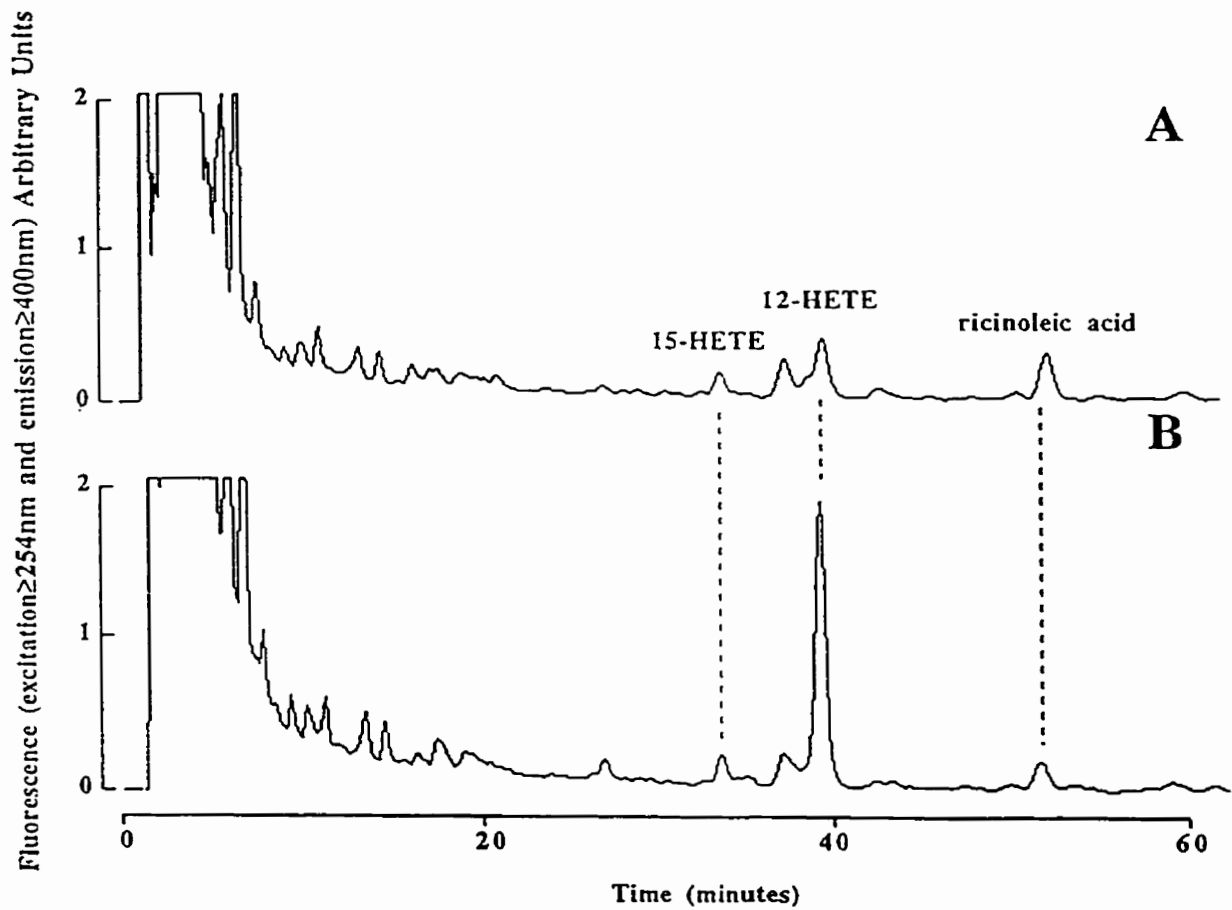
Figure 3-20. Application of ADAM derivatization and silicic acid column chromatography using *in vitro* preparation. Chromatograms of typical (A) control (EtOH) (B) 1μg AA stimulated samples. Ricinoleic acid (100ng-internal standard) was added to each sample before extraction with EtOAc (*see Materials and Methods* section for details).

Bradykinin

Figure 3-21 demonstrates the effects of increasing concentrations of BK on 15- and 12-HETE production. Figure 3-22 shows the results in chromatographic form. 15-HETE production was stimulated with lower doses of BK (+160% to +174%, $p \leq 0.05$ vs control), but was not concentration-dependent. BK-stimulated 12-HETE production increased +261% to +492%, versus control ($p \leq 0.0005$). LTB_4 or hepoxilins were not obvious in these chromatograms due to the lack of a clean window within the range of elution of these compounds.

Platelet-activating factor

Figure 3-23 presents the effects of increasing concentrations of PAF on 15- and 12-HETE production. Figure 3-24 illustrates typical results obtained from HPLC. PAF stimulated the production of 15-HETE at lower doses, but again the effect was not concentration-dependent (+149% to +162%, $p \leq 0.05$ vs control). In contrast, 12-HETE production was dependent on PAF concentrations, increasing +171% to +406% ($0.05 \leq p \leq 0.0005$ vs control). No LTB_4 or hepoxilins were clearly detectable.

3.4 APPLYING THE ADAM PROTOCOL TO AN *IN VIVO* PREPARATION

Figures 3-25 and 3-26 illustrate graphically and chromatographically the effects of *in vivo* intradermal administration of BK and PAF. The highest *in vitro* dose of each stimulant was tested. Both BK and PAF stimulated the production of 12-HETE (+411% and +255% respectively, $p \leq 0.05$ vs Krebs' control). No other compounds could clearly be discerned due to presence of other peaks in the TrX, LTB_4, and Hx regions.

3.5 RECOVERY OF INTERNAL STANDARD

Recovery of ADAM-ricinoleic acid from HPLC represented the extent to which the compound could be retrieved after the extraction (*in vitro* and *in vivo* only), derivatization and silicic acid column chromatography procedures. Figure 3-27A illustrates that optimal results were achieved when pure standards were used (i.e. the excess ADAM was eluted before the ADAM-12-HETE derivative). However, recovery of ricinoleic acid was reduced when *in vitro* or *in vivo* preparations were used (Figure 27B: -38% and -71% respectively). This may be due to irreversible tissue binding and the inability of EtOAc to fully dissociate this binding. Hence HETEs present in these tissues may not have been extracted fully by the methods used.
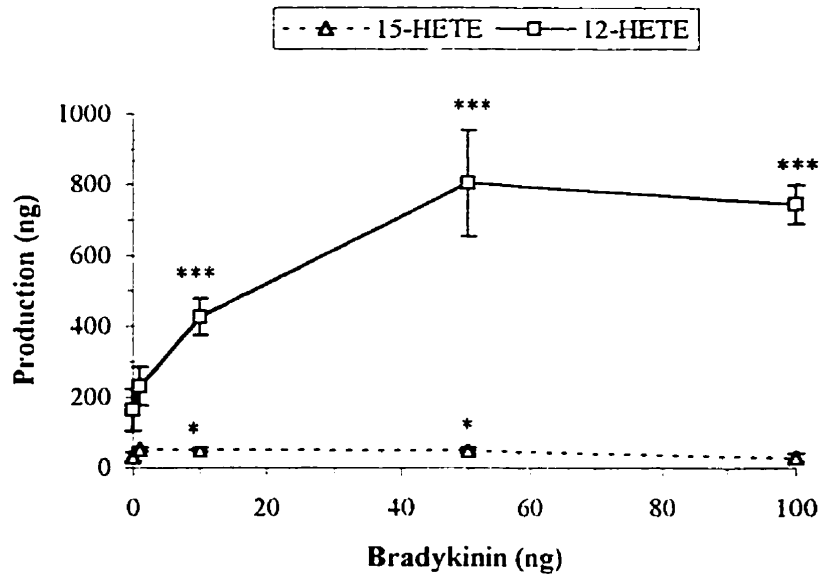
Figure 3-21. Application of ADAM derivatization and silicic acid column purification using *in vitro* model: 300µg of 10,000g supernatant enzyme batch + various concentrations of bradykinin incubated at 37*C for 60 minutes. Calculations are based on a known amount of ricinoleic acid (internal standard) added. 12- and 15-HETEs were the only products detected using 75%ACN/25%H$_2$O HPLC solvent system (flow rate 1.4mL/min). Results are mean±SD of n=3 samples. (*p≤0.05, *** p≤0.0005 vs control)
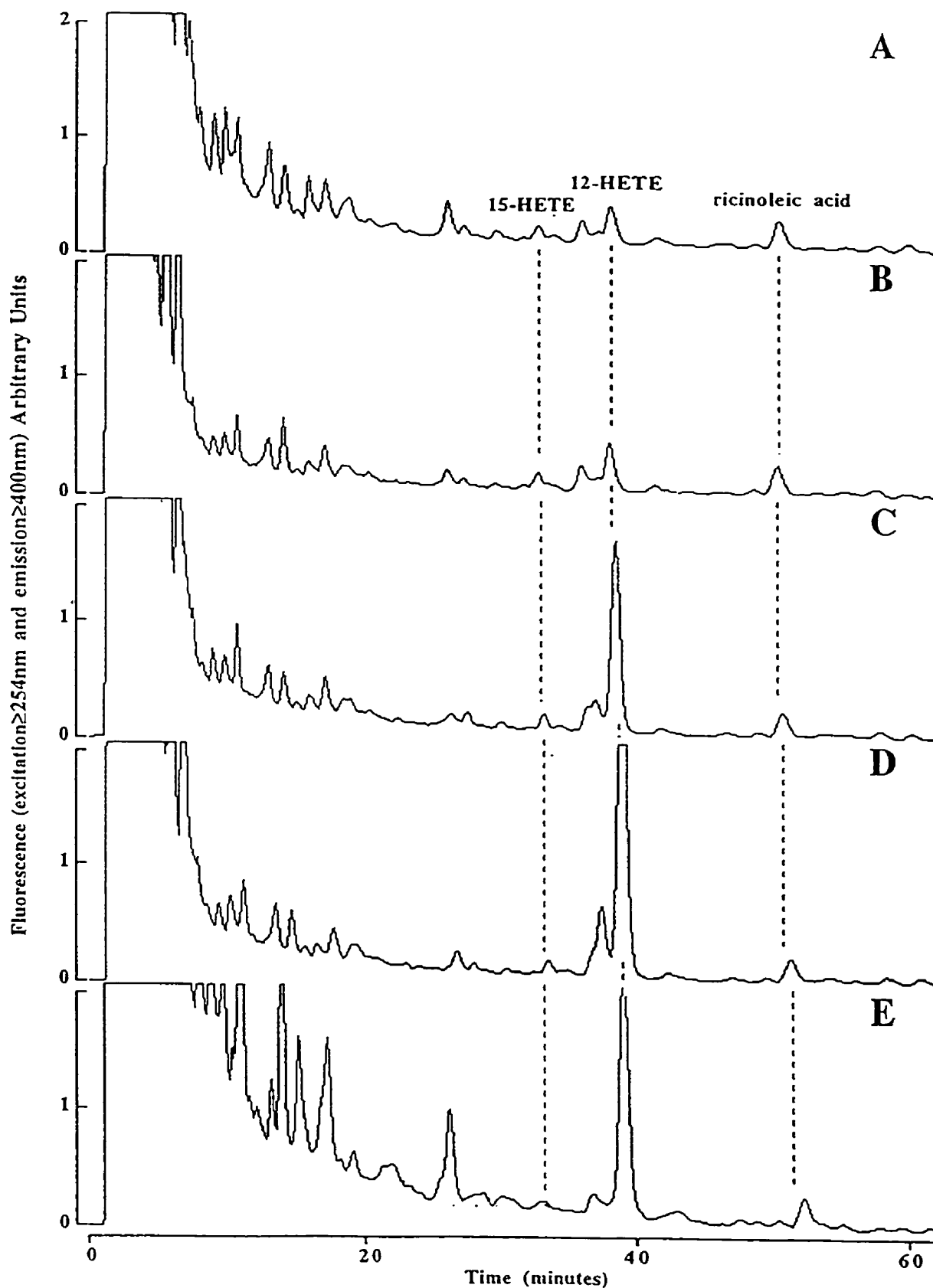
Figure 3-22. Application of ADAM derivatization and silicic acid column chromatography using *in vitro* preparation. Chromatograms of typical bradykinin dose-response (A) control (EtOH) (B) 1ng (C) 10ng (D) 50ng (E) 100ng. Ricinoleic acid (100ng-internal standard) was added to each sample before extraction with EtOAc (*see Materials and Methods* section for details).
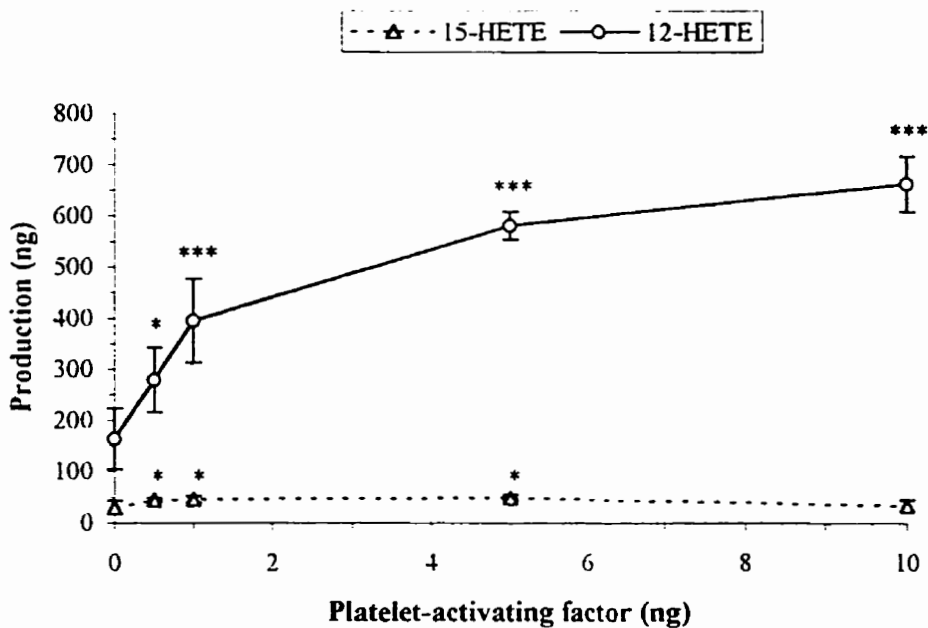
Figure 3-23. Application of ADAM derivatization and silicic acid column purification using *in vitro* model: 300μg of 10,000g supernatant enzyme batch + various concentrations of platelet-activating factor incubated at 37*C for 60 minutes. Calculations are based on known amount of ricinoleic acid (internal standard) added. 12- and 15-HETEs were the only products detected using 75%ACN/25%H_2O HPLC solvent system (flow rate 1.4mL/min). Results are mean±SD of n=3 samples. (*$p \leq 0.05$, *** $p \leq 0.0005$ vs control)
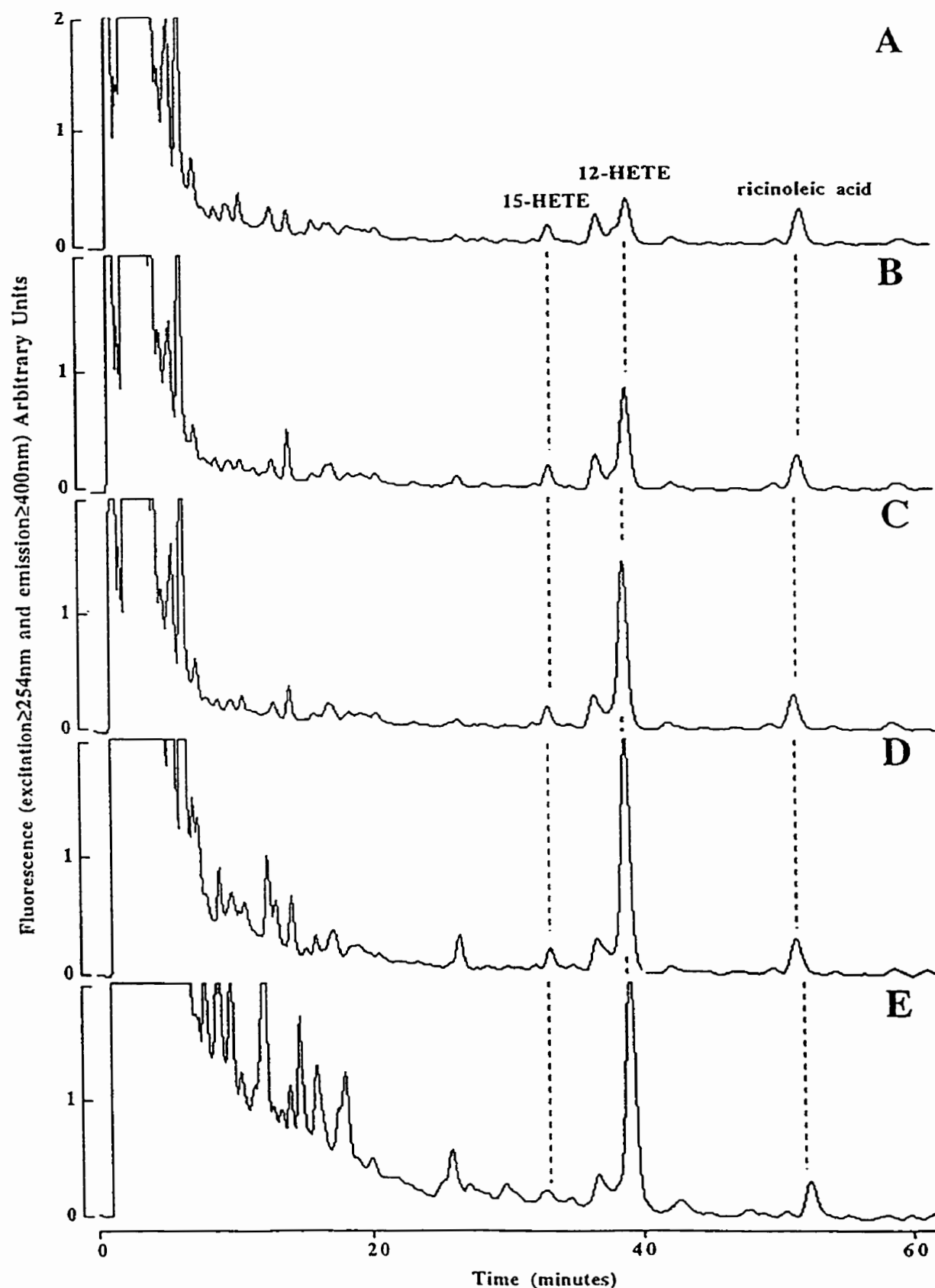
Figure 3-24. Application of ADAM derivatization and silicic acid column chromatography using *in vitro* preparation. Chromatograms of typical platelet-activating factor dose-response (A) control (EtOH) (B) 0.5ng (C) 1ng (D) 5ng (E) 10ng. Ricinoleic acid (100ng-internal standard) was added to each sample before extraction with EtOAc (*see Materials and Methods* section for details).
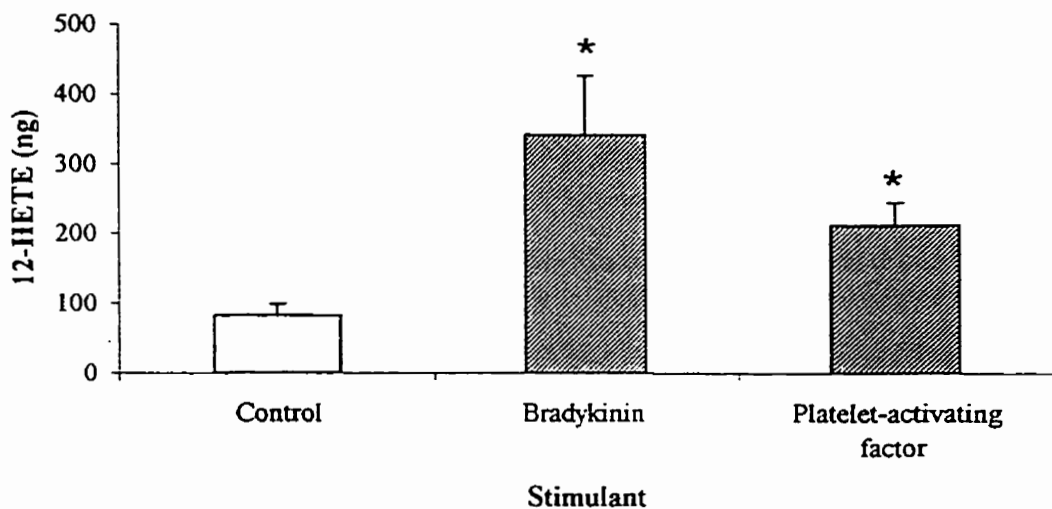
Figure 3-25. Application of ADAM derivatization and silicic acid column purification using *in vivo* model: 100μL intradermal injections of control (3%EtOH), bradykinin (100ng) and platelet-activating factor (10ng). After 30 minutes, circular patches of skin containing injections were excised, homogenized and extracted with EtOAc. Calculations are based on amount of ricinoleic acid (internal standard) added. 12-HETE was the only product detected using 75%ACN/ 25%H$_2$O HPLC system (flow rate 1.4mL/min). Results are mean±SD of n=3 (*p≤0.05 vs control).
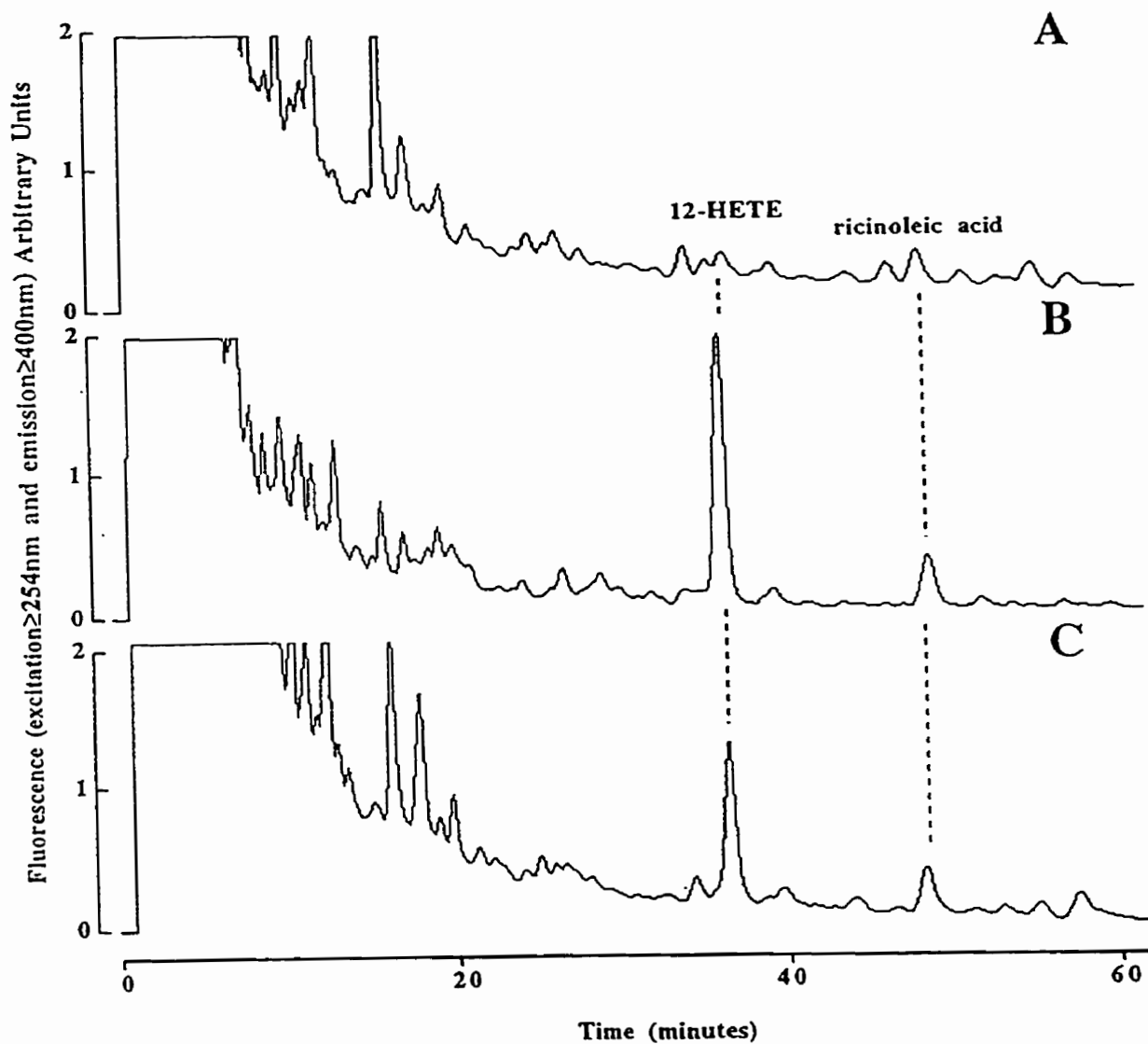
Figure 3-26. Application of ADAM derivatization and silicic acid column chromatography using *in vivo* preparation. Chromatograms of typical (A) control (Krebs) (B) 100ng bradykinin (C) 10ng platelet-activating factor. Ricinoleic acid (100ng-internal standard) was added to each sample before extraction with EtOAc (*see Materials and Methods* section for details).
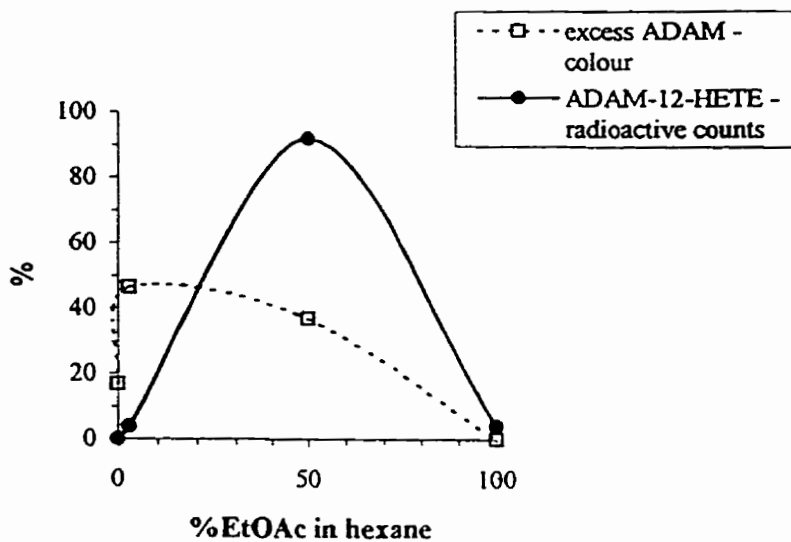
Figure 3-27A. Colour and counts separation using pure standards. Silicic acid column eluent fractions was analyzed for colour (spectrophotometrically) and radioactivity.
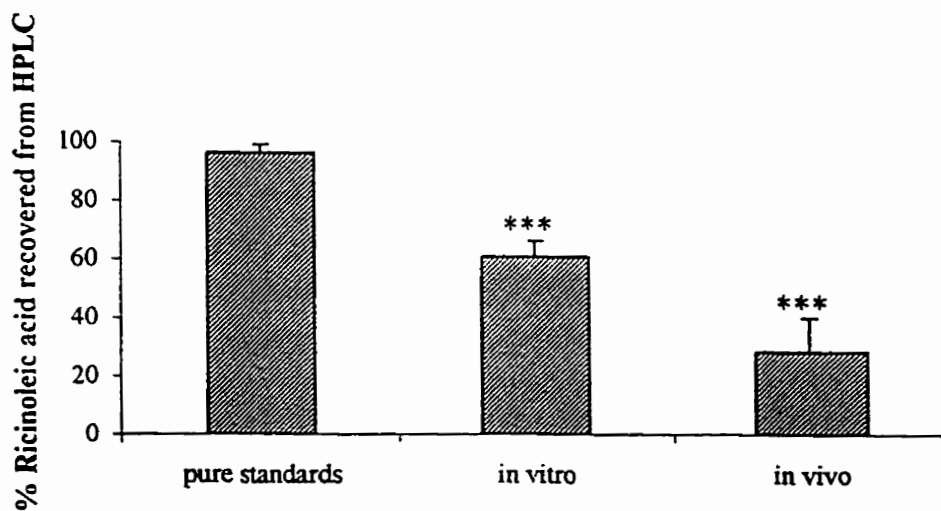
Figure 3-27B. Ricinoleic acid recovery. Indication of derivatization and silicic acid column chromatography. Results represent mean±SEM, pure standards n=7, *in vitro* : n=36, ***p<0.0005 vs pure standards, *in vivo* : n=6, ***p<0.0005 vs pure standards.

SECTION FOUR: DISCUSSION

GENERAL INTRODUCTION

"...to postulate the potential involvement of leukotrienes in the genesis of a pathological change and development of inflammatory skin diseases...several criteria should be satisfied (Rosenbach *et al.*, 1985; Camp and Derm, 1989). In addition to the reproduction, at least in part, of the pathological changes observed in the disease by introduction of the mediator into the tissue *in vivo*...other criteria must be fulfilled, such as: (a) the demonstration of the release of the mediator in appropriate concentrations in samples from the inflamed skin *in vivo*, (b) the attribution of the mediator release to resident tissue or to infiltrating inflammatory cells, and (c) the modification of the pathological process by administration of specific enzyme inhibitors or receptor antagonists *in vivo*." (Michel and Dubertret, 1992)

These were the criteria which LTB_4 possessed to emerge as one of the major contributors in the pathogenesis of psoriasis. In fact, the notion that a potential mediator of inflammation should encompass some, if not all, these characteristics has been around for some time and only slight modifications have been made to it over the years (Dale, 1929; Spector and Willoughby, 1963; Wilhelm, 1973). Histamine was the first of such mediators, and since then the list has grown to include 5-hydroxytryptamine, bradykinin and prostaglandins. The discovery of arachidonate products has extended this list even further. Certainly the aforementioned, LTB_4 is the most potent chemotactic factor yet described (Bray *et al.*, 1981). However, the possibility that other lipoxygenase products may be considered inflammatory mediators has not been thoroughly addressed.

One of the aims of this study was to examine the products of the 12-lipoxygenase pathway, in particular 12-HETE and determine if this compound was involved in the development of acute inflammation. In doing so, we set out to fulfill some of the above mentioned criteria for a potential inflammatory mediator. The first was to "demonstrate release of the mediator...from the inflamed skin *in vivo*". In order to do this, we needed to develop an effective method of profiling the products formed in the rat skin.

4.1 ESTABLISHING AND IMPLEMENTING THE ADAM PROTOCOL

With the advances in technology, newer and more specialized techniques of analyzing minute amounts of specific compounds have been created. But with such advances come the disadvantages of price and complexity of usage. For our purposes, gas-liquid chromatography (GLC) has been a common method for analyzing fatty acids and give limits of detection in the low nanogram to high picogram range (Perkins, 1975). However, gas-liquid chromatography does not allow injected samples to be recovered. In contrast, high pressure liquid chromatography (HPLC) systems are more affordable but are hampered by several factors. First, detection of compounds on HPLC is usually via an ultraviolet (UV) detector. The strength of UV absorbance is dependent on the conjugation of double bonds in the molecule. Therefore, without this

characteristic feature, compounds will fail to be detected even when present in submicrogram amounts. Second, without an appropriate internal standard, compounds cannot be accurately quantified. Using the ADAM reagent to label the fatty acids with a fluorescent tag prior to HPLC analysis permits non-UV absorbing compounds to be detected even at low nanogram levels. In fact, detection of the fluorescent derivative is so much improved that a sole fluorescent detector (with or without complementary UV detector) is all that is required to monitor the compound of interest. The addition of a suitable internal standard, such as ricinoleic acid (Figure 4-1), serves to quantify production of fatty acid-like substances such as HETEs as well as determine recovery of the sample work-up.
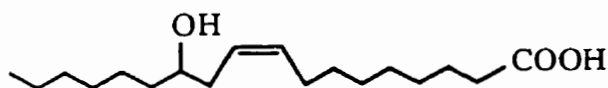
Figure 4-1. Chemical structure of ricinoleic acid (12-hydroxy-cis-9-octadecenoic acid)

4.1.1 The ADAM protocol

9-anthryldiazomethane (ADAM: Figure 4-2A) is a red solid that easily reacts with carboxylic acid to give fluorescent esters (Figure 4-2B). Because of its characteristic aromatic structure, ADAM derivatives have strong and specific absorbances.
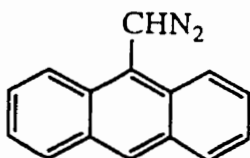
Figure 4-2A: 9-anthryldiazomethane (ADAM) excitation$\geq$254nm and emission$\geq$400nm.
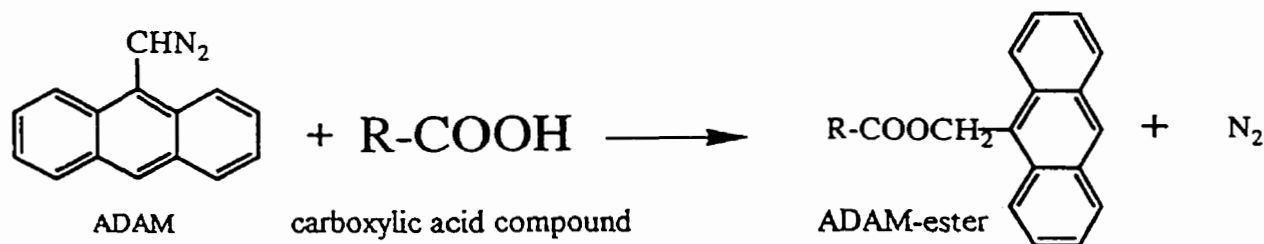
Figure 4-2B. ADAM reaction.

Derivatization, silicic acid column chromatography and reverse-phase HPLC

The use of ADAM to examine the compounds of a biological sample is not new. Nimura *et al.* first developed the fluorescence labeling reagent for fatty acids in 1980 and it has since been used by other investigators to label urinary oxalic acid (Imaoka *et al.*, 1983), free AA in rabbit alveolar macrophages (Nakagawa and Waku, 1985) and AA derivatives from rat peritoneal leukocytes (Yamaki and Oh-ishi, 1992) to name just a few. To our knowledge, this is the first time that ADAM has been used to detect lipoxygenase products from the skin.

The two main advantages of using ADAM were facility and sensitivity:

Facility

1. reaction time was relatively short (1 hour).
2. high reactivity with free fatty acid and compounds that possessed carboxyl, aromatic hydroxyl and sulfonyl groups.
3. reaction could take place in a variety of commercially available and inexpensive organic media such as MeOH, acetone, and EtOAc.
4. no specialized equipment was required as the reaction took place at room temperature, utilizing neither heat nor catalyst.

Sensitivity

1. non and/or low-absorbing UV compounds became detectable
2. fluorescence detection was 10-100 times greater than UV (Cooper and Anders, 1974; Borch, 1975; Pei *et al.*, 1976).
3. separated ADAM derivatives could be easily quantitated.

However, no method, no matter how successful nor useful, was without its faults and limitations. First, although the reaction proceeded to completion after 60 minutes using an ADAM concentration of 50μg/mL, variability in the derivatization still existed. This was due to the sensitive nature of ADAM to light and oxidation which could have altered its ability to function optimally. To account for this, a known quantity of internal standard was added so that changes during derivatization and HPLC analysis could be accounted for.

Second, because of the aforementioned variability in derivatization, not so much during the work done with pure standards but rather at the *in vitro* and *in vivo* stages, the amount of ADAM reagent used had to be increased. This in turn caused an increase in the background noise on the subsequent HPLC analysis. Since tissue productivity of a certain compound was unknown, it was necessary to develop a fast and effective way to reduce the amount of 'noise' without interfering with the derivatized compounds. Silicic acid column chromatography was selected for this purpose. The use of the column stemmed from the works of Borgeat and Samuelsson (1979) who used it to examine AA metabolism in PMNL and Ziboh *et al.* (1984) who similarly used it to look at lipoxygenation of AA from murine keratinocytes. In both cases, the column was used to elute

different fractions of lipids from the incubation extract. In our studies, the ability of the silicic acid column to separate the excess ADAM reagent from the desired ADAM derivatives was pivotal.

Finally, under the given solvent conditions, the hepoxilins and HETEs were the most easily identified, as their retention times did not coincide with the retention times of the excess and decomposed reagent that eluted earlier. Although, the system was originally set-up to detect ADAM-LTB$_4$, the region in the chromatogram where the compound eluted was not sufficiently cleaned up by the silicic acid column to permit its quantitation. This problem may be solved through use of a solvent program which can change from a slower system (i.e. more H$_2$O in the system) to a faster system (i.e. more ACN) over time. These procedures are easily achieved by HPLC except that our current system did no possess the capabilities to perform such solvent programming. Indeed PGE$_2$, PGF$_{2\alpha}$ and 6-keto PGF$_{1\alpha}$ have been detected using a 60:40 (ACN:H$_2$O) solvent system (unpublished observations).

4.1.2 The in *vitro* and *in vivo* models

Before the ADAM protocol was applied to an *in vivo* sample, it was first tested on an *in vitro* rat skin preparation. Of the three layers of skin, the epidermis has been shown to exhibit a high level of AA metabolizing activity, with 12-HETE as the predominant lipoxygenase compound (Hammarstrom *et al.*, 1979; Ruzicka *et al.*, 1983; Ziboh *et al.*, 1984; Henke *et al.*, 1986; Ruzicka and Aubock, 1987; Cameron *et al.*, 1990; von Zepelin *et al.*, 1991). With this in mind, the production of 12-HETE served as a positive control from which a crude extraction procedure and modifications to the existing derivatization protocol were made.

The first step in establishing the *in vitro* model was to obtain a viable enzyme mixture. Epidermis preparatory procedures were compiled from several labs (Ruzicka *et al.*, 1983; Cameron *et al.*, 1990; Falgueyret *et al.*, 1990; von Zepelin *et al.*, 1991). The main problem encountered was that adult rat skin was rarely used as investigators opted for the more manageable skins of mice, guinea pig and human subjects. In the end, two batches, a 10,000g and 100,000g supernatant, were tested for activity with radiolabelled AA. Of the two, it was observed that the 10,000g supernatant, which contained cytosol, microsomes and other membrane fragments, possessed the greatest enzymatic activity. This finding was supported by other investigators (Ruzicka and Printz, 1982a; Ruzicka and Printz, 1982b; Bedord *et al.*, 1983; Ruzicka *et al.*, 1983). To demonstrate that the product was enzymatically formed, it was found that the 10,000g batch was heat sensitive and that thawing at 37°C (as opposed to room temperature) inhibited its activity.

As was mentioned, *in vitro* and *in vivo* testing of the ADAM protocol required the involvement of an additional step to extract the compounds from the buffer (*in vitro*) and tissue (*in vivo*). Due to time constraints, a crude extraction was obtained. One of the drawbacks of such an unrefined extraction procedure was that capacity for complete derivatization decreased. Although ADAM has been shown to be extremely active, it is also non-specific in its actions. Since it was assumed that stimulation with AA, BK or PAF would produce more than just 12-HETE, and that

extraction with EtOAc would extract more than just 12-HETE, the accumulated presence of other derivatizable substrates could have easily interfered with the ability of ADAM to fully derivatize our compounds of interest. To compensate for this, the amount of ADAM used to initiate derivatization was increased, but this in turn reduced the effectiveness of the silicic acid column to elute the excess reagent. Attempts to normalize the results were achieved by basing subsequent calculations on the recovery of the internal standard, ricinoleic acid, as its ADAM-ester derivative, in the HPLC profile.

Special mention should be made at this time regarding the type of tissue taken for analysis at the *in vitro* and *in vivo* stages. In an effort to determine the usefulness of the ADAM protocol on a biological sample, it was decided that the due to the high enzymatic activity in the epidermis, this portion of the skin be examined first *in vitro*. Subsequent analyses on the dermis layer *in vivo* were based on the assumption that the epidermis *in vivo* would respond similarly to the epidermis *in vitro*. The second reason for looking at the dermis *in vivo* stemmed from earlier works in our laboratory which demonstrated enzymatic formation of hepoxilins in this layer (Pace-Asciak *et al.*, 1993). Needless to say that preparations will be made to examine both layers *in vivo* and *in vitro* in the near future.

Despite these nuances, application of the ADAM protocol to the *in vitro* and *in vivo* preparations poignantly demonstrated that 12-lipoxygenase activity was highly active in the rat skin. The main differences between the two skin preparations were that:

1) no 15-HETE was detected *in vivo* and

2) considerably lower amounts of 12-HETE were formed *in vivo*.

Several factors may have contributed to these incidences. First, 12- and 15-HETE production may have been time-dependent such that a reduction in incubation time (from 60 minutes *in vitro* to 30 minutes *in vivo*) may have slowed the formation of 15-HETE to amounts below the limits of detection for the current system (e.g. less than 5-10ng). Second, the reduced amount of 12-HETE formed may have been attributed to 15-HETE itself. Kragballe *et al.* (1986) demonstrated that dermis derived 15-HETE inhibited epidermal 12-HETE production. It could be speculated that the 15-lipoxygenase pathway would be more stable and more available in the *in vivo* system, allowing for the production of 15-HETE to proceed. This may have in turn, inhibited 12-lipoxygenase activity, thereby resulting in a lower production of 12-HETE *in vivo*. Although 15-HETE was not detected using ADAM, this may have been due to the localized distribution of this compound to the epidermis (and not the dermis) as compared to 12-HETE. Finally, since we were dealing with an *in vivo* system any number of unknown physiological parameters such as HETE uptake, further metabolism as well as the aforementioned 15-HETE inhibition could have affected its outcome. van de Sandt *et al.* (1995) have established a direct relation between clinical signs of irritation and *in vitro* release of 12-HETE from skin organ cultures of rabbit and human subjects after topical exposure to benzalkonium chloride, sodium dodecyl sulfate, and formaldehyde. This release was dose-dependent and occurred at irritant concentrations relevant to

the *in vivo* situation (Gad *et al.*, 1986; Willis *et al.*, 1988; Agner and Serup, 1990). This suggests that our *in vitro* results may hold some relevance to the events *in vivo*.

Clearly, the use of ADAM to label fatty acids has allowed the detection of 12-HETE and other lipoxygenase compounds at the low nanogram levels. Due to the fact that the HPLC system can be customized to suit possibly any ADAM derivative, many compounds can be analyzed with respectable ease. Although, some of its shortcomings include reagent clean-up and sample extraction, ADAM labeling is a viable alternative in identifying and quantifying compounds in the skin.

4.1.3   12-HETE production

Hydroxy fatty acids are known to be involved in chronic and acute skin inflammation *in vivo* (Ruzicka and Printz, 1982c; Camp *et al.*, 1983; Kobza Black *et al.*, 1985). In the course of this study, we were able to illustrate that stimulation of *in vitro* and *in vivo* rat skin preparations by AA, BK and PAF lead to 12-HETE production. The occurrence via AA stimulation was not surprising. Studies on the lipoxygenase pathway in both keratinocytes and Langerhans cells after AA challenge have shown that the main products were 5-, 12- and 15-HETE, with small amounts of LTB$_4$ (Rosenbach *et al.*, 1985; Rosenbach *et al.*, 1990). The major cyclooxygenase product of both cell types was PGD$_2$, with minor traces of PGE$_2$. Others have also detected, to a lesser extent PGF$_{2\alpha}$ and 11-HETE (Sola *et al.*, 1992).

Studies have shown that BK could stimulate the release of 12- and 15-HETE in tissues such as arterial endothelium (Ibe *et al.*, 1989; Legrand *et al.*, 1991), bronchial epithelium (Salari and Chan-Yeung, 1989) and platelets (Gesce *et al.*, 1986) in a variety of species. However, it seems that BK and PAF-stimulated production of 12-HETE in the skin is a novel finding. The mechanism of 12-HETE production by BK and PAF are still unclear. However, a few hypotheses can be postulated. Ziboh and Lord (1979) demonstrated that a membrane-bound phospholipase A$_2$ (PLA$_2$) activity was present in rat and human skin and BK enhanced this activity by causing hydrolysis of phospholipids and formation of AA. Since stimulation by AA can produce any of the HETE compounds, the fact that 12-HETE was the predominant monohydroxy product shows that 12-lipoxygenase is considerably active in the epidermis of the skin. Hence, 12-HETE as the main product of BK stimulation.

The mechanism of PAF actions may follow a similar route, with an added step. PAF is the acetylated product of lyso-PAF, a product concurrently formed with AA from PLA$_2$ activation (Chignard *et al.*, 1984). In the skin, there is no limiting PAF source as human epidermal cells and fibroblasts have demonstrated abilities to produce PAF (Michel *et al.*, 1988; Michel *et al.*, 1990). PAF actions are believed to be mediated by specific cell surface receptors that have been identified on human keratinocytes (Travers *et al.*, 1995). These receptors are functionally linked to phosphoinositol hydrolysis, and activation results in the production of inositol-1, 4, 5-triphosphate (IP$_3$) and diacylglycerol (DAG) (Shukla, 1985). IP$_3$ mobilizes intracellular calcium and DAG

activates protein kinase C. Since PLA$_2$ is calcium dependent, and the source of calcium is believed to be mainly intracellular (van den Bosch, 1980), the indirect release of calcium by PAF may in turn activate PLA$_2$ to release free AA which in turn undergoes similar metabolic processes, as outlined by BK actions, to produce 12-HETE.

4.2 VASCULAR PERMEABILITY EFFECTS OF 12-LIPOXYGENASE PRODUCTS

4.2.1 12-HETE

In demonstrating that 12-HETE was produced in the skin after administration of two known inflammatory mediators (BK and PAF) on both *in vivo* (and *in vitro*) samples, we had satisfied one of the criteria for an inflammatory mediator. The second criterion required "...reproduction of pathological changes by introducing mediators into the tissue *in vivo*".

Increased vascular permeability is one of the cardinal features of acute inflammation and is considered to accompany the early phase of wound healing. Normally, the capillary wall is freely permeable to water and electrolytes but only slightly so to proteins. During inflammation, contraction of endothelial cells results in the development of spaces through which plasma proteins and circulating leukocytes can pass.

The classical technique for determining changes in vascular permeability in cutaneous inflammation is well established (Ramsdell, 1928). The principle is to inject an animal with one of a number of dyes (e.g. Evans blue). This dye becomes attached to circulating plasma albumin to form a stable dye-protein complex (Rawson, 1943; Udaka *et al.*, 1970; Harada *et al.*, 1971). Modifications of this method have included intravenously injecting radiolabelled proteins such as ^{125}I-serum albumin to better quantify the leakage at the inflammatory sites (Williams and Jose, 1981; Rampart and Williams, 1986). Although the test has been used on rabbits, mice, guinea pigs, rats and even man, rats were selected for the following reasons. First, rats have been shown to be less susceptible to variations in anaesthesia, shock, chilling and increased air temperature; conditions which have been found to reduce the leakage effects of test compounds (Spector and Willoughby, 1968). Second, rats have demonstrated a linear relationship between log dose of a test compound and area of cutaneous dye leakage (Sparrow and Wilhelm, 1957) suggesting a cause-and-effect interpretation of the results. Finally, rats were economically more feasible, easy to handle and readily available.

In the skin, extensive work regarding inflammation has been done involving metabolites of the AA cascade (Ruzicka, 1990). Cyclooxygenase products such as PGs are present in many inflammatory exudates (Willis, 1969; Velo *et al.*, 1973; Willoughby *et al.*, 1975) and seem to be prime candidates as modulators. PGs (E$_1$, E$_2$, F$_{1\alpha}$, and F$_{2\alpha}$) have shown to evoke increased vascular permeability in the skin of rat and man (Crunkhorn and Willis, 1971) but have little effects on other species. Despite these differences, PGs have been shown to potentiate the effects of

vascular permeability elicited by direct and leukocyte-dependent mediators (Williams and Morley, 1973; Ikeda et al., 1975; Williams and Peck, 1977). It has been suggested that potentiation may be due either to sensitization of agonist receptors on vascular endothelial cells (Williams and Morley, 1973), or to modulation of cAMP levels in the endothelial cells through adenyl cyclase (Zurier et al., 1974). However, the effect seems best substantiated by modulations in arteriolar vasodilatation (Johnston et al., 1976; Teixeira et al., 1993; Fujii et al., 1994a; Fujii et al., 1994b) leading to an increase in blood flow in the microcirculation of the affected area.

In our study, the in vivo administration of BK and PAF elicited an increase in vascular permeability in the rat skin in a dose-dependent manner. These results were in agreement with other investigators (Williams and Morley, 1973; Ikeda et al., 1975; Chahl, 1976; Whalley et al., 1987; Khalil and Helme, 1992; Fujii et al., 1995). Moreover, the intradermal injection of a similar dose of 12-HPETE and 12-HETE also caused an increase in vascular permeability albeit lower than that observed with BK and PAF. This difference could be attributed to the ability of BK to vasodilate (Higgs et al., 1981) possibly through nitric oxide production (Khalil and Helme, 1992), and PAF to chemoattract PMNL (Archer et al., 1985; Wardlaw et al., 1986; Sigal et al., 1987), in addition to inducing gap formation between endothelial cells (Majno and Palade, 1961; Majno et al., 1969; Arfors et al., 1979). Although the cutaneous effects of 12-HETE have notably involved chemotaxis of PMNL (Turner et al., 1975; Goetzl et al., 1977; Goetzl and Gorman, 1978; Dowd et al., 1985), its influence on vascular permeability has been limited to a few tissues such as lung (Brigham, 1980) and dental pulp (Okiji et al., 1989). The works of Higgs et al. (1981) have shown that 12-HPETE causes a small but significant increase in plasma leakage, while 12-HETE was inactive. The former is consistent with the results we obtained with 12-HPETE, while the latter could be a matter of interspecies differences commonly found between rat and other animals. Indeed, this phenomenon has been consistently observed upon PG administration in rats and rabbits (Williams and Morley, 1973; Johnston et al., 1976; Chahl and Chahl, 1976).

A shortcoming of our present data is that a only one dose of 12-HETE was used to examine changes in vascular permeability. Testing for a dose-dependent effect of 12-HETE and subsequent comparison of these effects with BK and PAF are definitely in the works for the immediate future. Nonetheless, our results show that 12-HETE can mimic, in vivo, the increase in plasma protein leakage induced by BK and PAF, satisfying the second criteria for a potential mediator.

The third parameter, "...attribution of mediator release to resident cells or infiltrating inflammatory cells" has been fulfilled through works done in this study and by other investigators. Certainly the production of 12-HETE by the epidermis by us is in agreement with other studies (Hammarstrom et al., 1979; Ruzicka and Printz, 1982a; Ruzicka et al., 1983; Henke et al., 1986; Cameron et al., 1990; von Zepelin et al., 1991). In addition, 12-HETE has been shown to be synthesized by neutrophils (Borgeat and Samuelsson, 1979; Goetzl and Sun, 1979), vascular tissue (Greenwald et al., 1979), blood platelets (Hamburg and Samuelsson, 1974; Nugteren, 1975), macrophages (Rigaud et al., 1979), mast cells (Roberts et al., 1979) and psoriatic plaques

(Hammarstrom *et al.*, 1975; Hammarstrom *et al.*, 1979). Combined with the fact that BK is released from inflamed tissue (Movat, 1979; Marceau *et al.*, 1983) and PAF from many of the aforementioned inflammatory cell types (Henson, 1970; Lynch *et al.*, 1979; Camussi *et al.*, 1981; Vargaftig *et al.*, 1981; Benveniste *et al.*, 1982; Camussi *et al.*, 1983b) as well as skin fibroblasts (Camussi *et al.*, 1983a; Michel *et al.*, 1988), 12-HETE production during inflammation is very active.

Finally, experiments to "...(modify the) pathological process by administration of specific enzyme inhibitors or receptor antagonists in *vivo*" are also planned for the immediate future. The use of BK and PAF inhibitors as well as 12-HETE receptor antagonists to block the vascular permeability effects of 12-HETE should determine the extent of its involvement in cutaneous inflammation.

4.2.2 Hepoxilins

Much of the focus of this study was directed toward 12-HETE yet, the novel findings obtained with the hepoxilins merit some attention. Like 12-HETE, hepoxilins too, are products derived from the 12-lipoxygenase pathway. Although hepoxilins have been shown to modulate neurotransmission (Piomelli *et al.*, 1987; Carlen *et al.*, 1989; Carlen *et al.*, 1994) and release of insulin (Pace-Asciak and Martin, 1984; Pace-Asciak *et al.*, 1986), studies on the skin have been limited. Previous work demonstrated that co-injection of HxA3 with BK caused potentiation of plasma protein leakage over that produced by BK alone (Pace-Asciak, 1994). Since 12-HETE was shown to increase vascular permeability, it was of obvious interest to see if these hepoxilin compounds (naturally occurring HxA3 and HxB3 and their two structural analogs, HxΔA3 and HxΔB3) could evoke similar effects.

HxA3 and HxB3 are structurally similar compounds with the A and B denoting the position of the hydroxyl group, at C8 and C10 respectively. The epimers of each hepoxilin (R and S forms) represent the moRe polar and leSs polar configurations as determined by HPLC (Demin *et al.*, 1995). The hepoxilin analogs differ from the native hepoxilins by replacement of the epoxide moiety at C11(S) and C12(S) with a cyclopropyl group. It has been observed that the cyclopropane analogs can mimic the actions of HxA3 in blocking the calcium mobilizing effects of chemotactic agents (Laneuville *et al.*, 1993). Their effects appear more potent, possibly because their structure may afford them greater chemical and biological stability.

Application of the ADAM protocol on the *in vivo* and *in vitro* skin preparations failed to detect the presence of any hepoxilins, yet the possibility of their production cannot be entirely ruled out. It is suspected that due to the acidic work-up of the lipoxygenase products, the unstable epoxide moiety of the hepoxilins was converted to the more stable di-hydroxy form characteristic of trioxilins (TrXs). Selection of a more suitable HPLC solvent system to clearly distinguish products in the TrX region would certainly verify this hypothesis. However, it has been shown that hepoxilin production is generally low (as compared to 12-HETE), even after stimulation with

its direct precursor, 12-HPETE (Pace-Asciak *et al.* 1993; Reynaud *et al.*, 1994b). Therefore since the exogenously added AA in our experiments can be metabolized via both the cyclooxygenase and lipoxygenase pathways, the proportion of 12-HPETE actually available for further conversion into hepoxilins would be less. As a result the amount of hepoxilin produced would no doubt be below our levels of detection.

The absence of hepoxilins in the samples only adds to the mystery surrounding their vascular permeability effects *in vivo*. Despite not having exhibited any activity on their own, specific hepoxilin epimers were shown to selectively potentiate plasma protein leakage induced by BK and PAF. HxA_3 and its analogue $Hx\Delta A_3$ had greater effects on BK, $Hx\Delta B_3$ selectively affected PAF while HxB_3 potentiated both BK and PAF . In all cases, activity resided with the R/LP epimer forms while the S/MP forms remained relatively inactive. Interestingly, the 8R/10R and LP stereospecificity of hepoxilin action in the skin contrasted with the finding that the 8S hepoxilins potentiated noradrenaline-induced contraction of aorta and portal vein (Laneuville *et al.*, 1992).

The mechanism of action of the hepoxilins is still unclear but it can be speculated that these compounds may release other undetermined second messengers. Indeed, hepoxilins have been shown to promote the release of DAG and AA from human neutrophils (Nigam *et al.*, 1990) with the latter stimulating vascular permeability on its own (Ikeda *et al.*, 1975; Crummey *et al.*, 1987). Another explanation may be associated with calcium concentrations. It has been shown that injection of calcium-binding agents in rat skin causes an immediate leakage of circulating protein-bound dye (Spector, 1958). Since hepoxilins have demonstrated the ability to increase the transport of calcium across membranes (Derewlany *et al.*, 1984), this may contribute in part, to the increase in vascular permeability.

Issekutz (1981) has shown that hyperemia and hyperpermeability are related temporally and in magnitude to the rate of polymorphonuclear leukocyte (PMNL) migration across the microvascular wall and basement membrane resulting in the generation of other pro-inflammatory mediators. Some of these mediators are BK and PGs and have been described elsewhere. Others include lysosomal enzymes and superoxide, released from PMNLs during phagocytosis of particles at the inflammatory site (Cochrane and Janoff, 1974; Weissmann *et al.*, 1978; Movat, 1979). Lysosomal enzymes may produce tissue damage directly (Goldstein, 1974), while superoxide can damage endothelial cells (Sacks *et al.*, 1978). No doubt experiments involving inhibitors of kinin generation and superoxide dismutase will need to be performed to determine whether hepoxilins affect PMNL migration and/or release these mediators.

A final consideration of hepoxilin action may involve the endothelium-derived relaxing factor, nitric oxide (NO) (Ignarro *et al.*, 1987; Palmer *et al.*, 1987; Moncada *et al.*, 1991). It has been shown that large amounts of NO are produced at the site of inflammation through inducible form of NO synthase present in leukocyte and resident cells. NO has been shown to modulate substance P-induced oedema formation (Hughes *et al.*, 1990) as well as BK-induced vasodilatation

(Khalil and Helme, 1992). This effect may directly or indirectly be associated with cyclic guanylyl monophosphate (cGMP) production resulting in phosphorylation of the endothelial skeleton (Yuan *et al.*, 1993). Administration of L-NAME, a NO inhibitor, demonstrated a dose-dependent inhibition of BK-induced oedema formation in guinea pig skin (Teixeira *et al.*, 1993).

Finally, stereospecificity of hepoxilin action warrants further mention. Endothelial cells are known to possess receptor sites for catecholamines, angiotensin, acetylcholine, histamine and serotonin (Buonassisi and Colburn, 1980). We have demonstrated that binding of hepoxilin exists in human neutrophils (Reynaud *et al.*, 1995) and that this binding results in a rise in intracellular calcium (Dho *et al.*, 1990). Since this study revealed that the R and LP epimers were the preferred forms, it may be possible that specific binding of these epimers exist in the rat skin.

4.2.3 The final word

The 12-lipoxygenase pathway catalyzes a reaction involving removal of a hydrogen atom from AA at C10 with subsequent insertion of molecular O_2 at C12, to yield 12-hydroperoxy-eicosatetraenoic acid (12-HPETE). We conclude from this study that the reduction of unstable 12-HPETE to 12-HETE by a glutathione-dependent peroxidase (Chang *et al.*, 1982) predominates over the enzymatic isomerization to hepoxilins. Although the reasons for this are unclear, it could be speculated that the lipoxygenase and peroxidase activity in the skin are closely linked (e.g. spatially or temporally) such that there is a more automatic conversion to 12-HETE. Perhaps if the conversion of 12-HPETE to 12-HETE can be selectively blocked, this would in turn enhance hepoxilin production. There is also the possibility that in the rat pineal gland and lung where hepoxilin production has been documented (Pace-Asciak *et al.*, 1983; Reynaud *et al.*, 1994a, Reynaud *et al.* 1994b), the combination of more 'hepoxilin synthase' in the tissue and longer stability time of 12-HPETE creates an optimal environment for hepoxilin formation.

4.3 Future Considerations

Much of the work planned for the immediate future has been alluded to elsewhere. These include, testing for HETE and hepoxilin production in the dermis and epidermis for both *in vitro* and *in vivo* preparations, normalizing the incubation time of *in vitro* and *in vivo* preparations to 30 minutes, and examining the dose-dependent effects of 12-HETE alone and in the presence of BK, PAF and 12-lipoxygenase inhibitors. A further consideration is to expand the ADAM protocol to detect cyclooxygenase products to determine the extent of their contribution to BK- and PAF-induced vascular permeability.

In lieu of the stereoselective effects of hepoxilins, steps undertaken to further elucidate their mechanism of action would include testing the combined effects of NO and PGs on vascular permeability with and without pre-administration of cAMP and nitric oxide inhibitors. The ADAM protocol can also be utilized here to detect changes in cyclooxygenase and lipoxygenase activity when hepoxilins are added alone and in combination with other compounds. Although it seems

unlikely that hepoxilins are direct-acting mediators of vascular permeability (since they do not have any effects on their own), they may belong to one of the other two groups, namely vasodilators or leukocyte-dependent mediators. The possibility of the latter can be achieved by using nitrogen mustard to deplete circulating PMNL.

Finally, in light of the specific actions of selective hepoxilins demonstrated in this study, these compounds may serve as additional tools to investigate the roles of other mediators in acute inflammation.

SUMMARY

We determined that the 12-lipoxygenase pathway is highly active in the skin resulting predominantly in the production of 12-HETE after stimulation with BK and PAF *in vitro and in vivo*. The amount of 12-HETE formed was determined as a ratio of ricinoleic acid (internal standard) recovered after derivatization with a fluorescent tag, ADAM, purification through silicic acid column chromatography and analysis on reverse-phase HPLC.

The presence of 12-HETE in the skin preparations and its ability to evoke an increase in vascular permeability on its own *in vivo*, suggest that the leakage effects induced by BK and PAF may be, in part, mediated by 12-HETE, possibly via binding to its receptors located in the epidermis (Gross *et al.*, 1988; Gross *et al.*, 1990). All this, combined with the ability of 12-HETE to induce infiltration of leukocytes (Dowd *et al.*, 1985; Ruzicka and Burg, 1987), chemotaxis of epidermal cells (Hein *et al.*, 1991) and activation of neutrophils (Naccache *et al.*, 1981) provide further support to the idea of 12-HETE as an inflammatory mediator.

The absence of hepoxilin production in the skin at this point, does not diminish the fact that hepoxilins have interesting effects on vascular permeability. This pertains to the selectivity and specificity of $HxA_3(8R)$, $Hx\Delta A_3(LP)$ and $HxB_3(10R)$ to potentiate BK-induced vascular permeability in addition to $HxB_3(10R)$ and $Hx\Delta B_3(LP)$ to potentiate PAF effects. This modulatory characteristic of hepoxilins may be of importance in other areas of inflammation.

The inflammatory response is designed to rid the body of a foreign invader and effectively dispose of it so that healing can occur. In clinical medicine, the hope is to control the inflammatory process such that the reaction itself does not bring about local damage as seen in many chronic conditions (e.g. Arthus reaction, psoriasis, rheumatoid arthritis). The ability to pharmacologically control inflammation by antagonizing the release of mediators or directly affecting the function of inflammatory cells are just some ways in which relief may be achieved.

REFERENCES

Agner T, Serup J. Sodium lauryl sulphate for irritant patch testing - a dose response study using bioengineering methods for determination of skin irritation. *J Invest Dermatol* 1990; **95**: 543-547.

Archer CB, Page CP, Paul W, Morley J, MacDonald DM. Inflammatory cell accumulation in response to intracutaneous Paf-acether: a mediator of acute and persistent inflammation? *Br J Dermatol* 1985; **113 [Suppl 28]**: 133-135.

Arfors KE, Rutili G, Svensjo E. Microvascular transport of macromolecules in normal and inflammatory conditions. *Acta Physiol Scand* 1979; **463 [Suppl]**: 93-103.

Baars AJ, Mukhtar H, Zoetemelk CEM, Jansen M, Breimer DD. Glutathione-S-transferase activity in rat and human tissues and organs. *Comp Biochem Physiolol [C]* 1981; **70**: 285-288.

Bedord CJ, Young JM, Wagner BM. Anthralin inhibition of mouse epidermal arachidonic acid lipoxygenase *in vitro*. *J Invest Dermatol* 1983; **81**: 566-571

Benveniste J, Roubin R, Chignard M, Jouvin-Marche E, Le Couedic JP. Release of platelet-activating factor (PAF-acether) and 2-lyso PAF-acether from three cell types. *Agents Actions* 1982; **12**: 711-713.

Bhattacherjee P, Eakins KA, Hammond B. Chemotactic activity of arachidonic acid lipoxygenase products in the rabbit eye. *Br J Pharmacol* 1981; **73**: 254P-255P.

Bickers DR, Dutta-Choudhury T, Mukhtar H. Epidermis: a site of drug metabolism in neonatal rat skin. Studies on cytochrome P-450 content and mixed-function oxidase and epoxide hydrolase activity. *Mol Pharmacol* 1982; **21**: 239-247.

Borch RF. Separation of long fatty acids as penacyl esters by high pressure liquid chromatography. *Anal Chem* 1975; **47**: 2437-2438.

Borgeat P, Samuelsson B. Arachidonic acid metabolism in polymorphonuclear leukocytes: effects of ionophore A23187. *Proc Natl Acad Sci USA* 1979; **76**: 2148-2152.

Bray MA, Ford-Hutchinson AW, Smith MJH. Leukotriene B_4 and leucocyte movement. *Br J Pharmacol* 1980; **73**: 259P-260P.

Bray MA, Ford-Hutchinson AW, Smith MJH. Leukotriene B_4: an inflammatory mediator in vivo. *Prostaglandins* 1981; **22**: 213.

Brigham KL. Pulmonary dysfunction of diffuse lung inflammation. Role of mediators of arachidonic acid. *Prog Biochem Pharmacol* 1980; **20**: 26-37.

Buonassisi V, Colburn P. Hormone and surface receptors in vascular endothelium. In: B.M. Altana, eds. Advances in Microcirculation. Karger: Bassel, 1980: 76.

Cameron GS, Baldwin JK, Jashway DW, Patrick KE, Fischer SM. Arachidonic acid metabolism varies with the state of differentiation in density gradient-separated mouse epidermal cells. *J Invest Dermatol* 1990; **94**: 292-296.

Camp RDR, Greaves MW, Hensby CN, Plummer NA, Warin AP. Irradiation of human skin by short wavelength ultraviolet radiation (100-290nm) (UV-C): increased concentration of arachidonic acid and prostaglandins E_2 and F_2 alpha. *Br J Clin Pharmacol* 1978; **61**: 145-148.

Camp RDR, Derm FF. Cutaneous pharmacology: perspectives on the growth of investigation of mediators of inflammation. *J Invest Dermatol* 1989; **92**: 78S-83S.

Camp RDR, Mallet AI, Woollard PM, Brain SD, Kobza Black A, Greaves MW. The identification of hydroxy fatty acids in psoriatic skin. *Prostaglandins* 1983; **26**: 431-447.

Camussi G, Aglietta M, Coda R, Bussolino F, Piacibello W, Tetta C. Release of platelet-activating factor (PAF) and histamine. II. The cellular origin of human PAF: monocytes, polymorphonuclear neutrophils and basophils. *Immunology* 1981; **42**: 191-199.

Camussi G, Aglietta M, Malavasi F, Tetta C, Piacibello W, Sanavio F, Bussolino F. The release of platelet-activating factor from human endothelial cells in culture. *J Immunol* 1983a; **131**: 2397-2403.

Camussi G, Pawlowski I, Bussolino F, Caldwell PRB, Brentjens J, Andres G. Release of platelet activating factor in rat antibody-mediated injury of the lung: the role of leukocyte pulmonary endothelial cells. *J Immunol* 1983b; **131**: 1804-1807.

Carlen PL, Gurevich N, Wu PH, Su WG, Corey EJ, Pace-Asciak CR. Actions of arachidonic acid and hepoxilin A_3 on mammalian CA1 neurons. *Brain Res* 1989; **497**: 171-176.

Carlen PL, Gurevich N, Zhang L, Wu PH, Reynaud D, Pace-Asciak CR. Formation and electrophysiological actions of the arachidonic acid metabolites, hepoxilins, at nanomolar concentrations in rat hippocampal slices. *Neurosciences* 1994; **58**: 493-502.

Carr SC, Higgs GA, Salmon JA, Spayne JA. The effects of archidonate lipoxygenase products on leukocyte migration in rabbit skin. *Br J Pharmacol* 1981; **73**: 253P-254P.

Chahl JS, Chahl LA. The role of prostaglandins in chemically induced inflammation. *Br J Exp Path* 1976; **57**: 689-695.

Chahl LA. Interactions of bradykinin, prostaglandin E_1, 5-hydroxytryptamine, histamine and adenosine-5'-triphosphate on the dye leakage response in rat skin. *J Pharm Pharmac* 1976; **28**: 753-757.

Chang WC, Nakao J, Orimo H, Murota SI. Effects of reduced glutathione on the 12-lipoxygenase pathways in rat platelets. *Biochim J* 1982; **202**: 771.

Chignard M, Le Couedic JP, Coeffier E, Benveniste J. PAF-acether formation and archidonic acid freeing from platelet ether-linked glyceryl phosphorylcholine. *Biochem Biophys Res Commun* 1984; **124**: 637-643.

Cochrane CG, Janoff A, The Arthus reaction: a model of neutrophil and complement mediated injury. In: B. Zweifach, L. Grant and R. T. McClusky, eds. The Inflammatory Process. New York: Academic Press, 1974: 85.

Conheim J. Inflammation lectures in general pathology. New Sydenham Society, 1889: 1:242-382

Cooper MJ, Anders MW. Determination of long chain fatty acids as 2-napthacyl esters by high-pressure liquid chromatography and mass spectrometry. *Anal Chem* 1974; **46**: 1849-1852.

Crummey A, Harper GP, Boyle EA, Mangan FR. Inhibiton of arachidonic acid-induced ear oedema as a model for topical anti-inflammatory compounds. *Agents Actions* 1987; **20**: 69-76.

Crunkhorn P, Willis AL. Cutaneous reactions to intradermal prostaglandins. *Br J Pharmacol* 1971; **41**: 49-56.

Dale HH. Some chemical factors in the control of the circulation. *Lancet* 1929; **1**: 1285.

Demin P, Reynaud D, Pace-Asciak CR. High performance liquid chromatographic separation of fluorescent esters of hepoxilin enanatiomers on a chiral stationary phase. *J Chromatography B: Biomedical applications* 1995; **672:** 282-289.

Demin PM, Pivnitsky KK, Vasiljeva LL, Pace-Asciak CR. Synthesis of methyl [5,6,8,9,14,15-^{3}H6] hepoxilin B$_3$ and its conversion to methyl [5,6,8,9,14,15-^{3}H6] hepoxilin A$_3$. *J Labelled Compounds and Radiopharmaceuticals* 1994; **34:** 221-230.

Derewlany LO, Pace-Asciak CR, Radde IC. Hepoxilin A, hydroxyepoxide metabolite of arachidonic acid stimulates transport of calcium-45 across the guinea pig visceral yolk sac. *Can J Physiol Pharmacol* 1984; **62:** 1466-1469.

Dho S, Grinstein S, Corey EJ, Su WG, Pace-Asciak CR. Hepoxilin A$_3$ induces changes in cytosolic calcium intracellular pH and membrane potential in human neutrophils. *Biochem J* 1990; **266:** 63-68.

Dowd PM, Black AK, Woollard PM, Camp RDR, Derm FF, Greaves MW. Cutaneous responses to 12-hydroxy-5,8,10,14-eicosatetraenoic acid (12-HETE). *J Invest Dermatol* 1985; **84:** 537-541.

Dunn CJ, Willoughby DA, The inflammatory response-a review. In: M. W. Greaves and S. Shuster, eds. Pharmacology of the skin. Berlin: Springer-Verlag, 1989 : 465-477.

Eckert RL. Structure, function, and differentiation of the keratinocyte. *Physiol Rev* 1989; **69:** 1316-1345.

Falgueyret JP, Leblanc Y, Riendeau D. Stereoselective carbonyl reductases from rat skin and leukocyte microsomes converting 12-ketoeicosatetraenoic acid to 12(S)-HETE. *FEBS* 1990; **262:** 197-200.

Finnen MJ, Herdman ML, Shuster S. Distribution and sub-cellular localization of drug metabolizing enzymes in the skin. *Br J Dermatol* 1985; **113:** 713-721.

Ford-Hutchinson AW, Bray MA, Doig MV, Shipley ME, Smith MJH. Leukotriene B, a potent chemokinetic and aggregating substance released from polymorphonuclear leucocytes. *Nature* 1980; **286:** 264-265.

Fujii E, Irie K, Muraki T. Nitric oxide plays a role in increase in vascular permeability induced by bradykinin but not by platelet-activating factor (PAF) or histamine in mouse skin. *Jpn J Pharmacol* 1994a; **64 [Suppl]:** 312P.

Fujii E, Irie K, Uchida Y, Ohba K, Muraki T. Role of eicosanoids but not nitric oxide in the platelet-activating factor-induced increase in vascular permeability in mouse skin. *Eur J Pharmacol* 1995; **273:** 267-272.

Fujii E, Irie K, Uchida Y, Tsukahara F, Muraki T. Possible role of nitric oxide in 5-hydroxytryptamine-induced increase in vascular permeability in mouse skin. *Naunyn-Schmiedeberg's Arch Pharmacol* 1994b; **350:** 361-364.

Gad SC, Walsh RD, Dunn BJ. Correlation of ocular and dermal irritancy of industrial chemicals. *J Toxicol Cutaneous Ocul Toxicol* 1986; **5:** 195-213.

Gesce A, Mezei Z, Telegdy G. The action of peptide and protease on the arachidonate cascade of human and rat platelets. *Adv Exp Med Biol* 1986; **198 (pt B):** 121-128.

Goetzl EJ, Gorman RR. Chemotactic and chemokinetic stimulation of human eosinophil and neutrophil polymorphonuclear leukocytes by 12-L-hydroxy-5,8-heptadecatrienoic acid (12-HHT). *J Immunol* 1978; **120:** 526-531.

Goetzl EJ, Sun FF. Generation of unique mono-hydroxy-eicosatetraenoic acids from arachidonic acid by human neutrophils. *J Exp Med* 1979; **150:** 406-411.

Goetzl EJ, Woods JM, Gorman RR. Stimulation of human eosinophil and neutrophil polymorphonuclear leukocyte chemotaxis and random migration by 12-L-hydroxy-5,8,10,14-eicosatetraenoic acid. *J Clin Invest* 1977; **59:** 179-183.

Goldstein IM, Lysosomal hydrolases and inflammatory materials. In: G. Weissmann, eds. Mediators of Inflammation. New York: Plenum Press, 1974:51-60.

Green H. Terminal differentiation of cultured human epidermal cell. *Cell* 1977; **11:** 405-416.

Greenwald JE, Bianchine JR, Wong LK. The production of the arachidonate metabolite HETE in vascular tissue. *Nature* 1979; **281:** 588-589.

Gross E, Ruzicka T, Mauch C, Krieg T. Evidence for LTB₄/12-HETE binding sites in a human epidermal cell line. *Prostaglandins* 1988; **36:** 49-58.

Gross E, Ruzicka T, Restoff B, Stolz W, Klotz KN. High-affinity binding and lack of growth-promoting activity of 12(S)-hydroxyeicosatetraenoic acid (12(S)-HETE) in human epidermal cell line. *J Invest Dermatol* 1990; **94:** 446-451.

Gschwendt M, Furstenberger G, Kittstein W, Beseemfelder E, Hull WE, Hagedorn H, Opferkuch HJ, Marks F. Generation of the arachidonic acid metabolite 8-HETE by extracts of mouse skin treated with phorbol ester *in vivo*: identification of ^{H}-n.m.r. and GC-MS spectroscopy. *Carcinogenesis* 1986; **7:** 449-455.

Habif TP, In: E.A. Klein, B.S. Menczer, S. Walker, eds. Clinical Dermatology. A Color Guide to Diagnosis and Therapy. St. Louis: C.V. Mosby Company, 1990:10

Hamberg M, Samuelsson B. Prostaglandin endoperoxides. Novel transformation of arachidonic acid in human platelets. *Proc Natl Acad Sci* 1974; **71:** 3400-3404.

Hammarstrom S, Hamberg M, Samuelsson B, Duell EA, Stawiski M, Vorhees JJ. Increased concentrations of non-esterified arachidonic acid, 12L-hydroxy-5,8,10,14-eicosatetrenoic acid, prostaglandin E₂ and prostaglandin F₂-alpha in epidemis of psoriasis. *Proc Natl Acad Sci* 1975; **72:** 5130-5134.

Hammarstrom S, Lindgren JA, Marcelo C, Duell EA, Anderson TF, Voorhees JJ. Arachidonic acid transformations in normal and psoriatic skin. *J Invest Dermatol* 1979; **73:** 180-183.

Harada M, Takeuchi M, Fukao T, Katagiri K. A simple method for the quantitative extraction of dye extravasated into the skin. *J Pharm Pharmac* 1971; **23:** 218-219.

Harper KH, Calcutt G. Conjugation of 3,4-benz-pyrenols in mouse skin. *Nature (London)* 1960; **186:** 80-81.

Hein R, Gross E, Ruzicka T, Krieg T. 12-hydroxyeicosatetraenoic acid (12-HETE) is a chemotactic stimulus for epidermal cells. *Arch Dermatol Res* 1991; **28:** 135-137.

Henke D, Danilowicz R, Eling T. Arachidonic acid metabolism by isolated epidermal basal and differentiated keratinocytes from the hairless mouse. *Biochim Biophys Acta* 1986; **876:** 271-279.

Hensby CN, Plummer NA, Black AK, Fincham N, Greaves MW. Time-course of arachidonic acid, prostaglandins E_2 and F_2 alpha in human abdominal skin, following irradiation with ultraviolet wavelengths (290-320nm). *Adv Prost & Thromb Res* 1980; **7:** 857-850.

Henson PM. Release of vasoactive amines from rabbit platelets induced by sensitized monouclear leukocytes and antigen. *J Exp Med* 1970; **131:** 287-306.

Higgs GA, Salmon JA, Spayne JA. The inflammatory effects of hydroperoxy and hydroxy acid products of arachidonate lipoxygenase in rabbit skin. *Br J Pharmac* 1981; **74:** 429-433.

Holbrook KA, Wolff K, The structure and development of skin. In: T. B. Fitzpatrick, A. Z. Eisen, K. Wolff, I. M. Freedberg and K. F. Austen, eds. Dermatology in General Medicine. New York: McGraw-Hill, 1987 : 93.

Hughes SR, Williams TJ, Brain SD. Evidence that endogenous nitric oxide modulates oedema formation induced by substance P. *Eur J Pharmacol* 1990; **191:** 481-484.

Ibe BO, Falck JR, Johnson AR, Campbell WB. Regulation of synthesis of prostacyclin and HETE in human endothelial cells. *Am J Physiol* 1989; **256 (6 pt1):** C1168-C1175.

Ignarro LJ, Buga GM, Wood KS, Byrns RE, Chaudhuri G. Endothelium-derived relaxing factor produced and released from artery and vein is nitric oxide. *Proc Natl Acad Sci USA* 1987; **84:** 9265-9269.

Ikeda K, Tanaka K, Katori M. Potentiation of bradykinin-induced vascular permeability increase by PGE_2 and arachidonic acid in rabbit skin. *Prostaglandins* 1975; **10:** 747-758.

Imaoka S, Funae Y, Sugimoto T, Hayahara N, Maekawa M. Specific and rapid assay of urinary oxalic acid using high-performance liquid chromatography. *Anal Biochem* 1983; **128:** 459-464.

Irvine RF. How is the level of free arachidonic acid controlled in mammalian cells? *Biochem J* 1982; **204:** 3-16.

Issekutz AC. Vascular responses during acute neutrophilic inflammation. *Lab Invest* 1981; **45:** 435-441.

Jimbow K, Queuedo WC, Fitzpatrick TB, Szabo G. Some aspects of melanin biology:1950-1970. *J Invest Dermatol* 1976; **67:** 72-89.

Johnston MG, Hay JB, Movat HZ. The modulation of enhanced vascular permeability by prostaglandins through alterations in blood flow (hyperemia). *Agents Actions* 1976; **6:** 705-711.

Kellaway CH, Trethewie ER. The liberation of slow reacting smooth muscle-stimulating substances in anaphylaxis. *Q J Exp Physiol Cogn Med Sci* 1940; **30:** 121-145.

Khalil Z, Helme RD. The quantitative contribution of nitric oxide and sensory nerves to bradykinin-induced inflammation in rat skin microvasculature. *Brain Res* 1992; **589:** 102-108.

Kobza Black A, Barr RM, Wong E, Brain S, Greaves MW, Dickinson R, Shroot B, Hensby CN. Lipoxygenase products of arachdionic acid in human inflamed skin. *Br J Clin Pharmacol* 1985; **20:** 185-190.

Kragballe K, Pinnamaneni G, Desjarlais L, Duell EA, Voorhees JJ. Dermis-derived 15-hydroxy-eicosatetraenoic acid inhibits epidermal 12-lipoxygenase activity. *J Invest Dermatol* 1986; **87:** 494-498.

Lands WEM, Samuelsson B. Phospholipid precursors of prostaglandins. *Biochim Biophys Acta* 1968; **164:** 426-429.

Laneuville O, Corey EJ, Couture R, Pace-Asciak CR. Hepoxilin A_3 (HxA_3) is formed by the rat aorta and is metabolized into HxA_3-C, a glutathione conjugate. *Biochim Biophys Acta* 1991a; **1084:** 60-68.

Laneuville O, Corey EJ, Couture R, Pace-Asciak CR. Hepoxilin A_3 increases vascular permeability in the rat skin. *Eicosanoids* 1991b; **4:** 95-97.

Laneuville O, Couture R, Pace-Asciak CR. Hepoxilins sensitize blood vessels to noradrenaline-stereospecificity of action. *Br J Pharmacol* 1992; **105:** 297-304.

Laneuville O, Reynaud D, Grinstein S, Nigam S, Pace-Asciak CR. Hepoxilin A_3 inhibits the rise in free intracellular calcium evoked by formyl-methionyl-leucyl-phenylalanine, platelet-activating factor and leukotriene B_4. *Biochem J* 1993; **295:** 393-397.

Legrand AB, Lawson JA, Meyrick BO, Blair IA, Oates JA. Substitution of 15-hydroxyeicosatetraenoic acid in phosphinositide signalling pathway. *J Biol Chem* 1991; **266:** 7570-7577.

Lynch JM, Lotner GZ, Betz SJ, Henson PM. The release of platelet-activating factor by stimulated rabbit neutrophils. *J Immunol* 1979; **123:** 1219-1226.

Maas RL, Turk J, Oates JA, Brash AR. Formation of a novel dihydroxy acid from arachidonic acid by lipoxygenase-catalyzed double oxygenation in rat mononuclear cells and human leukocytes. *J Biol Chem* 1982; **257:** 7056-7067.

MacNicoll AD, Grover PL, Sims P. The metabolism of a series of polycyclic hydrocarbons by mouse skin maintained in short-term organ culture. *Chem Biol Interact* 1980; **29:** 169-188.

Majno G, Palade GE. Studies on inflammation I. The effect of histamine and serotonin on vascular permeability: an electron microscopic study. *J Biophys Biochem Cytol* 1961; **11:** 571-605.

Majno G, Palade GE, Schoefl GI. Studies in Inflammation. II. The site of action of histamine and serotonin along vascular tree. A topographic study. *J Biophys Biochem Cytol* 1961; **11:** 607-632.

Majno G, Shea SM, Leventhal M. Endothelial contraction induced by histamine-type mediators: an electron microscopic study. *J Cell Biol* 1969; **42:** 647-672.

Marceau F, Lussier A, Regoli D, Giroud JP. Pharmacology of kinins: their relevence to tissue injury and inflammation. *Gen Pharmacol* 1983; **14:** 209-29.

Mayer B, Rauter L, Zenzmaier E, Gleispach H, Esterbauer H. Characterization of lipoxygenase metabolites of arachidonic acid in cultured human skin fibroblasts. *Biochim Biophys Acta* 1984; **795:** 151-161.

Michel L, Denizot Y, Thomas Y, Jean-Louis F, Heslan M, Benveniste J, Dubertret L. Production of Paf-acether by human epidermal cells. *J Invest Dermatol* 1990; **95:** 576-581.

Michel L, Denizot Y, Thomas Y, Jean-Louis F, Pitton C, Benveniste J, Dubertret L. Biosynthesis of Paf-acether by human skin fibroblasts *in vitro*. *J Immunol* 1988; **141:** 948-953.

Michel L, Dubertret L. Leukotriene B_4 and platelet-activating factor in human skin. *Dermatol Res* 1992; **284 [Suppl 1]:**S12-S17.

Moncada S, Palmer RMJ, Higgs EA. Nitric oxide: physiology, pathophysiology and pharmacology. *Pharmacol Rev* 1991; **43:** 109-142.

Movat HZ, The acute inflammatory reaction. In: H. Z. Movat, eds. Inflammation, Immunity and Hypersensitivity. Hagerstown, Maryland: Harper and Row, 1979: 1-162.

Mukhtar H, The structure and function of the skin. In: H. Mukhtar, eds. Pharmacology of the skin. Boca Raton: CRC Press Inc., 1992: 3-10.

Mukhtar H, Bresnick E. Glutathione-S-epoxidetransferase in mouse skin and human foreskin. *J Invest Dermatol* 1976; **66:** 161-164.

Mukhtar H, Khan WA. Cutaneous cytochrome P-450. *Drug Metab Rev* 1989; **20:** 657-673.

Naccache PH, Sha'afi RI, Borgeat P, Goetzl EJ. Mono- and dihydroxyeicosatetraenoic acids alter calcium homeostasis in rabbit neutrophils. *J Clin Invest* 1981; **67:** 1584-1587.

Nakagawa Y, Waku K. Determination of the amounts of free arachidonic acid in resident and activated rabbit alveolar macrophages by fluorometric high performance liquid chromatography. *Lipids* 1985; **20:** 482-486.

Nigam S, Nodes S, Cichon G, Corey EJ, Pace-Asciak CR. Receptor-mediated action of hepoxilin A3 releases diacylglycerol and arachidonic acid from human neutrophils. *Biochem Biophys Res Commun* 1990; **171:** 944-948.

Nimura N, Ishida K, Kinoshita T. Novel post-column derivatization method for the fluorimetive, determination of norepinephrine and epinephrine *J Chromatogr* 1980; **221:** 249-255.

Nugteren DH. Arachidonate lipoxygenase in blood platelets. *Biochim Biophys Acta* 1975; **380:** 299-307.

Nugteren DH, Kiviti GA. Conversion of linoleic acid and arachidonic acid by skin epidermal lipoxygenase. *Biochim Biophys Acta* 1987; **921:** 135-141.

Okiji T, Morita I, Sunada I, Murota S. Involvement of arachidonic acid metabolites in increases in vascular permeability in experimental dental pulpal inflammation in rat. *Arch Oral Biol* 1989; **34:** 523-528.

Pace-Asciak CR. Formation and metabolism of hepoxilin A3 by rat brain. *Biochem Biophys Res Commun* 1988; **151:** 493-198.

Pace-Asciak CR. Hepoxilins: a review on their cellular actions. *Biochim Biophys Acta* 1994; **1215:** 1-8.

Pace-Asciak CR, Granstrom E, Samuelsson B. Arachidonic acid epoxides isolation and structure of 2 hydroxy epoxide intermediates in the formation of 8,11,12-trihydroxyeicosatetraenoic acid and 10,11,12-hydroxyeicosatetraenoic acid. *J Biol Chem* 1983; **258:** 6835-6840.

Pace-Asciak CR, Martin JM. Hepoxilin, a new family of insulin secretagogues formed by intact rat pancreatic islets. *Prost Leuk Med* 1984; **16:** 173-180.

Pace-Asciak CR, Martin JM, Corey EJ. Hepoxilins, potential endogenous mediators of insulin release. *Prog Lipid Res* 1986; **25:** 625-628.

Pace-Asciak CR, Martin JM, Corey EJ, Su WG. Endogenous release of hepoxilin A3 from perfused pancreatic islets of Langerhans. *Biochem Biophys Res Commun* 1985; **128:** 942-946.

Pace-Asciak CR, Reynaud D, Demin P. Enzymatic formation of hepoxilins A₃ and B₃. *Biochem Biophys Res Commun* 1993; **197**: 869-873.

Palmer RMJ, Ferrige AG, Moncada S. Nitric oxide release accounts for the biological activity activity of endothelium-derived relaxing factor. *Nature* 1987; **327**: 524-526.

Pei PT, Kossa WC, Ramachandran S, Henly RS. High pressure reverse phase liquid chromatography of fatty acid p-bromophenacyl esters. *Lipids* 1976; **11**: 814-816.

Perkins EB, In: E. G. Perkins, eds. Analysis of lipids and lipoproteins. Champaign,Ill: American Oil Chemists' Society, 1975 : 183-203.

Piomelli D, Feinmark SJ, Schwarzy JH (1987). 12-hydroperoxyeicosatetraenoic acid (12-HPETE) a lipoxygenase metabolite of arachidonic acid that produces pre-synaptic inhibition in aplysia is metabolized to the hepoxilin A and B in neural tissue. 17th Annual Meeting of the Society of Neuroscience, New Orleans,

Quevedo WC, Fleischmann RD. Developmental biology of mammalian melanocytes. *J Invest Dermatol* 1980; **75**: 116-120.

Rampart M, Williams TJ. Polymorphonuclear leukocyte-dependent plasma leakage in rabbit skin is enhanced or inhibited by prostaglandin, depending on route of administration. *Am J Path* 1986; **124**: 66-73.

Ramsdell SG. The use of trypan blue to demonstrate the immediate skin reaction in rabbits and guinea pigs. *J Immunol* 1928; **15**: 305-311.

Rawson RA. The binding of T-1824 and structurally related diazo dyes by the plasma proteins. *Am J Physiol* 1942; **138**: 708-717.

Reynaud D, Delton I, Gharib A, Sarda N, Lagarde M, Pace-Asciak CR. Formation, metabolism, and action of hepoxilin A₃ in the rat pineal gland. *J Neurochem* 1994a; **62**: 126-133.

Reynaud D, Demin P, Pace-Asciak CR. Hepoxilin A₃ formation in the rat pineal gland selectively utilizes (12S)-hydroperoxyeicosatetraenoic acid (HPETE) but not (12R)-HPETE. *J Biol Chem* 1994b; **269**: 23976-23976.

Reynaud D, Demin P, Pace-Asciak CR. Hepoxilin binding in human neutrophils. *Biochem Biophys Res Commun* 1995; **207**: 191-194.

Rigaud M, Durand J, Breton JC. Transformation of arachidonic acid into 12-hydroxy-5,8,10,14-eicosatetraenoic acid by mouse peritoneal macrophages. *Biochim Biophys Acta* 1979; **573**: 408-412.

Roberts LJ, Lewis RA, Oates JA, Austen KF. Prostaglandin, thromboxane and 12-hydroxy-5,8,10,14-eicosatetraenoic acid production by ionophore-stimulated rat serosal mast cells. *Biochim Biophys Acta* 1979; **575**: 185-192.

Rosenbach T, Czarnielewski BM, Hecker M, Czarnetzski B. Comparison of eicosanoid generation by highly purified human Langerhans cells and keratinocytes. *J Invest Dermatol* 1990; **95**: 104-105.

Rosenbach T, Grabe J, Moller A, Schwanitz HJ, Czarnetski BM. Generation of leukotrienes from normal epidermis and their demonstration in cutaneous disease. *Br J Dermatol* 1985; **113** [Suppl 28]: 157-167.

Rowden G. The Langerhans cell. *CRC Crit Rev Immunol* 1981; 95-180.

Ruzicka T, Eicosanoids in inflammatory skin diseases. In: T. Ruzicka, eds. Eicosanoids and the skin. Boca Raton: CRC Press, 1990 : 53-65.

Ruzicka T, Aubock J. Arachidonic acid metabolism in guinea pig Langerhans cells: studies on cyclooxygenase and lipoxygenase pathways. *J Immunol* 1987; **138:** 539-543.

Ruzicka T, Burg G. Effect of chronic intracutaneous administration of arachidonic acid and its metabolites. Induction of leukocytoclastic vasculitis by leukotriene B_4 and 12-hydroxyeicosatetraenoic acid and its prevention by prostaglandin E_2. *J Invest Dermatol* 1987; **88:** 120-123.

Ruzicka T, Printz MP. Arachidonic acid metabolism in guinea pig skin. *Biochim Biophys Acta* 1982a; **711:** 391-397.

Ruzicka T, Printz MP. Arachidonic acid metabolism in guinea pig skin: effects of chloroquine. *Agents Actions* 1982b; **12:** 527-529.

Ruzicka T, Printz MP. Arachidonic acid metabolism in skin: Experimental contact dermatitis in guinea pigs. *Int Arch Allergy Appl Immunol* 1982c; **69:** 347-352.

Ruzicka T, Vitto A, Printz MP. Epidermal arachidonate lipoxygenase. *Biochim Biophys Acta* 1983; **751:** 369-374.

Ryan GB, Majno G, Inflammation. In: B. A. Thomas, eds. Kalamazoo: Upjohn Company, 1977: 5.

Sacks T, Moldow CF, Craddock PR, Bowers TK, Jacob HS. Oxygen radicals mediate endothelial cell damage by complement-stimulated granulocytes: an *in vitro* model of immune vascular damage. *J Clin Invest* 1978; **61:** 1161.

Salari H, Chan-Yeung M. Release of 15-hydroxyeicosatetrenoic acid (15-HETE) and prostaglandin E_2 (PGE_2) by cultured human bronchial epithelial cells. *Respir Cell Mol Biol* 1989; **1:** 245-250.

Serhan CN, Hamberg M, Samuelsson B. Lipoxins: novel series of biologically active compounds formed from arachidonic acid in human leukocytes. *Proc Natl Acad Sci* 1984a; **81:** 5335-5339.

Serhan CN, Hamberg M, Samuelsson B. Trihydroxytetraenes: a novel series of compounds formed from arachidonic acid in human leukocytes. *Biochem Biophys Res Commun* 1984b; **118:** 943-949.

Shak S, Perez DH, Goldstein IM. A novel dioxygenation product of arachidonic acid possesses potent chemotactic activity for human polymorphonuclear leukocytes. *J Biol Chem* 1983; **258:** 14948-14953.

Shukla SD. Platelet-activating factor-stimulated formation of inositol-tris phosphate in platelets and its regulation by various agents including calcium, indomethacin, CV3988 and forskolin. *Arch Biochem Biophys* 1985; **240:** 674-679.

Sigal CE, Valone FH, Holtzmann MJ, Goetzl EJ. Preferential human eosinophil chemotactic activity of the platelet activating factor (1-O-alkyl-2-acetyl-sn-glycerol-3-phosphatidylcholine). *J Clin Immunol* 1987; **7:** 179-185.

Smith MJH, Ford-Hutchinson AW, Bray MA. Leukotriene B: a potential mediator of inflammation. *J Pharmac Pharmacol* 1980; **32:** 517-518.

Sola J, Godessart N, Vila L, Puig L, de Moragas JM. Epidermal cell-polymorphonuclear leukocyte cooperation in the formation of leukotriene B4 by transcellular biosynthase. *J Invest Dermatol* 1992; **98:** 333-339.

Sparrow EM, Wilhelm DL. Species differences in susceptibility to capillary permeability factors. Histamine, 5-hydroxytryptamine and compound 48/80. *J Physiol* 1957; **137:** 51-65.

Spector WG. Substances which affect capillary permeability. *Pharmacol Rev* 1958; **10:**475-505.

Spector WG, Willoughby DA. The inflammatory response. *Bacteriol Rev* 1963; **2:** 117-154.

Stenn KS, The skin. In: L. Weiss, eds. Histology, Cell and Tissue Biology. New York: Elsevier Biomedical, 1983 : 569.

Summer KH, Goggelmann W. 1-Chloro-dinitrobenzene depletes glutathione in rat skin and is mutagenic in Salmonella typhimurium. *Mutation Res* 1980; **77:** 91-93.

Teixeira MM, Williams TJ, Hellewell PG. Role of prostaglandins and nitric oxide in acute inflammatory reactions in guinea pig skin. *Br J Pharamacol* 1993; **110:** 1515-1521.

Travers JB, Clark Huff J, Rola-Pleszczynski M, Gelfand EW, Morelli JG. Identification of functional platelet-activating factor receptors on human keratinocytes. *J Invest Dermatol* 1995; **105:** 816-823.

Turk J, Maas RL, Brash AR, Roberts LJ, Oates JA. Arachidonic acid 15-lipoxygenase products from human eosinophils. *J Biol Chem* 1982; **257:** 7068-7076.

Turner SR, Tainer JA, Lynn WS. Biogenesis of chemotactic molecules by the arachidonate system of platelets. *Nature* 1975; **257:** 680-681.

Udaka K, Takeuchi Y, Movat HZ. Simple method for qunatitation of enhanced vascular permeability. *Proc Soc Exp Biol Med* 1970; **133:** 1384-1386.

van de Sandt JJ, Maas WJ, Doornink PC, Rutten AA. Release of arachidonic and linoleic acid metabolites in skin organ cultures as characteristics of *in vitro* skin irritancy. *Fundam Appl Toxicol* 1995; **25:** 20-28.

van den Bosch H. Intracellular phospholipase A. *Biochim Biophys Acta* 1980; **604:** 191-246.

Vanderhoek JY, Bryant RW, Bailey JM. Regulation of leukocyte and platelet lipoxygenase by hydroxy eicosanoids. *Biochem Pharmacol* 1982a; **31:** 3463-3467.

Vanderhoek JY, Tare NS, Bailey JM, Goldstein AL, Pluznik DH. New role for 15-hydroxyeicosatetraenoic acid. Activator of leukotriene biosynthesis in PT-18 mast and basophil cells. *J Biol Chem* 1982b; **257:** 12191-12195.

Vargaftig BB, Chignard M, Benveniste J, Lefort J, Wal F. Background and present status of research on platelet-activating factor (PAF-acether). *Ann NY Acad Sci* 1981; **370:** 119.

Velo GP, Dunn CJ, Giroud J, Timsit J, Willoughby DA. Distribution of prostaglandins in inflammatory exudate. *J Path* 1973; **111:** 149-158.

von Zepelin HHH, Schroder JM, Smid P, Reusch MK, Christophers E. Metabolism of arachidonic acid by human epidermal cells depends upon maturational stage. *J Invest Dermatol* 1991; **97:** 291-297.

Wardlaw AJ, Moqbel R, Cromwell O, Kay AB. Platelet-activating factor: a potent chemotactic and chemokinetic factor for human eosinophils. *J Clin Invest* 1986; **78**: 1701-1706.

Wedmore CV, Williams TJ. Control of vascular permeability by polymorphonuclear leukocytes in inflammation. *Nature* 1981; **289**: 646-650.

Weissmann G, Smolen JE, Hoffstein S. Polymorphonuclear leukocytes as secretory organs of inflammation. *J Invest Dermatol* 1978; **71**: 95-99.

Whalley ET, Nwator IA, Stewart JM, Vavrek RJ. Analysis of the receptors mediating vascular actions of bradykinin. *Naunyn-Schmiedeberg's Arch Pharmacol* 1987; **336**: 430-433.

Wilhelm DL, Chemical mediators. In: B. W. Zweifach, L. Grant and R. T. McClusky, eds. The inflammatory process. New York: Academic Press, 1973 : 251-301.

Williams TJ, Jose PJ. Mediation of increased vascular permeability after complement activation. *J Exp Med* 1981; **153**: 136-153.

Williams TJ, Morley J. Prostaglandins as potentiators of increased vascular permeability in inflammation. *Nature* 1973; **246**: 215-217.

Williams TJ, Peck MJ. Role of prostaglandin-mediated vasodilation in inflammation. *Nature* 1977; **270**: 530-532.

Willis AL. Parallel assay of prostaglandin-like activity in rat inflammatory exudate by means of cascade perfusion. *J Pharm Pharmacol* 1969; **21**: 126-128.

Willis CM, Stephens CJM, Wilkinson JD. Experimentally-induced irritant contact dermatitis. Determination of optimum irritant concentrations. *Contact Dermatitis* 1988; **18**: 20-24.

Willoughby DA, Dunn CJ, Yamamoto S, Capasso F, Deporter DA, Giroud JP. Calcium pyrophosphate-induced pleurisy in rats. A new method of acute inflammation. *Agents Actions* 1975; **5**: 35-38.

Yamaki K, Oh-ishi S. Comparison of eicosanoids production between rat polymorphonuclear leukocytes and macrophages: detection by high-performance liquid chromatography with precolumn fluorescence labeling. *Jpn J Pharmacol* 1992; **58**: 299-307.

Yuan Y, Granger HJ, Zawieja DC, DeFily DV, Chilian WM. Histamine increases venular permeability via a phospholipase C-NO synthase-guanylate cyclase cascade. *Am J Physiol* 1993; **264**: H1734-1739.

Ziboh VA, Casebolt TL, Marcelo CL, Voorhees JJ. Lipoxygenase of arachidonic acid by subcellular preparations from murine keratinocytes. *J Invest Dermatol* 1984; **83**: 248-251.

Ziboh VA, Lord JT. Phospholipase A activity in the skin. Modulators of arachidonic acid release from phosphatidylcholine. *Biochem J* 1979; **184**: 283-290.

Zurier RB, Weissmann G, Hoffstein S, Kammerman S, Tai HH. Mechanism of lysosomal enzyme release from human leukocytes II. Effects of cAMP and cGMP, autonomic agonists and agents which affect microtubule function. *J Clin Invest* 1974; **53**: 297-309.

IMAGE EVALUATION
TEST TARGET (QA-3)

150mm

6"
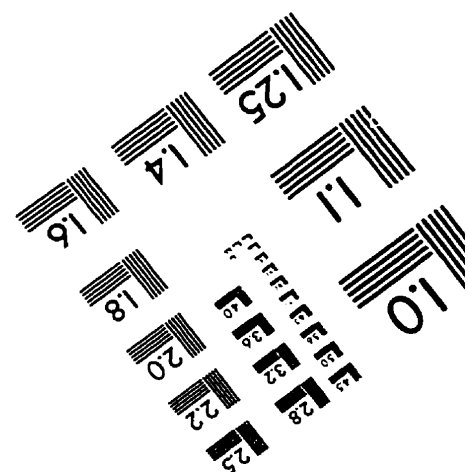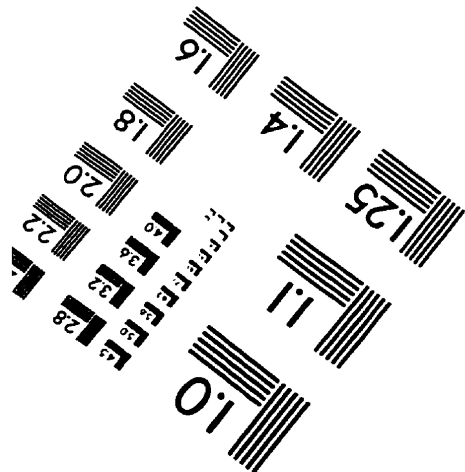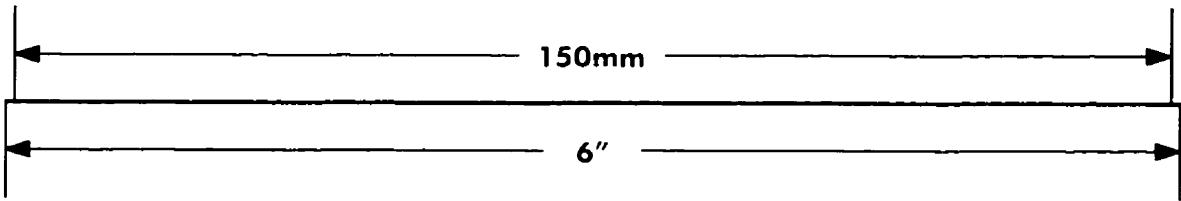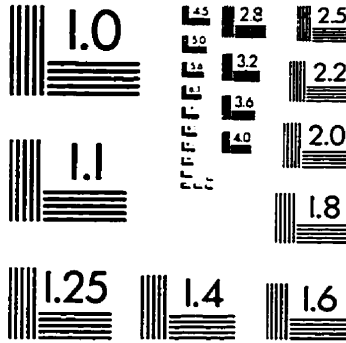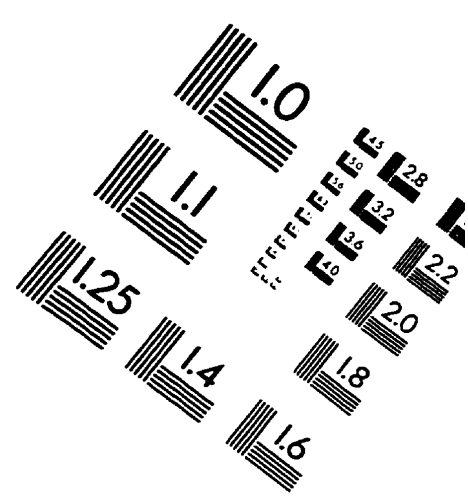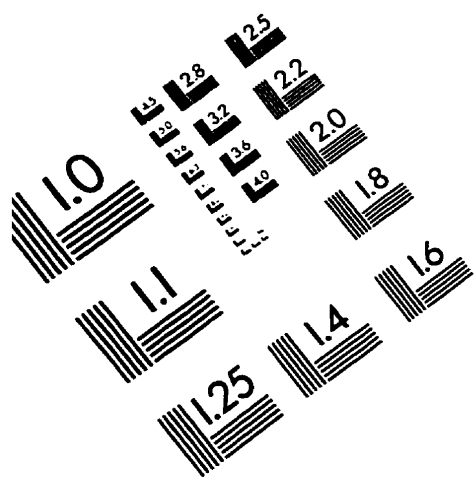
APPLIED IMAGE . Inc
1653 East Main Street
Rochester, NY 14609 USA
Phone: 716/482-0300
Fax: 716/288-5989